Valorisation of Unavoidable Food Supply Chain Wastes:

Mango Peels, Peach Peels and Pea Vines

Hao Xia

Doctor of Philosophy

University of York

Chemistry

July 2020

DEDICATION

I dedicate this work to my dear mother and father.

ABSTRACT

Traditionally, chemical and allied industries have been reliant on fossil fuels as a feedstock for their chemical, material and energy needs. Simultaneously, global population, resource consumption and waste (global megatrends) continue to increase leading to an unsustainable future if we continue to rely on crude oil as a feedstock for daily needs. As a result, biomass or renewable resources, such as unavoidable food supply chain wastes, represent an interesting opportunity to transition from linear, petroleum-based economies to circular, biobased bioeconomies (cradle to cradle).

Herein, the valorisation of three unavoidable feedstocks, namely: mango peel; pea vines, and; peach peel, is reported. Subcritical water extraction and microwave extraction were used as novel green techniques and they turned out to be better in both yield and greenness, achieving highest pectin yield of 18.34 % with over 70 % degree of esterification (DE) for mango peel waste, highest pectin yield of 7.47 % (78 % DE) for peach peel waste and highest biopolymer yield of 15.89 % from pea vine waste. Apart from extraction of pectin and microfibrillated cellulose (MFC), hydrothermal liquefaction was studied in mango peel; lye peeling simulation was studied in peach peel; and microwave pyrolysis was studied in pea vine waste. The potential applications of the extracted products were also investigated.

This study provides a green route for the valorisation of food supply chain waste and contributes as a source of biobased materials and chemicals for a sustainable 21st century.

Declaration of Interests

I declare that this thesis is a presentation of original work and I am the sole author.

This work has not previously been presented for an award at this, or any other,

University. All sources are acknowledged as References.

Table of Contents

List of Figures

List of Tables

List of Publications/ Conferences

Gao, Y., Xia, H., Sulaeman, A., de Melo, E., Dugmore, T. and Matharu, A.S., "Defibrillated celluloses via dual twin-screw and microwave hydrothermal treatment (MHT) of spent pea biomass", 2019, *ACS Sustainable Chem. Eng.*, **7**, p. 11861−11871.

Xia, H. and Matharu, A. S., "Unavoidable food supply chain waste: Acid-free pectin extraction from mango peel *via* subcritical water", 2017, *Faraday Discuss.*, **202**, p. 31-42.

Xia, H., Houghton, J. A., Clark, J. H. and Matharu, A. S., "Potential Utilization of Unavoidable Food Supply Chain Wastes–Valorization of Pea Vine Wastes", 2016, *ACS Sustainable Chem. Eng.*, **4** (11), p. 6002–6009.

"Potential Utilization of Unavoidable Food Supply Chain Wastes – Valorisation of Mango Peel Waste", 14th International Conference on Renewable Resources & Biorefineries, May 30 – June 1, 2018, Ghent, Belgium. (poster presentation)

"Acid-free Pectin Extraction from Mango Peel via Subcritical Water", Systems Change Thinking - Creating Value and Closing the Loop from Unavoidable Food Supply Chain Wastes, December 3, 2018, York, UK. (poster presentation)

Acknowledgements

First and foremost, I'd like to thank my two supervisors, Dr. Avtar Matharu and Prof. James Clark for the patient guidance and kind support throughout my PhD training.

I would also like to thank all the staffs and technicians in Green Chemistry Centre of Excellence, especially Paul Elliott, Dr. Hannah Briers, Dr. Thomas Dugmore and Dr. Joseph Houghton for the introduction and training on instruments and the guidance on experimental. Also, I'd like to thank all the green chemistry fellows in the department for creating a nice working atmosphere and sharing excellent ideas. Special thanks go to these folks: Allyn, Andy, James Shannon, Long, Xiangju and Yang.

I'd like to acknowledge Dr Tony Wild for wild funding financial assistance which has been highly beneficial.

Lastly and most importantly, I'd like to thank my families who have always supported me.

Thank you all.

Thesis Structure and Navigation

This thesis is intended for new and experienced researchers interested in valorisation of unavoidable food supply chain wastes. Although, all abbreviations are expanded in the main text a list of full abbreviations is given at the end of the thesis. The thesis is split in to four main chapters. All references are consolidated and found towards the end of thesis and not after every chapter.

Chapter 1 contextualises the impact of global megatrends on consumption and production based on fossil fuel resources as well generation of waste. Continued use of crude oil is unsustainable. The United Nations Sustainable Development Goals are given, and the 12 principles of green chemistry are introduced. The aims of the research are articulated, i.e., valorisation of unavoidable food supply chain wastes, namely: mango peels; pea vines, and; peach peels, as renewable source chemicals, materials and (bio)energy, using green extraction technologies. Each feedstock is explored with respect to its availability and chemical potential. An overview of some exemplar green extraction technologies with focus on sub-critical water and microwaves.

Chapter 2 provides all the experimental procedures and instruments used during the course of this research. It contains sufficient details for those new and skilled in-the-art of scientific experimentation. Two green extraction techniques (microwave extraction and pseudo – subcritical water extraction) were performed in this research. Meanwhile, a variety of analytic techniques are described in order to characterise the properties of pectin and MFC extracted from the biomass, namely ATR-IR, TGA, ^{13}C Solid NMR, GC-MS, HPLC, CHN, CV, DE, SEM/TEM, WHC, pectin gelation and MFC hydrogel formation.

Chapter 3 discusses the results generated from experiments conducted in Chapter 2. Chapter is sub-divided in to three sections: mango peel, peach peel and pea vine waste. In each section, the properties of pectin and MFC from these three feedstocks were studied via the techniques described in Chapter 2. The results are presented following the order how the biomass was processed.

Chapter 4 summarises and concludes the research conducted. Meanwhile, some green content, such as energy consumption, life cycle assessment and E-factor, are calculated and summarised. It gives some point of view that to what extent this work fits the green chemistry concept and what is the biggest problem in this work. Lastly, it also provides useful insights into the future work such as potential application for pectin/ MFC gel and scale-up issues.

Chapter 1 Introduction

1.1 Contextualisation

Our current methods of resource consumption and production, based on fossil fuels (crude oil, petroleum, gas and coal) as feedstock for chemicals, materials and energy, are incommensurate with the needs of a sustainable 21st Century. Crude oil has been at the heart of traditional chemical- and allied-manufacturing industries but has led to significant and sustained increases in anthropogenic carbon dioxide and climate change. We have been guilty of taking from Mother Earth, manufacturing without due care to either the environment or personal health, using articles with a mind-set of plentiful and one-use only and, thus, confining to them waste at end of life, *i.e.* a take-make-use-abuse culture akin to a linear economy that consigns resource from cradle to grave.

We can predict the needs of our current and future generation via monitoring of global megatrends. Megatrends are defined as 'sequences of events or observed phenomena that have some momentum in a particular direction and some level of durability'.[1] For example, global population is forecast to reach 9.5 billion by 2050 from 7.5 billion today (2020), which is interlinked to increased resource consumption and production because of increased need for housing and infrastructure (construction and urbanisation), healthcare, clean water and sanitation, affordable energy and, importantly, food and agriculture - it is anticipated that 70% more food will be required.[2] Thus, future efforts will focus on increased food productivity, minimisation of preventable food waste and valorisation of non-preventable food waste.[3] Hajkowicz

and Eady summarised five key megatrends in food and agriculture that will significantly influence food security in the next 20 years (Table 1.1)[4].

Table 1.1 Megatrends in food and agribusiness

Megatrend	Consequences
A less predictable planet	Supply of limited resources is being further constrained by more severe and unpredictable climate events and more potent microbes, pests and diseases, causing food producers to more seriously consider the environmental life cycle impact of food production activities.
Health on the mind	An ageing population, rising levels of chronic disease and increasing social awareness around health and wellbeing are creating demand for foods that provide specific and holistic health outcomes.
Choosey customers	Rising wealth, increasing choice and greater market access are driving demand for a more diverse range of foods and food service options that are tailored to individual preferences and lifestyles.
One world	As food and beverage value chains become increasingly global, new market opportunities are created while at the same time introducing competition and supply resilience risks in a volatile world.
Smarter Food Chains	Increasing demand for food, the use of big data and more sophisticated e-commerce platforms are driving the creation of leaner, faster, more agile and low waste value chains.

Additionally, on 25th September 2015, the UN Sustainable Development Summit adopted the document entitled "Transforming our world: the 2030 Agenda for Sustainable Development"[5], which set out 17 Sustainable Development Goals (SDGs) to end poverty, protect the planet, and ensure prosperity for all (Figure 1.1). Many of these are highly relevant to food production, agri-resilience and food security. For instance:

i. SDG 2: *End hunger, achieve food security and improved nutrition and promote Sustainable agriculture.*
    This seeks to simultaneously address global environmental sustainability and food security challenges.[6]

ii. SDG 8&9: *Promote sustained, inclusive and sustainable economic growth, full and productive employment and decent work for all & Build resilient infrastructure, promote inclusive and sustainable industrialization and foster innovation.*
    These two points are closely correlated. *The innovation of food industry will not only create smarter food chain, but also potentially create more opportunities for employment.*

iii. SDG 12.3: *By 2030, halve per capita global food waste at the retail and consumer levels and reduce food losses along production and supply chains, including post- harvest losses.*
    This was declared on European Circular Economy Action Plan in 2015 as well.[7]

iv. SDG 13: *Take urgent action to combat climate change and its impacts.*
    According to the Paris Agreement in 2015, a target of limiting global warming to increase below 1.5–2 °C by 2030 has been set.[8]

More recently, the United Nations COP 25 (Conference of the Parties) Climate Change Conference in Madrid (under the chairship of Chile) confirmed to note with concern the state of the global climate system. It also recognised that Recognizes that action taken to address climate change is most effective if it is based on best available science and continually re-evaluated in the light of new findings.[9]

Figure 1.1   17 Sustainable development goals (SDGs) (original in color)

However, crude oil alone cannot support our future resource needs as its supply is limited and its continued use pollutes the environment with anthropogenic carbon dioxide. Thus, biomass (both terrestrial and marine) represents an interesting alternative feedstock for our future chemical, material and energy needs especially if it resides as a residue (waste) and does not compete with food/feed. For example, food supply chains waste (FSCW), defined as "the organic material produced for human consumption discarded, lost or degraded primarily at the manufacturing and retail stages"[10], can be viewed as a rich source of biomolecules with inherent structure and

function designed by Nature. Food losses can arise from a variety of points along the supply chain (Figure 1.2).

Harvesting	—	handling at harvest
Threshing		
Drying	—	transport and distribution
Storage		
Primary processing	—	cleaning, classification, de-hulling, pounding, grinding, packaging, soaking, winnowing, drying, sieving, milling
Secondary processing	—	mixing, cooking, frying, molding, cutting extrusion
Product evaluation	—	quality control: standards recipes
Packaging	—	weighing, labelling, sealing
Marketing	—	publicity, selling, distribution
Post-consumer	—	over- or inappropriate purchasing, storage, preparation, portioning and cooking
End of life	—	disposal of food waste/loss at different stages of supply chain

Figure 1.2 Examples of food waste from various stages of the supply chain (original in color)

There is no shortage of food supply chain wastes (FSCW). Approximately 1.3 billion tonnes is wasted (30-50% of produce) globally per annum[11,12]. Food waste is a

significant contributor to greenhouse emissions and global warming. If, food waste was a mythical country, then it would be the third largest contributor of carbon dioxide (4.4 gigatonnes of carbon dioxide equivalents).[13] In the UK alone, 10 million tonnes of food is wasted each year and this is expected to rise by a further 1.1 million by 2025.[14] More than one half (60%) of this waste could be avoided. The value of wasted food in 2018 was estimated at £19 billion and is associated with greenhouse gas emissions of over 25 million tonnes.[15]

Furthermore, unlike crude oil, which is essentially a source of carbon and hydrogen, biomass (food waste) provides chemical heterogeneity, i.e., oxygen, sulfur, nitrogen as well as mineral elements. There is an urgent need to move from traditional petroleum-based linear economies (petroleum refineries) to forward-thinking biobased circular economies (biorefineries) that use biomass rather than crude oil as a feedstock. According to IEA Bioenergy Task 42, biorefining is "the sustainable processing of biomass into a spectrum of marketable products and energy"[16]. This concept is analogous to petrochemical refineries, which produce multiple fuels and products from petroleum. According to The U. S. National Renewable Energy Laboratory (NREL), the biorefinery concept is built on two different "platforms", which are "sugar platform" based on biochemical processes with a focus on sugar fermentation and the "syngas platform" based on thermochemical processes with a focus on biomass gasification (Figure 1.3).[17] Biomass tends to be the only viable alternative to fossil resources as it

is the only C-rich material source available on Earth besides fossils.[16] As a result, the development of biorefinery will be more and more important for human beings to meet their demands on fuels (and also chemicals and materials).
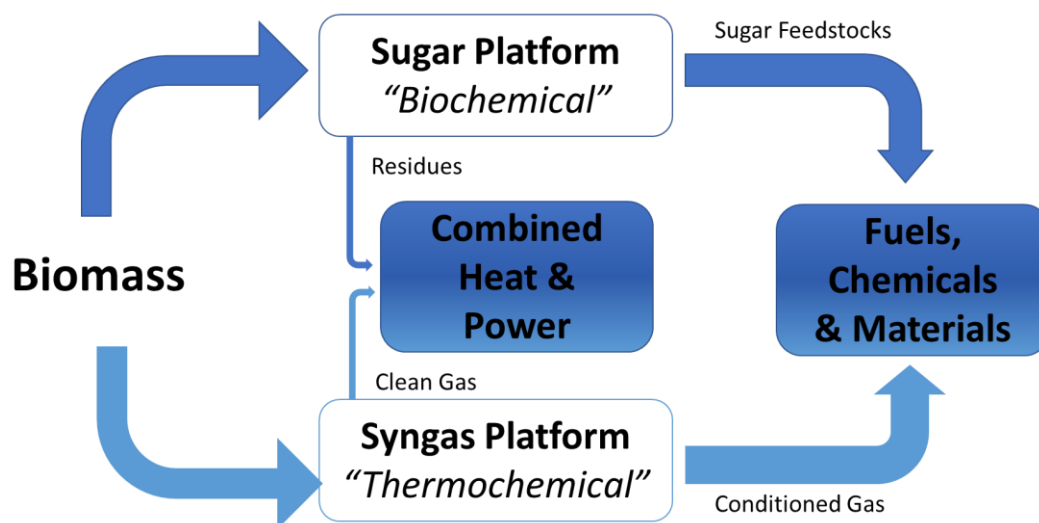
Figure 1.3   Biorefinery concept with biomass as feedstock[17] (original in color)

It is also very important that when developing chemistry for biorefineries, the methods and techniques used should minimize impact to the environment and the final products should be truly green and sustainable.   Herein, green chemistry will play an important role is this transition as it invokes the use of renewable resources and development of biorefineries.

1.2 Green Chemistry

Green chemistry is widely accepted as a philosophy or way of thinking to reduce damage to the environment associated with chemical processes and practices traditionally associated with crude oil as a feedstock.[18] Green chemistry as an

established scientific discipline came to the fore the mid-1980s when Anastas and Warner established a set of guidelines known as the 12 Principles[19]:

i. Prevention: It is better to prevent waste than to treat or clean up waste after it has been created.

ii. Atom Economy: Synthetic methods should be designed to maximize incorporation of all materials used in the process into the final product.

iii. Less Hazardous Chemical Syntheses: Wherever practicable, synthetic methods should be designed to use and generate substances that possess little or no toxicity to human health and the environment.

iv. Designing Safer Chemicals: Chemical products should be designed to preserve efficacy of function while reducing toxicity.

v. Safer Solvents and Auxiliaries: The use of auxiliary substances (e.g., solvents, separation agents, etc.) should be made unnecessary wherever possible and innocuous when used.

vi. Design for Energy Efficiency: Energy requirements of chemical processes should be recognized for their environmental and economic impacts and should be minimized. If possible, synthetic methods should be conducted at ambient temperature and pressure.

vii. Use of Renewable Feedstocks: A raw material or feedstock should be renewable rather than depleting whenever technically and economically practicable.

viii. Reduce Derivatives: Unnecessary derivatization (use of blocking groups, protection/deprotection, and temporary modification of physical/chemical processes) should be minimized or avoided if possible, because such steps require additional reagents and can generate waste.

ix. Catalysis: Catalytic reagents (as selective as possible) are superior to stoichiometric reagents.

x. Design for Degradation: Chemical products should be designed so that at the

end of their function they break down into innocuous degradation products and do not persist in the environment.

xi. Real-time analysis for Pollution Prevention: Analytical methodologies need to be further developed to allow for real-time, in-process monitoring and control prior to the formation of hazardous substances.

xii. Inherently Safer Chemistry for Accident Prevention: Substances and the form of a substance used in a chemical process should be chosen to minimize the potential for chemical accidents, including releases, explosions, and fires.

1.3 High-Value Compounds from FSCW

Food waste is a treasure of high value chemicals and materials as exemplified by Figure 1.4. Herein, only pectin and microfibrillated cellulose are discussed as these outputs are the main focus of thesis. For a detailed account of the chemical potential of food waste the reader is directed to reference 20.
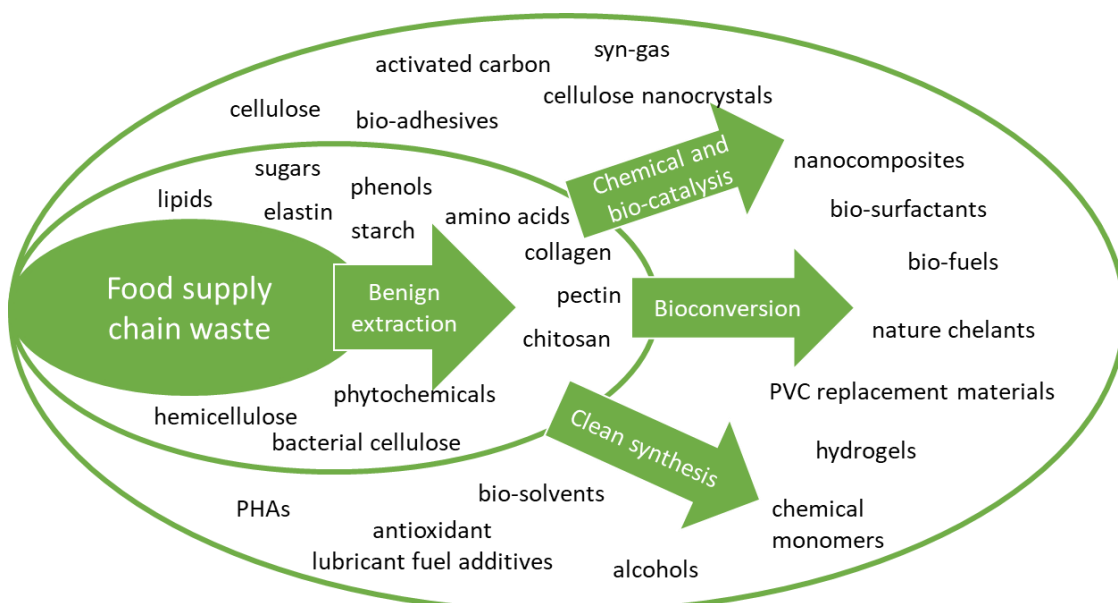
Figure 1.4   Components present in FSCW and their potential applications[20] (original in color)

1.3.1 Pectin

Pectin is a family of complex heteropolysaccharides, also known as pectic polysaccharides, consisting of a few hundred to about 1000 D-galacturonic acid (GalA) units (Figure 1.5)[21]. Homogalacturonan (HG) is most abundant pectic polysaccharide. It is a linear homopolymer of α-1,4-linked GalA that comprises about 65 % of pectin, which is partially methyl esterified at the C-6 carboxyl, and may be *O*-acetylated at *O*-2 or *O*-3[22]. Rhamnogalacturonan I (RG I) consists of the repeating disaccharide rhamnose-galacturonic acid, while Rhamnogalacturonan II (RG II) is a homo-galacturonan chain with complex side chains attached to the galacturonic residues. Both RG chains are also called the "hairy" regions of pectin molecule.[23] Other neutral sugars are also present as side chains in different amount depending on the source of pectin. Pectin is the major component of cell walls, which is distributed in the primary cell wall of all plant[24].
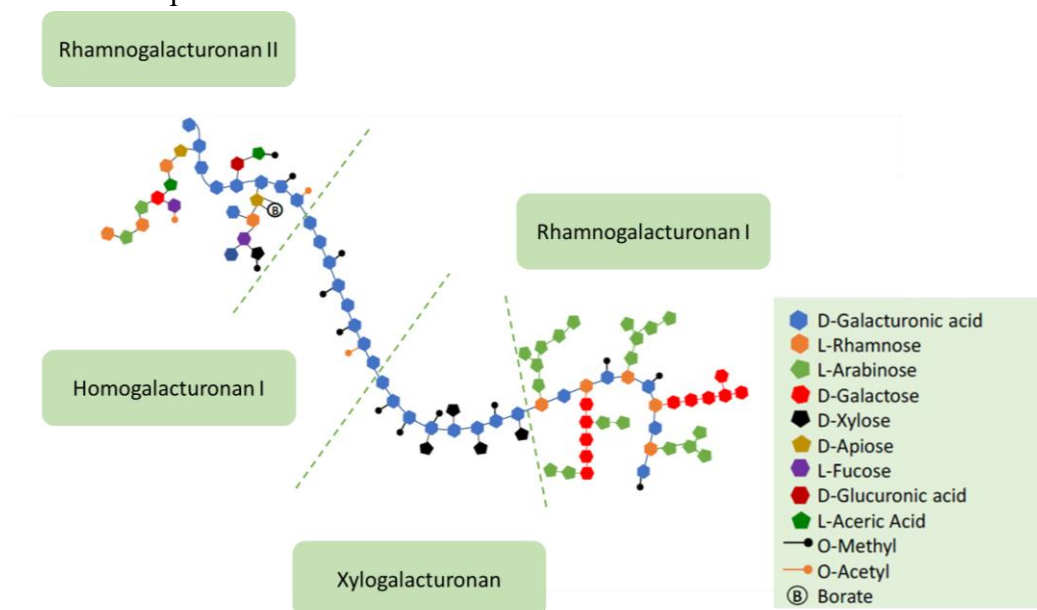
Figure 1.5 Representation of a complex pectin structure comprising different

polymeric regions (original in color)[25]Pectin is characterised by its degree of esterification (DE), *i.e.*, the ratio of methyl esterified GalA groups to total GalA groups. The DE affects the behaviour of pectin, especially its gelling property. For commercial pectin, the values of DE for high methoxyl (HM) pectin typically range from 60 to 75 % while those for low methoxyl (LM) pectin range from 20 to 40 %[21]. These two groups of pectin gel by different mechanisms. HM-pectin requires a minimum number of soluble solids and a strict pH around 3.0, and its gels are thermally reversible. LM-pectin can produce gels independent of sugar content, but it requires the presence of a controlled amount of divalent cation (typically Ca^{2+})[26].

The degree of esterification of pectin can be determined by using Fourier transform-infrared (FT-IR) spectroscopy as a straightforward method. Guillermo *et al.* measured the absorbance spectra of pectin samples isolated from papaya (*Carica papaya*) fruit and the bulk pectin without isolation from the cell wall, and then they calculated the degree of esterification by using a relationship involving absorbance intensities for 1630 and 1745 cm^{-1} bands which could be assigned to the stretching frequencies for the carbonyl groups of galacturonic acid and its methyl ester, respectively[27].

Although pectin occurs commonly in most of the plant tissues, its gelling ability varies due to the molecular size and degree of esterification of different species. Considering both quality and quantity of raw materials, apple pomace and citrus peel are most commonly used for commercial pectin manufacture[28]. The pectin produced by these

two raw materials is slightly different. Apple pectin forms a heavier and more viscous gel, while citrus pectin has the lighter colour. Besides, sugar beets and sunflower head residues are also used for commercial pectin production[29].

Pectin is widely used as a gelling, thickening (a structure formation by increasing the viscosity of a system[30]) and stabilizing agent in the food and cosmetic industries[22,31]. It is also reported to be used as carrier polymer for the encapsulation of food ingredients[32] and fat replacer in spreads, salad dressing, ice cream and emulsified meat products.[33] Meanwhile, it also has applications in pharmaceutical industries.[34] For example, pectin has been reported to be effective in removing lead and mercury from the gastrointestinal tract and respiratory organs, favourably influences cholesterol levels in blood, treatment of iron deficiency anaemia and many other health issues. [29]
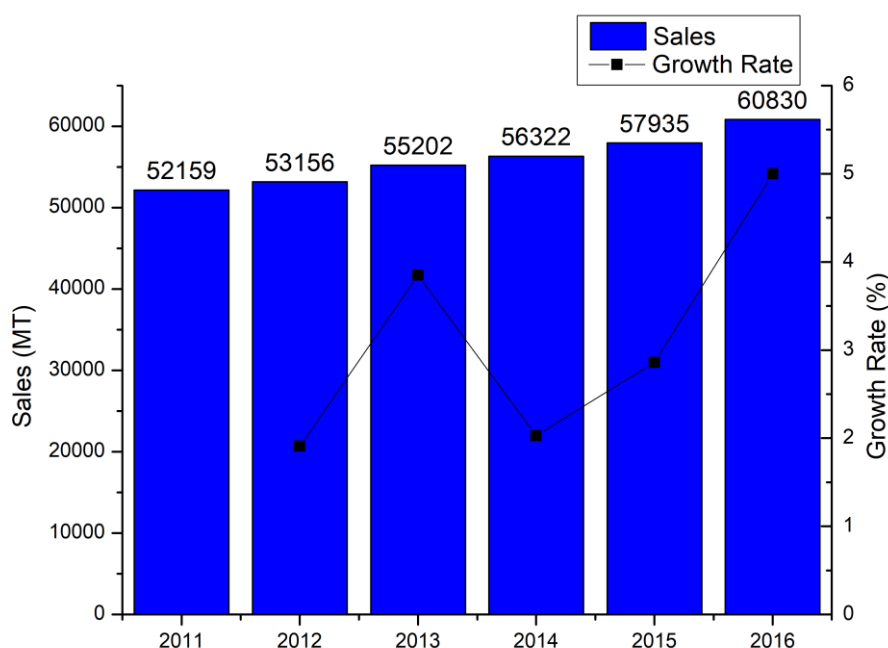
Figure 1.6 Global pectin sales and growth (2011-2016) (original in color)
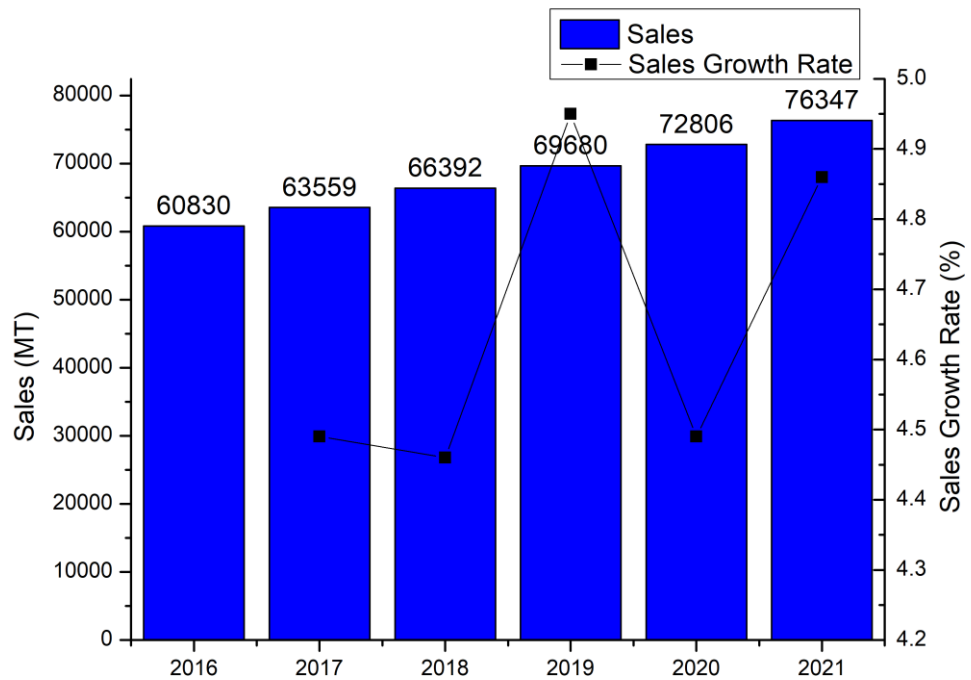
Figure 1.7   Global pectin sales and growth rate (2016 -2021) (original in color)

The global sales of pectin and its growth rate from 2011 to 2016 are shown in Figure 1.7[35]. An obvious increase can be observed during the past few years and a maximum growth rate of 5 % was achieved between 2015 and 2016, which indicates its increasing demand and promising value (CP Kelco, the world's biggest pectin manufacturer, made a $ 360 M revenue in 2016). It was predicted to maintain a 4-5 % of annual growth rate from 2016 to 2021 (Figure 1.6) and achieved a highest global revenue of $ 1320.58 M.

The conventional method of pectin extraction, including industrial production, is to heat the raw materials with acidic solvent, normally at a pH of 2.0 and a temperature of 80–100 °C, and the process lasts more than 1 hour. Various acids have been used for

pectin extraction, such as hydrochloric acid, sulfuric acid, nitric acid, and citric acid etc.[36–39] Besides, alkaline extraction was also studied. Diluted alkaline (normally NaOH or Na_2CO_3) were used and unlike the acidic extraction, it was usually carried out under low temperature (*ca.* 25 °C).[40,41] Compared with acid-extracted pectin, alkaline-extracted pectin has very low degree of esterification and small particle size.[42] It is reported that low DE pectin at pH 8.5 had the greatest gel strength and structure development rate. However, as mentioned earlier, the gelation of low DE pectin usually required the inclusion of Ca^{2+}, and this will result in lower degree of crystallinity.[43]

These acid/ alkaline extraction methods were usually time-consumed, which might lead to the degradation of pectin due to the long process of heating. Herein, some novel techniques have been developed recent years in order to increase the extraction efficiency.

i.   Ultrasound-assisted Extraction (UAE)

Y.T Xu *et al.* studied on ultrasound-assisted heating extraction and a higher yield and shorter extraction time was reported compared with conventional heating extraction[31]. S.S. Hosseini *et al.* reported an ultrasound-assisted extraction of pectin from sour orange peel. The optimal condition was power of 150 W, irradiation time of 10 min and pH of 1.5 and a highest extraction yield and DE of $28.07 \pm 0.67\%$ and $6.77 \pm 0.43\%$ were achieved.[44] A. Grassino *et al.* worked on the ultrasound-assisted extraction of pectin from tomato waste. A highest yield of 35 % was achieved at power of 37 kHz

and temperatures of 60 °C. The comparison with conventional heating showed 15 min

of UAE extraction gave a similar pectin yield with 24 h of conventional heating.[45]

ii.   Microwave Extraction (MWE)

L. Pfaltzgraff *et al*. studied acid-free MAE of milled orange peels with water as solvent,

at 120 °C for 15 min, and obtained a 7 % (lab-scale) and 10 % (pilot-scale) pectin

yield[10]. Y. Liu *et al.* also studied on the extraction of orange peel and combined the

MWE with hand-pressure (the cloth-wrapped peel was pressed by hand and leached

with deionized water), resulting in 12 % higher yield than hand-pressure alone[46]. J.

Maran *et al.* studied microwave-assisted extraction of pectin from waste mango peel,

and obtained the highest pectin yield of 28.86 % at microwave power of 413 W, pH of

2.7, time of 134 s and solid–liquid ratio of 1:18 g mL^{-1}.[47] M. Kazemi *et al.* reported

extraction of Pistachio green hull pectin, which obtained a highest pectin yield of 18.13 %

in microwave power of 700 W, irradiation time of 165 s, and pH of 1.5. Interestingly, a

very low DE (12.1 %) was reported.[48] M. Fishman *et al.* studied microwave-assisted

extraction of pectin from lime (albedo, pulp and flavedo), and found the optical heating

time was 3 min, with microwave power of 630 W, pH of 2 and solid–liquid ratio of

1:25 g mL^{-1}, which gave a total pectin yield of 14.6 %.[49] Recently Fishman *et al.* have

reported on the long term storage of the pectin first extracted in 2006. The pectin

showed approximately 50% less degree of esterification and more total sugar content,

while the galacturonic acid content remained almost same following cold storage.[50]

iii.   Subcritical Water Extraction (SWE)

X. Wang *et al*. studied the extraction of pectin from citrus peel and apple pomace by subcritical water, achieving maximum yield of 21.95 % for citrus peel pectin and 16.68 % for apple pomace pectin, respectively[51]. H. Ueno *et al*. reported pectin extraction from the flavedo of *Citrus junos* using subcritical water, combined with sodium hexametaphosphate and hydrochloric acid, for a three-step extraction, and a maximum total pectin yield of 21.74 %[52]. S.Q. Liew *et al*. used subcritical water on extraction of pectin from pomelo peels. A highest yield of 19.6 % was achieved at 120 °C and 30 bar with a relatively low DE (41.1 %), which was pointed out due to the absence of acid.[53] W. Li *et al*. carried out the subcritical water extraction of pectin from jackfruit peel, and achieved a highest pectin yield of 14.96 % at 138 °C for 9.15 min. They also did the traditional citric acid heating. The results showed that pectin from SWE had more hairy region and side chains than traditional heating, but the molecular weight (113.3 kDa) was much lower (174.3 kDa for pectin from traditional heating).[54]

Strictly speaking, all the yields reported above should be mass extract/ mass raw materials (dry weight basis) instead of pure pectin yield. However, in most cases, they are taken as pectin yield by default.

1.3.2 Cellulose and Microfibrillated Cellulose (MFC)

Cellulose is the most abundant biopolymers in most plants.[55] It is a linear, stereoregular polysaccharide which is made of 1,000 to 30,000 D-glucopyranose units and linked by β - (1,4) - glycosidic bonds (Figure 1.8). The lateral size of the cellulose chain is about 0.3 nm, and the chain length normally varies from 500 to 15000 nm.[56]
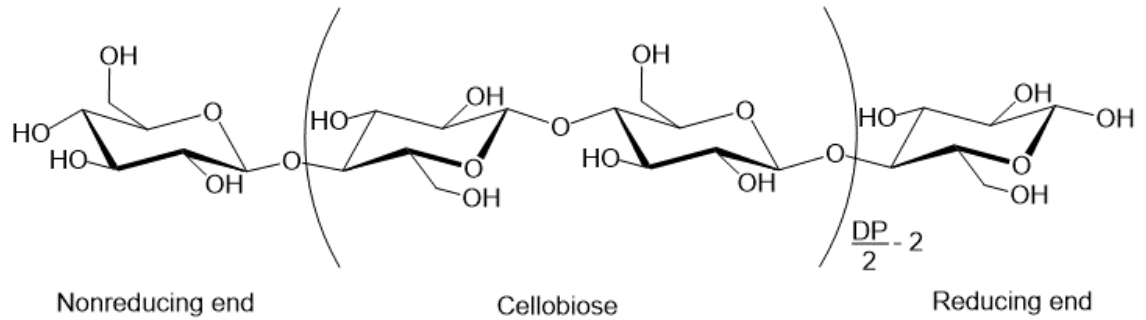
Figure 1.8 Chemical structure of cellulose[57]

Microfibrillated Cellulose (MFC, Figure 1.9) is also described as microfibril/ nanofibril (aggregates) or microfibrillar/ nanofibrillar cellulose in other literature. According to G. Chinga-Carrasco, MFC materials may be composed of (1) nanofibrils, (2) fibrillar fines, (3) fibre fragments and (4) fibres based on their dimensions as listed in table 1.2.[58] The thickness of its nano-elements (elementary fibril) is typically 3-10 nm, but due to the aggregation, it is usually 20- 40 nm.[59]
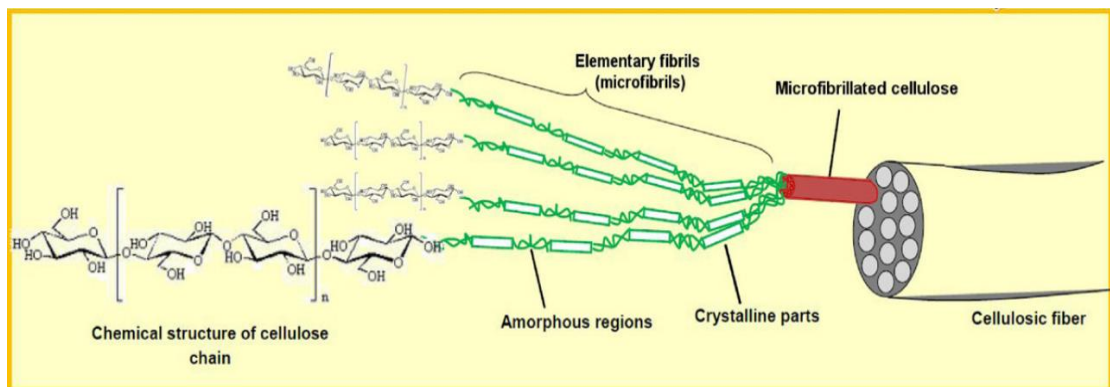
Figure 1.9   Detailed structure of microfibrillated cellulose (original in color)

Meanwhile, the term "Microfibrillated Cellulose" is also confused with some other similar names such as Nanofibrillar cellulose (NFC), Nanocrystalline cellulose (NCC)

Table 1.2 Components of microfibrillated cellulose

Diameter (µm)	Biological structures
10 – 50	Cellulose fibre
<1	Macrofibrils - fibrillar fines, fibrils
<0.1	Nanofibril, nanofibers
<0.035	Microfibril
0.0035	Elementary fibril

or Microcrystalline cellulose (MCC) although they are different concept. The differences are summarised in table 1.3.[60]

Wood pulp and fibre is the most important biomass for micro- and nano-fibrillated cellulose production, but they can also be derived from a lot of other sources, such as seed fibre, bast fibre, grasses, marine animals, algae fungi and bacteria *etc.*[61] The conventional processes for cellulose production (see Figure 1.10) mainly involve biological and chemical pretreatments (*e.g.* KOH/ NaOH treatment, for removal of hemicellulose and lignin in biomass) and mechanical disintegration/ fractionation (e.g. homogenisation, grinding, blending *etc.*)[61]. However, these methods lead to many environmental concerns such as lye waste disposal and high energy consumption. Thus, recently more environmental-benign techniques (e.g. superheated steam pretreatments[62] and enzymatic pretreatments[63]) have been studied and developed.

Table 1.3   Cellulosic nanomaterials dimensions

Terminology and nomenclature of cellulose nanomaterials	Width (nm)	Length (nm)	Aspect ratio (length/ width)
Cellulose nanofibril (CNF) Nanofibrillar cellulose (NFC)	2-10	>10,000	> 1000
Cellulose nanocrystals (CNC) Nanocrystalline cellulose (NCC) Cellulose nanowhiskers	2-20	100 – 600	10 – 100
Cellulose microcrystal (CMC) Microcrystalline cellulose (MCC)	>1000	>1000	≈1
Cellulose microfibril (CMF) Microfibrillar cellulose (MFC)	10 – 100	500 – 10,000	50 – 100
Bacterial cellulose (BC) Microbial cellulose	10 – 40	>1000	100 – 150

Compared with inorganic reinforcements, cellulose/cellulosic materials have many advantages. For instance, it has low cost and energy consumption due to its abundance and renewability. On the other hand, it has low density but a high specific strength, modulus and reactive surface.[64] Because of these advantages, it has been widely used in papermaking,[65] food[66] and pharmaceutical industry,[67] as well as the manufacture of multilayer film,[68] supercapacitors[69] and compressibility or porous materials (*eg.*

hydrogels and aerogels).[70] Therefore, the global market of MFC continues to increase, and has doubled from 2012 ($ 5.4 M) to 2014 ($ 10.3 M). The market is expected to reach 40.7 M $ in 2019. Especially in EU region, it is forecasted to share more than half of the global market ($ 20.5 M), which is almost ten times the number of its market size in 2012 ($ 2.2 M).[71]
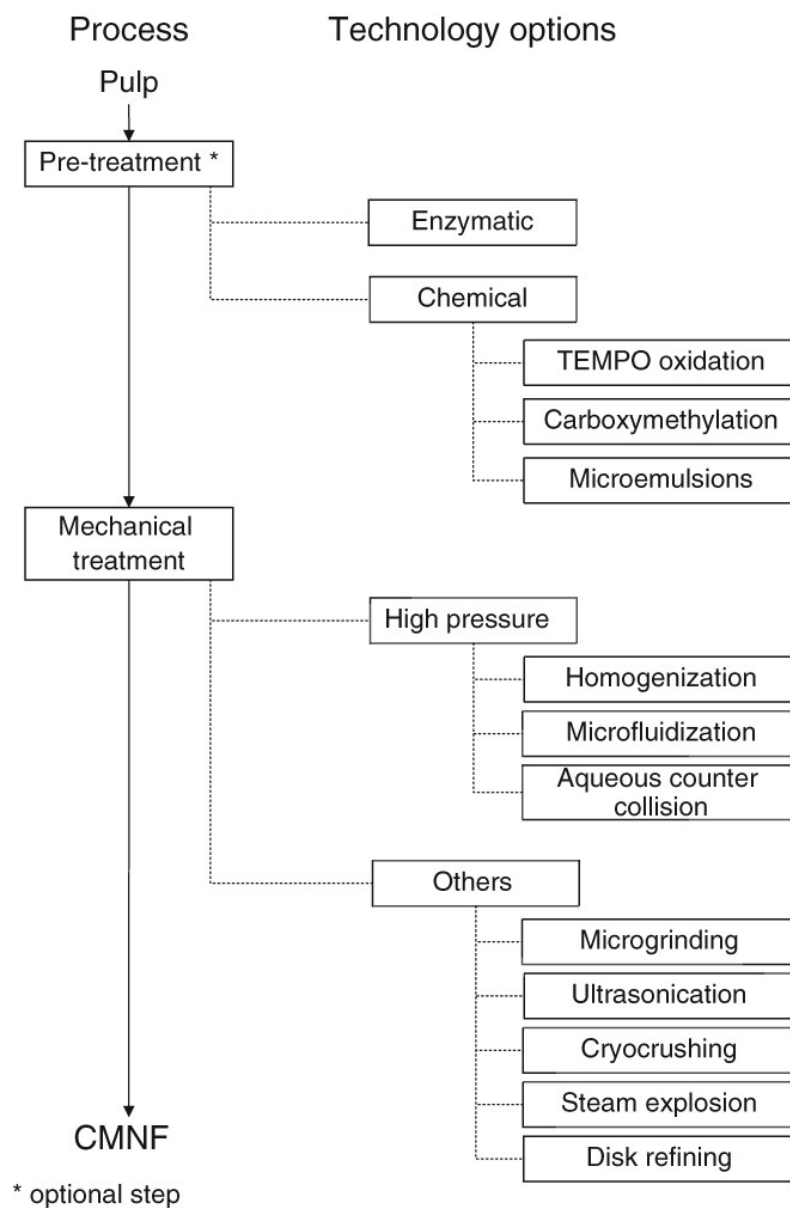
Figure 1.10 A typical list of pre-treatments and mechanical treatments for cellulose

micro- and nanofibrils (CMNF) production.[72]

1.4 Aims and Objectives

With a desire to move from crude oil to renewable feedstocks to aid a sustainable 21st

Century, this research aims to valorise three different FSCWs, namely:

i.   *mango peels;*

ii.   *peach peels, and;*

iii. *pea vines,*

with focus (but not exclusively limited to) on pectin, cellulose, sugars etc. using

microwave and (pseudo)subcritical water extraction processes.

In the following sections, a brief overview of some exemplar green extraction technologies is given with focus on microwaves and sub-critical water. Additionally, each feedstock is reviewed with respect to its production volumes and chemical potential.

1.4.1 Green Extraction Techniques

1.4.1.1 Microwave Extraction (MWE)

Microwaves are non-ionising electromagnetic waves located between the radio-frequency range at the lower frequency and infrared at the higher frequency in the electromagnetic spectrum, within the frequency band of 300 MHz to 300 GHz; 915

MHz is considered most useful for industrial applications with its greater penetration depth, while 2,450 MHz frequency is generally used for extraction applications with a wide range of commercial units designed for analytical chemistry purposes[73,74]. Microwaves cause molecular motion by migration of ionic species and/ or rotation of dipolar species.[75] Unlike conventional heating, heat is dissipated inside the irradiated medium in microwave heating,[76] so there is no heat and energy transfer and it is non-contact heating. Therefore, it gains huge advantages against conventional heating, such as higher heating rates (efficiency), selectivity, greater control of process (higher safety) and reduced size and waste for equipment.[77]

However, microwave extraction is still not widely used in industry and this is mainly because of its scaling-up issue. As it draws more and more attention within lab-scale, some pilot-scale research has been conducted as well to explore the potential of large-scale extraction. Polyphenols[78], essential oils[79] and have been studied for their pilot-scale microwave extraction. As for pectin, pilot-scale was also studied and reported by G. Garcia-Garcia *et al.* where a Sairem Labotron Pyro 60K Pyro microwave (see Figure 1.11). Up to 4 L of orange peels were processed and achieved a pectin yield of 5 % on wet basis, which was higher than conventional heating method (3 % on wet basis). Meanwhile, the specifications of the pectin (Degree of esterification, Galacturonic Acid, Loss on Drying *etc.*) were also analysed and they all met the commercial criteria.[80]
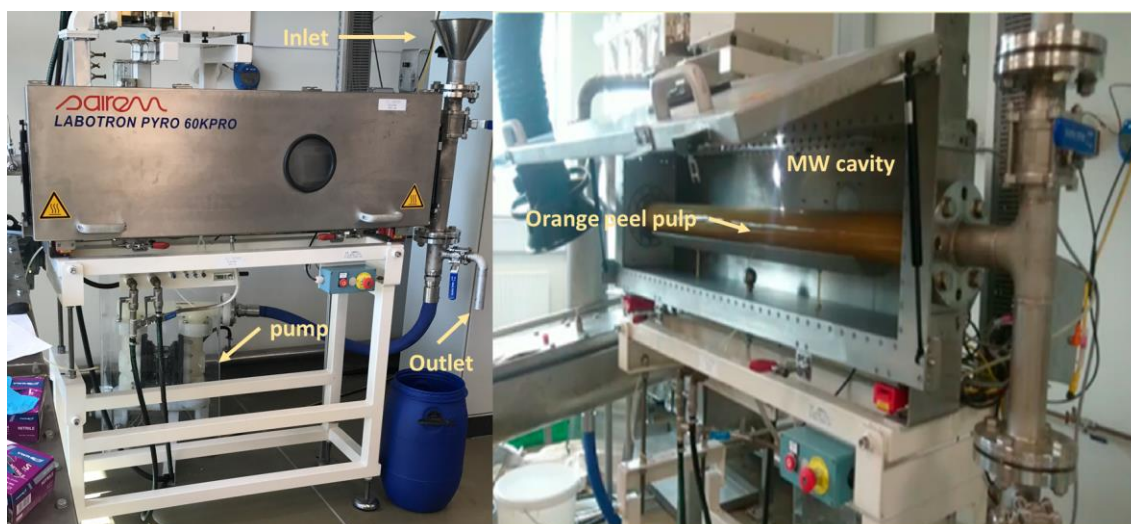
Figure 1.11 Sairem Labotron Pyro 60K Pyro microwave (original in color)[80]

1.4.1.2 Subcritical Water Extraction (SWE)

Subcritical water, also known as "Superheated water", is water at temperatures between

the usual boiling point (100 °C) and the critical temperature (374 °C) with pressure

high enough to maintain the liquid state (see Figure 1.12). It is an excellent solvent for

both polar and non-polar compounds due to its tunable polarity, which is directly

dependent upon the temperature[81]. The dielectric constant of water decreases when

increasing the temperature. And when it is in subcritical state (between 100 °C and

374 °C), the dielectric constant of water will become similar to some common organic

solvents such as DMSO, methanol, ethanol and acetone. Therefore, subcritical water

can extract various polar and non-polar organic compounds by choice, through varying

the temperature. As a result, subcritical water extraction (SWE) has become more and

more attractive because it reduces the use of organic solvent as well as improves the

extraction methods of constituents of plant materials.
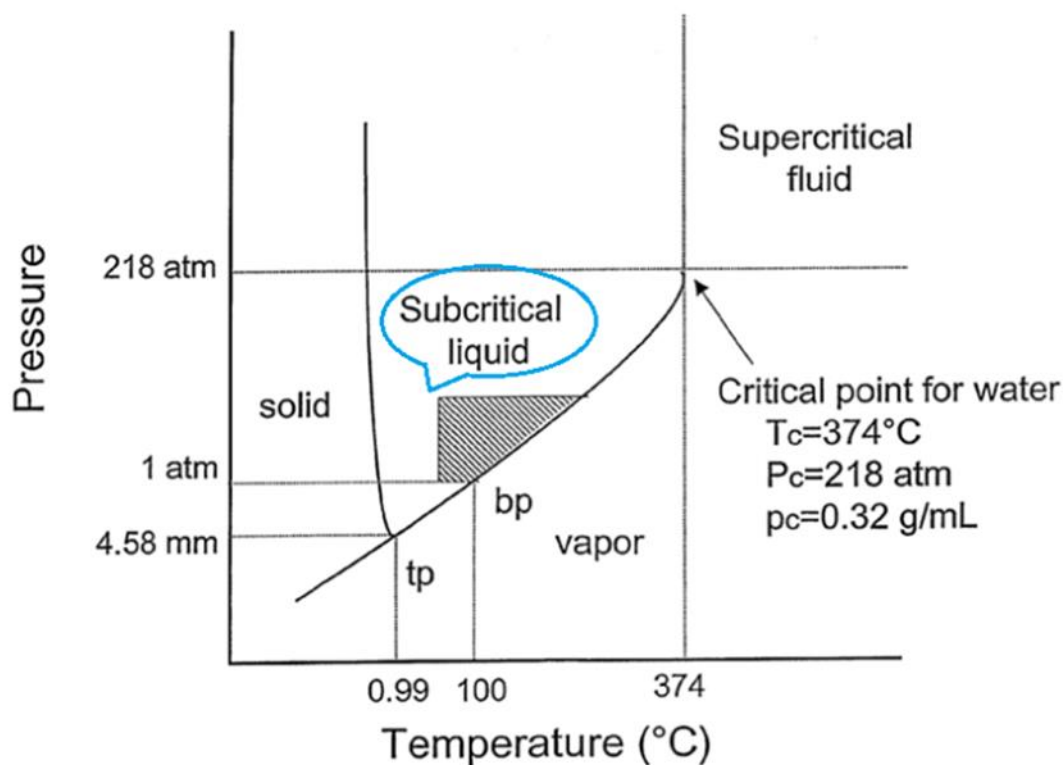
Figure 1.12 Phase diagram of water as a function of temperature and pressure (Cross-hatched area indicates the preferred region (SWE))[82] (original in color)

The mechanism of SWE process can be described to six sequential steps (Figure 1.13):

i.   rapid fluid entry;

ii.   desorption of solutes from matrix active sites;

iii.   diffusion of solutes through organic materials;

iv.   diffusion of solutes through static fluid in porous materials;

v.   diffusion of solutes through layer of stagnant fluid outside particles, and;

vi.   elution of solutes by the flowing bulk of fluid.

This mechanism suggests that the flow rate plays an important role in affecting the extraction efficiency. [83]
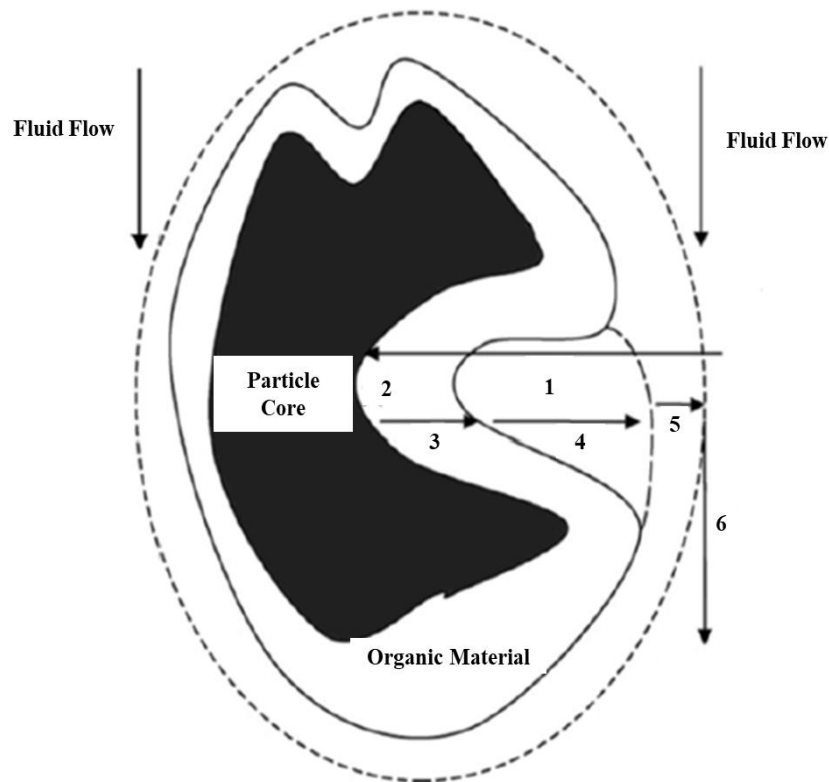
Figure 1.13 Proposed schematic presentation of the extraction steps in SWE[83]

Due to the pressure issue, subcritical water extraction was mostly limited within lab-scale. Recently, pilot-scale subcritical water extraction has started to be explored. M. Co *et al.* reported pilot-scale subcritical water extraction of flavonoids from satsuma mandarin (*Citrus unshiu Markovich*) peel.[84] An 8 L stainless-steel extraction cell was used, and the extraction temperature and pressure were reported up to 280 °C and 15 MPa respectively. The yield of flavonoids (113.4 mg/g) from pilot-scale was similar to

that from lab-scale (117.8 mg/g), and a high recovery rate of flavonoids (96.3 %) was also reported. H. Kwon *et al.* reported a pilot-scale subcritical solvent extraction of curcuminoids from *Curcuma long L.*[85] Curcuminoids from turmeric were extracted using the subcritical solvent (mixture of water and ethanol) with a 8 L extraction system. The highest extraction temperature and pressure were 150 °C and 100 atm, and a highest curcuminoids yield of 13.58 % was reported.

1.4.1.3 Ultrasound-assisted Extraction (UAE)

Ultrasound is one of the novel alternative technologies used to extract target compounds from biomass. The mechanism of ultrasound is related to many physical and chemical phenomena. However, acoustic cavitation is the main driving force for its extraction effects[86]. When ultrasound propagates through a medium, it induces a series of compressions and rarefactions in its molecules. Such alternating pressure changes cause the formation and, ultimately, the collapse of bubbles in a liquid medium. This phenomenon of creation, expansion, and implosive collapse of microbubbles in ultrasound-irradiated liquids is known as "acoustic cavitation".

Ultrasound can be used in various systems (Figure 1.14). It is efficient, effective and easy to use, which leads to its wide application in degassing, filtration, demoulding, defoaming, emulsification *etc*.
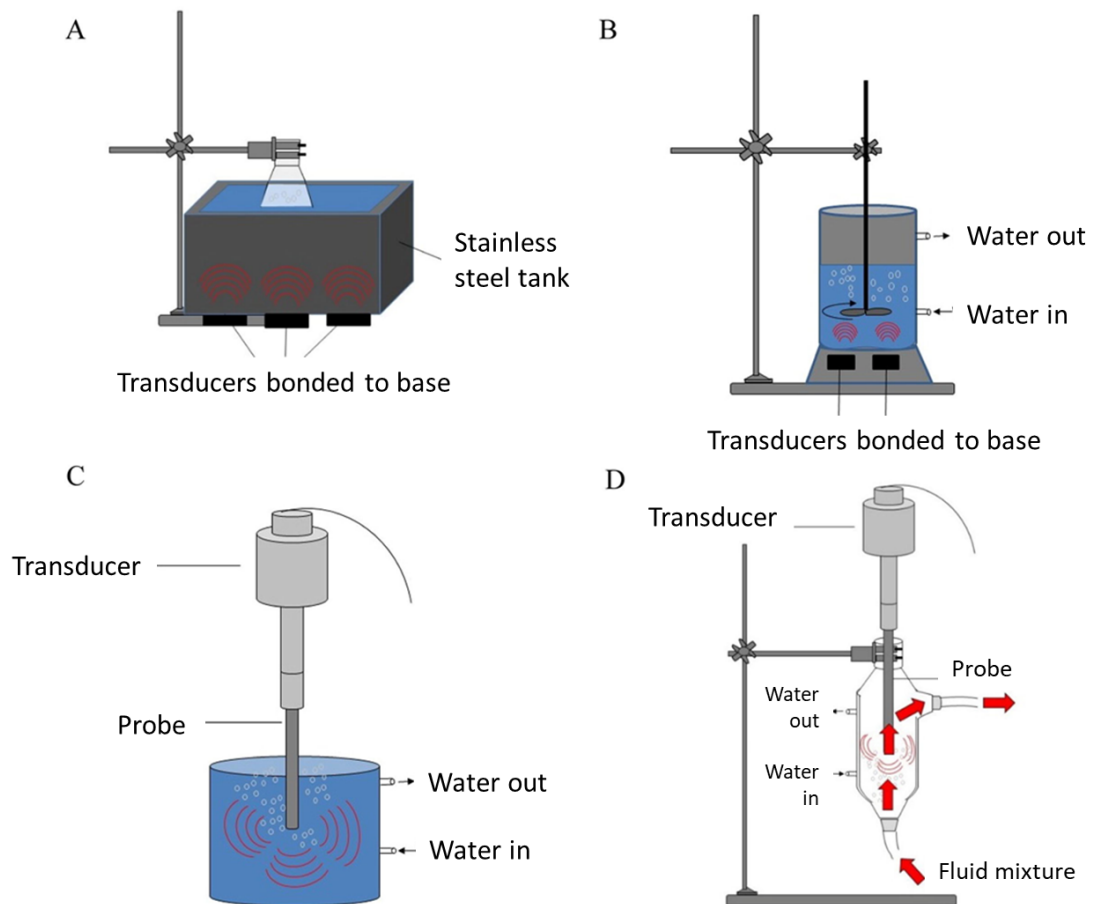
Figure 1.14 Commonly used ultrasonic systems (A: Ultrasound bath, B: Ultrasound reactor with stirring, C: Ultrasound probe, D: Continuous sonication with ultrasound probe)[87] (original in color)

1.4.1.4 Pulsed Electric Field (PEF) Extraction

Pulsed electric field (PEF) technique has been studied over 50 years and become one of the most popular technology in food processing.[88] It is an efficient technology with short treatment time (from several nanoseconds to several milliseconds) and high voltage (pulse electric field strength varying from 100- 300 V/cm to 20- 80 kV/cm).[89] The mechanism is call "electroporation" and can be explained as the reversible or

irreversible pores (damage) which plant cells form when exposed to a given electric field[90]. Some of the applications of PEF are shown in Figure 1.15. Moreover, industrial scale with up to 10,000 l/ h has been reported as well.[91]
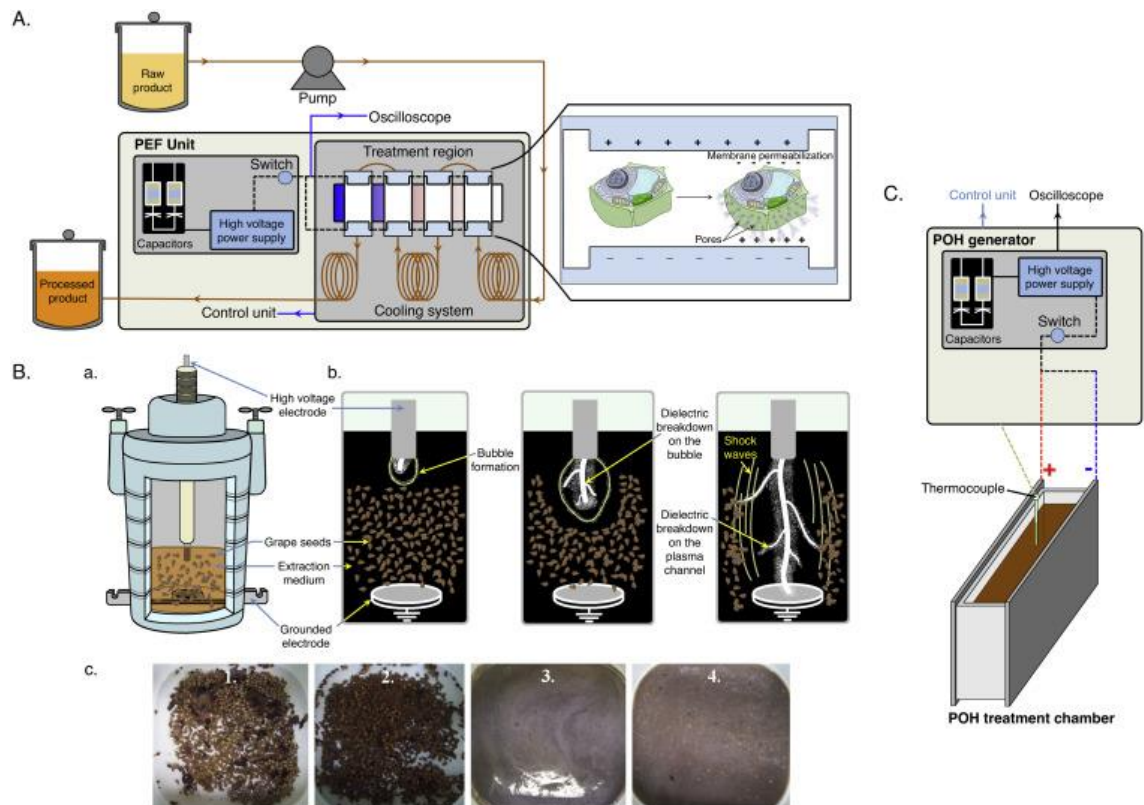
Figure 1.15 A) Schematic representation of a continuous PEF treatment system. B) a. Schematic representation of a laboratory scale HVED cell used for grape seed processing. b. Schematic representation of dielectric breakdown formation during HVED treatment and associated phenomena. c. Effect of the energy input per pulse and the specific energy input per pulse on the fragmentation of grape seeds suspensions: (1) control samples, (2) pilot HVED treated samples (EB = 0.16 kJ, EBm = 0.02 kJ/kg), (3) laboratory HVED treated samples (EB = 0.16 kJ, EBm = 0.53 kJ/kg) and (4) pilot HVED treated samples (EB = 0.4 kJ, EBm = 0.53 kJ/kg) with a total specific energy input of 160 kJ/kg with permission. C) Schematic representation of a laboratory scale pulsed ohmic heating (POH) system[90] (original in color)

1.4.2 Overview of Used Feedstocks

1.4.2.1 Mango Peel Waste

Mangoes (*Mangifera Indica*) are the second most important tropical fruit after banana. In 2017, the global production of mangoes was in excess of 50 M tonnes (FAO). India is largest producer of mango peel, accounting for almost two-thirds of global production, followed by China, Thailand and Indonesia (Figure 1.16).
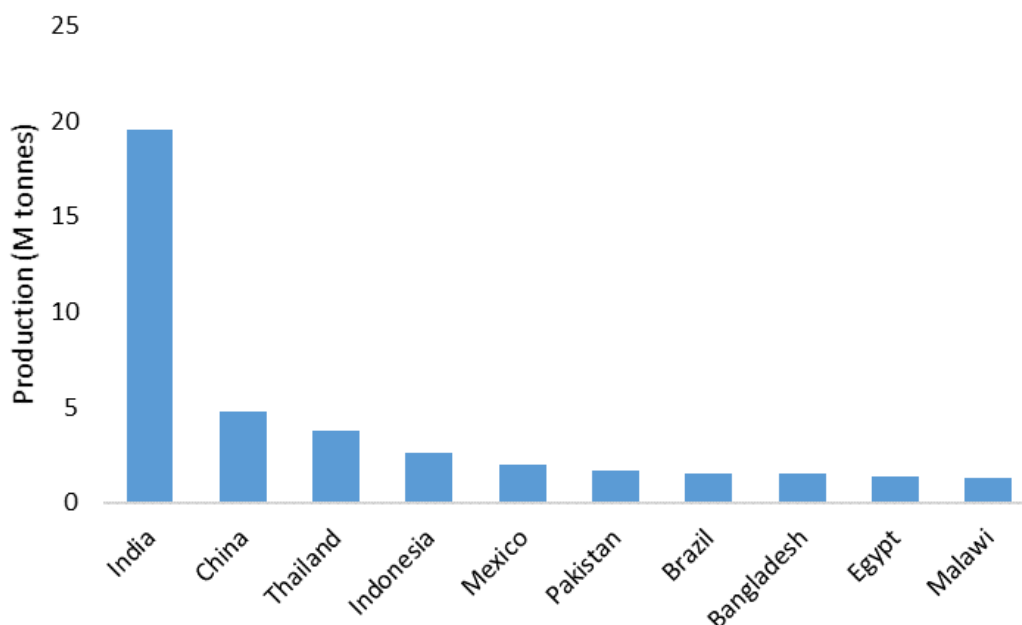
Figure 1.16 Top ten global mango producers in 2017 (original in color)

Peels and stones (Figure 1.17) are the major by-products of industrial mango processing, which consists 7 – 24 % and 30 – 45 % of total mango weight, respectively.[92, 93] Normally, these by-products are directly discarded and left to decay, which is an environmental concern. However, mango peel is a rich source of many valuable compounds, such as (poly)phenols (Figure 1.18), enzymes and dietary fibre

[94,95] and the basic composition of mango peel powder, also known as *amchur* (derived from *ambh* meaning mango and *chur* meaning powder in Hindi, respectively), is listed in table 1.4.
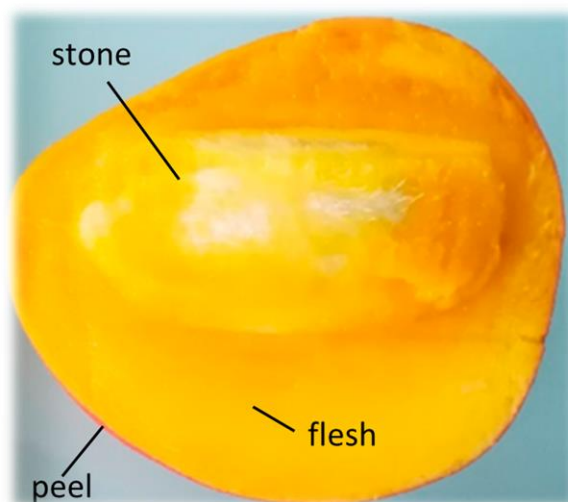
Figure 1.7 Cross section of a *Kesar* mango used in this thesis[96] (original in color)

Table 1.4   Exemplar proximate composition of mango peel powder (Kodagu Foods, Mysore, India)[97]

Component	Content
Moisture (%)	10.5 ± 0.5
Fat (%)	2.2 ± 0.06
Ash (%)	3.0 ± 0.18
Total protein (%)	3.6 ± 0.6
Total carbohydrate (%)	80.7 ± 1.2
Total dietary fiber (%)	51.2 ± 1.08
Soluble dietary fiber (%)	19.0 ± 0.26
Insoluble dietary fiber (%)	32.1 ± 1.34
Total polyphenols (mg GAE/g MPP) [a]	96.2 ± 1.4
Total carotenoids (μg/g MPP) [b]	3092 ± 98

a. GAE = gallic acid equivalents; b. MPP = mango peel powder

Mango peels have been studied for various applications in recent years. C. Sampaio *et al.* reported that the seeds and peels of mango cultivars could be used for absorption of chromium(VI) in aqueous solutions,[98] which is because of the high amount of gallates and galloyl glucosides (see Figure 1.15). On average, with use of a Cr(VI) concentration of 100 mg/L, a maximum adsorption capacity of 90 % (g/g) was achieved at pH 1.0, sorbent concentration of 3 g/L, and a contact time of 180 min. Similarly, A. Haq *et al.* [99] reported sorption of chromium(III) and chromium(VI) showing that pH 5.0 and 7.0, respectively were best conditions. L. Silva *et al.* studied mango peel extracts as a potential alternative method of post-harvest disease control.[100] They found that mango peel extracts treated with methanol, hexane and ethyl acetate had an inhibitory effect on *in vitro C. gloeosporioides* (causing anthracnose - a group of diseases that cause dark, sunken lesions on leaves, stems, flowers, and fruits) development, which could be helpful in plant disease control. E. Coelho *et al.* processed mango peels with alcoholic maceration and maceration with pectinase to yield antioxidant compounds such as polyphenols (*e.g.* Figure 1.17, epicatechin-gallate, epigallocatechin-gallate), flavonols (quercetin-3-*O*-glucopyranoside and rutin), and phenolic acids (gallic acid, *o*-coumaric acid, and syringic acid).[101]

Conventionally, pectin is extracted from waste mango peels with the addition of mineral acids (mainly HCl and H_2SO_4). Recently, citric acid is also widely used in pectin extraction. Literature examples for pectin extraction from mango peel are

summarised in table 1.5.

Table 1.5   Exemplar literature data for pectin isolation from mango peel (all with conventional heating)

Reference	Acid	Condition	Pectin Yield (%)	DE (%)
92	H_2SO_4	pH=1.5, 90 °C, 2.5 h	16.4	NP*
102	H_2SO_4	pH=2.5, 80 °C, 2 h	21.0	NP*
103	H_2SO_4	pH=1.5, 90 °C, 2.5 h	21.2	66
104	HCl	0.05 N, 100 °C, 1 h	20.8	76
105	HCl	pH=1.5, 85 °C, 1 h	19.8	57
106	Citric acid	pH=2.5, 80 °C, 2 h	NP*	78

*NP = not reported

Apart from conventional acidic extraction, some novel techniques have now been developed. For instance, M. Wang *et al.* used ultrasound-assisted extraction (UAE) with citric acid and achieved high DE pectin (85 – 88 %) at 80 °C.[107] Maran *et al.* used acid-assisted (pH 2.7) microwave extraction to obtain a very high yield of pectin (29%) under the condition: microwave power of 413 W, time of 134 s and solid–liquid ratio of 1:18 g/ml.[108] J. Banerjee *et al.* reported pressurised hot water extraction (1:20 w/v, 16.2 Psi and 121 °C) from mango peels (*Totapuri* variety) to yield pectin (27 %) with high DE (77 - 89 %).[109] A. Matharu *et al.* reported an acid-free microwave-assisted hydrothermal extraction (1:6 w/v, 110 °C, 600 W, 5 min) of pectin from mango peel and achieved a pectin yield of 11.6 % (dry weight basis) and high DE (76 – 88 %). [110]
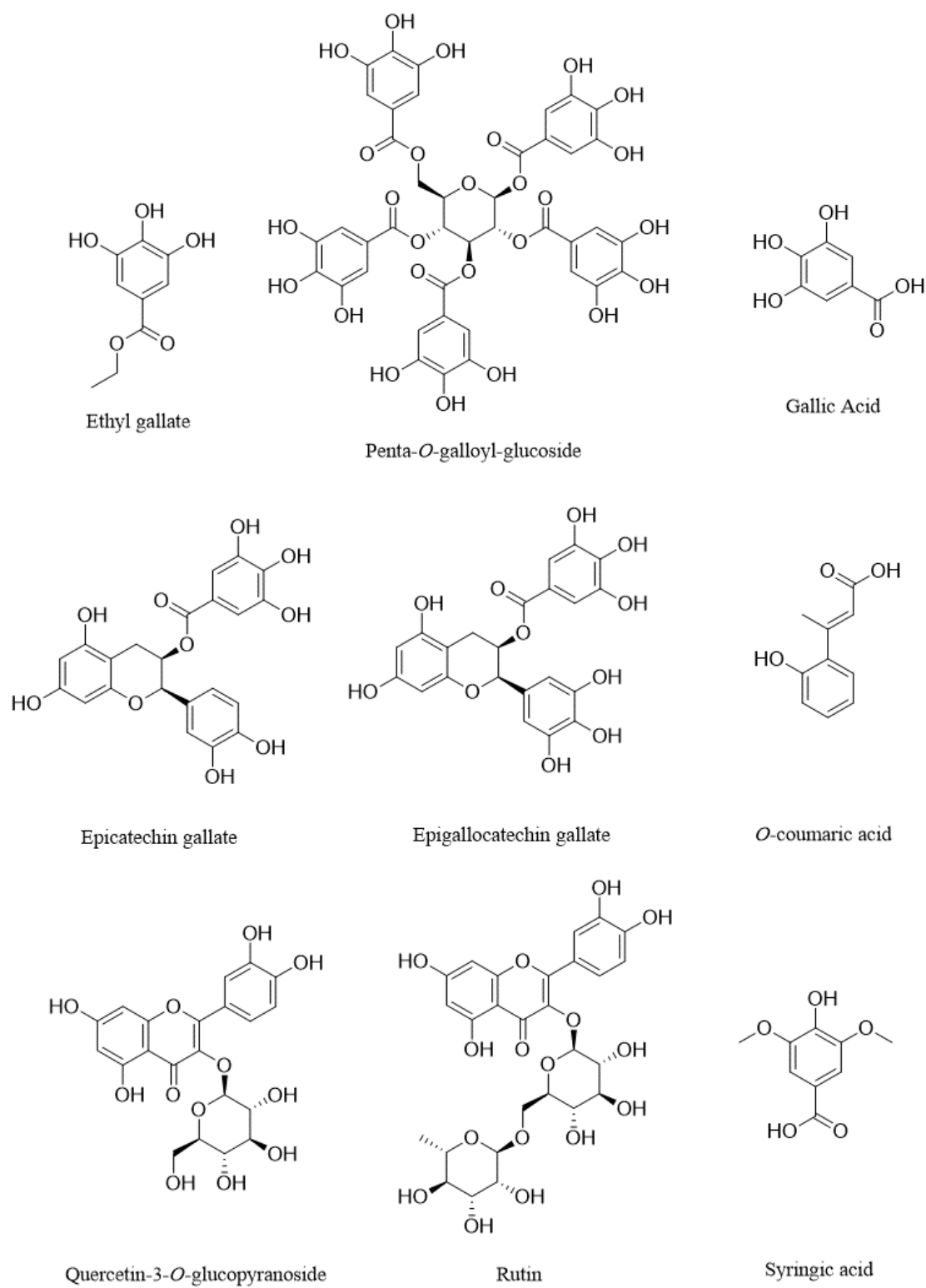
Figure 1.18 Examples of (poly)phenols in mango peel

Thus, this study aims to investigate both mango peel pectin extracted by (pseudo)SWE with water as sole solvent as well as generation of MFC from post extracted residue as outlined in Figure 1.19. Two different systems (flow and batch) will be studied in this project to compare the effectiveness on extraction of pectin and cellulose from mango peel waste. All samples will be characterised accordingly, in particular ATR-IR, [13]CP-MAS NMR and TGA and their properties determined. Gelation for pectin and residues will be important as will water holding capacity and water retention value for the latter.

Due to the limit of flow system equipment, the temperature probe was only attached to the oven instead of the reactor vessel. This made it unable to monitor the real-time temperature of the reacting matrix, which means it may not be guaranteed to maintain subcritical state all the time. As a result, "*pseudo*" was used here to describe the subcritical waster extraction. For batch system, the temperature probe was attached to the reactor vessel so there was no such issue.

Prior to either microwave or SWE extraction, extractives from mango peel will be removed using either boiling (reflux) ethanol or heptane. The former is expected to remove polar compounds such as phenolics and sugars, including residual water. The latter is expected to remove oils, lipids and fats.
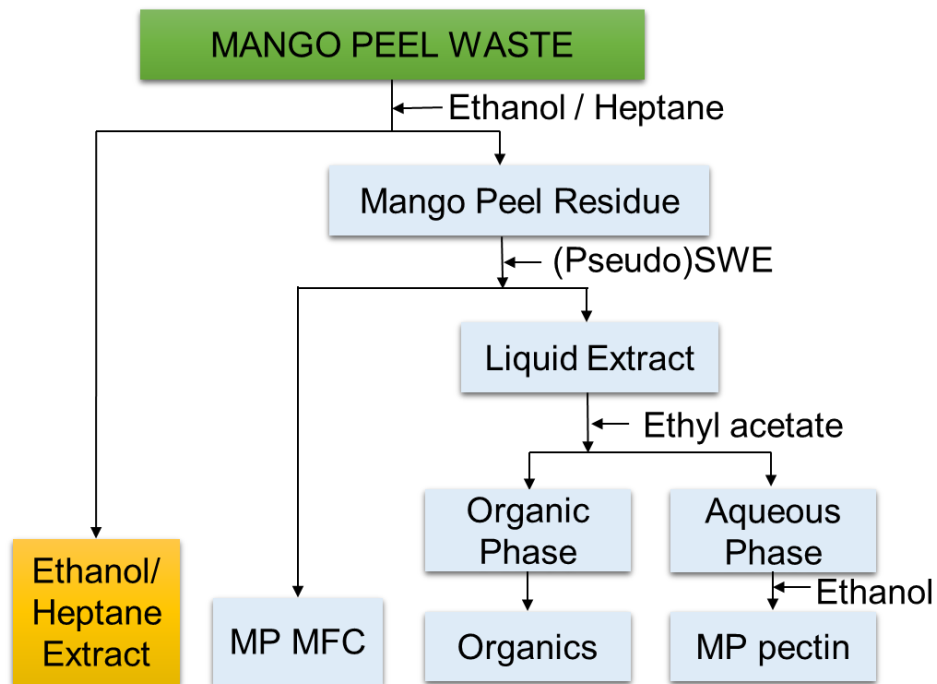
Figure 1.19 Valorisation protocol for mango peel wastes (original in color)

1.4.2.2 Pea Vine Waste

Peas (*Pisum sativum*) are the second most important legume food worldwide.[111] In 2017, the global pea production exceeded 20.7 Million tonnes. Typically, the pea growing season is approximately 8−10 weeks and harvesting removes peas (seeds) leaving behind other parts of the plant pods, stalks, vines, and leaves (also known as haulm) as unavoidable waste which is re-ploughed or left to rot on the land (Figure 1.20).[112] These pea vine wastes account for approximately 45% of total crop weight.[113] The main composition of pea vine wastes is shown in Table 1.6.[114]

Figure 1.20 Pea vine waste (also known as haulm) used in this thesis (original in color)

Table 1.6   Chemical and mineral composition of pea vine waste (dehydrated)

Component	Content (% of dry matter)	Minerals	Content (g/kg of dry matter)
Crude protein	18	Calcium	12
Holocellulose and lignin	43	Phosphorous	12
Ether extract	2		
Ash	15		
Starch (polarimetry)	22		

Thus, there is significant volume of unavoidable waste biomass that is currently under-exploited for its chemical and economic potential let alone enhancing environmental credentials. Pea pods have been explored by many researchers. For example, A. Gomez *et al.* reported the physical fractionation from postharvest pea vines to yield chloroplast- rich compounds, which could be a promising source of lipid-soluble micronutrients.[115] P. Nimbalkar *et al.* studied pea pod waste as a carbon source for biofuels. The high content of cellulose (32 %) and hemicellulose (21 %) on dry basis makes it a good candidate for biobutanol production.[116] Verma *et al.* have used pea peel waste as a cost-effective carbon source for bacterial cultivation (*Trichoderma reesei*)

to produce cellulase, an enzyme that is widely used in food processing, detergent market and textile industry.[111] M. Aparicio *et al.* extracted many functional compounds from waste pea pod (Figure 1.21), including soluble sugars (sucrose, glucose and fructose), fatty acid (oleic acid), and minerals (potassium, calcium and iron), suggesting the added value of waste pea pod and its potential as a source of dietary fiber.[117] Anwar *et al.* utilized the carboxylic and phenolic groups in waste pea pods for the adsorption of bioaccumulative heavy metal (chromium) from aqueous solution.[118] Similarly, Khan *et al.* studied on the waste pea shells as an environmental benign absorbent for removal of malachite green, which is a toxic cationic triphenylmethane dye with high environmental persistence, from aqueous solutions.[119]
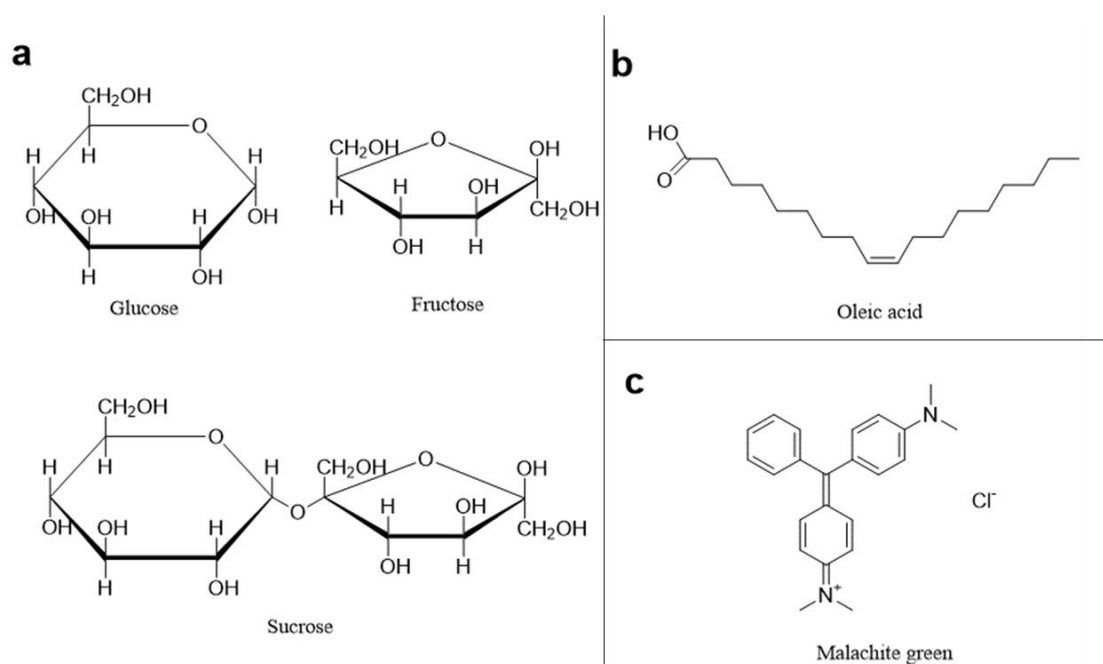
Figure 1.21 Compounds mentioned in pea vine waste literature a) sugars (found in pea pod); b) fatty acid (found in pea pod); c) malachite green(toxic dye from aqueous solutions which could be removed by pea shell waste)

Herein, this study aims to report a valorisation route for real, on-farm, pea vine wastes generated in the UK in order to establish the preliminary basis for a potential pea vine waste biorefinery. The valorisation protocol is summarized in Figure 1.22, which adopts a cascade process critically evaluating (pseudo)subcritical water as a benign solvent extraction technique to isolate biopolymers while the resultant residues are thereafter subjected to microwave pyrolysis for their small molecule potential (bio-oil) and calorific value (biochar).
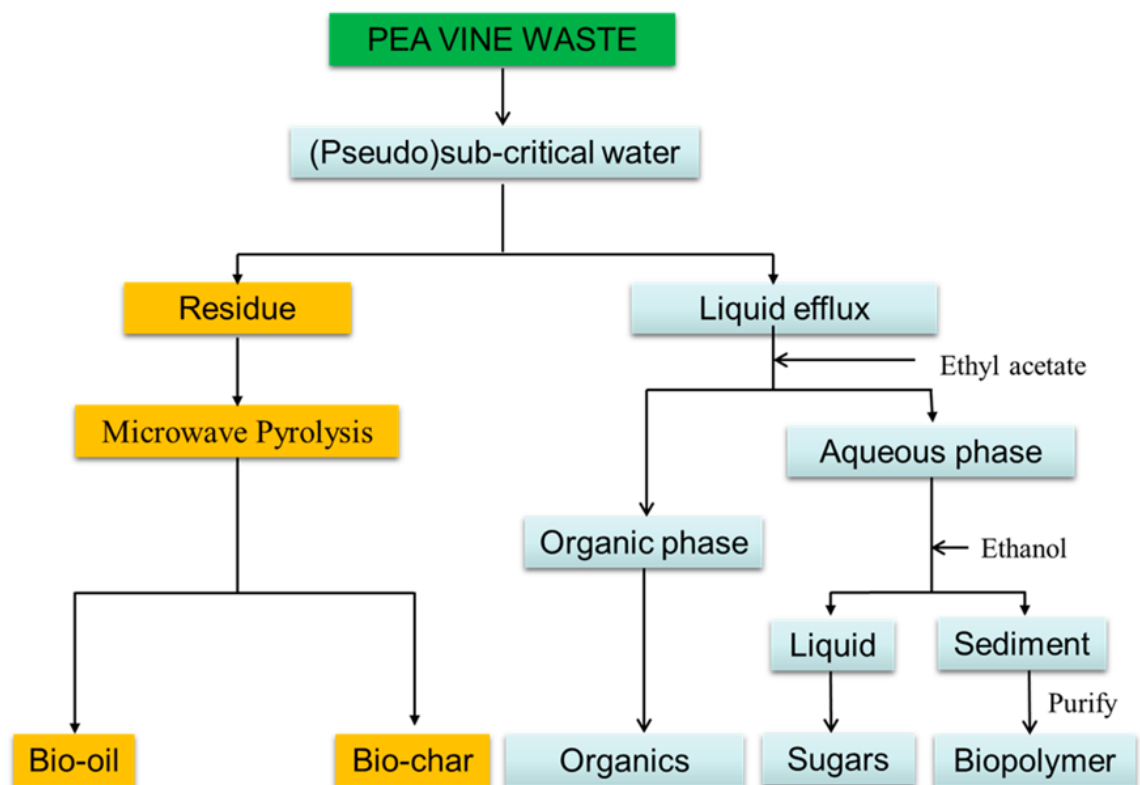
Figure 1.22 Valorisation protocol for pea vine wastes (original in color)

Subcritical water extraction (flow system) will be used for the extraction of compounds from pea vine waste. Various parameters such as temperature, time and flow rate will be tested to optimise the extraction condition. The extracts will be analysed for potential pectin, protein and starch contents and the post extract residue will be submitted to microwave pyrolysis for bio-oil and bio-char study.

1.4.2.3 Peach Peel Waste

Peach (*Prunus persica*, Figure 1.23) is a juicy fruit with over 24 million tonnes of production in 2017. China is the largest production country, which shares almost 60 % of the world total amount, followed by Spain, Italy and Greece (Figure 1.24).[120]
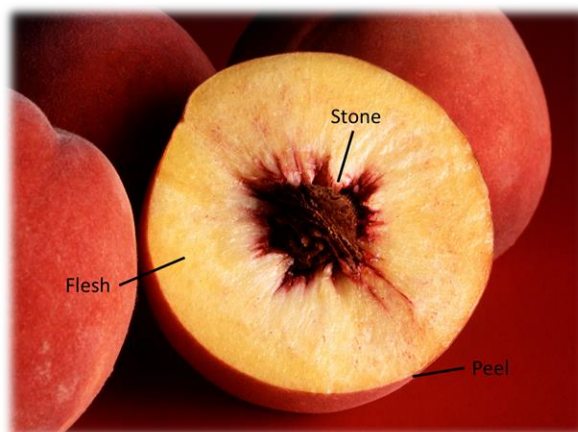
Figure 1.23 Cross section of Autumn Red peaches used in this thesis (original in color)
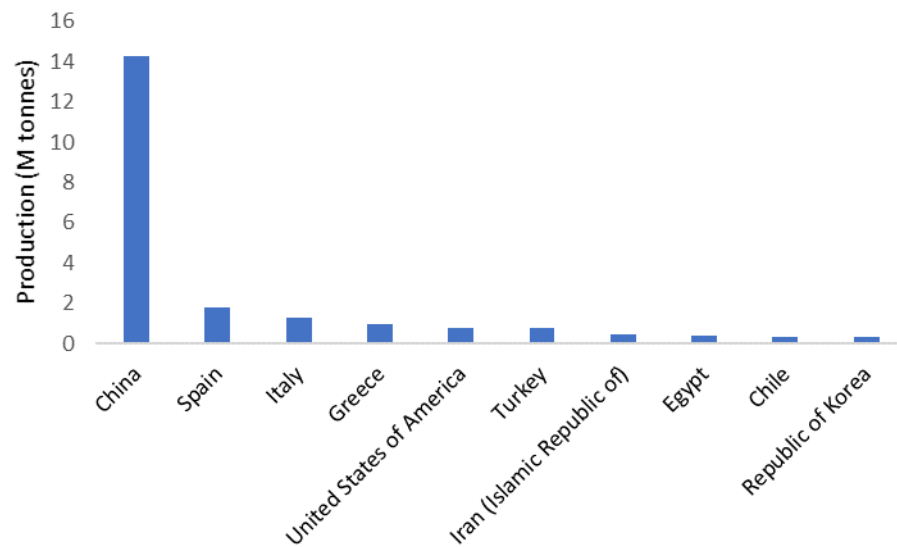
Figure 1.24 Top ten global peach producers in 2017 (original in color)

Although sometimes peach was consumed with skin, there are still large amounts of by-products from food industry which can be considered as waste, The peel of peaches is very soft and "clings" to the flesh especially when it is relatively raw. Therefore, in industry, peaches are usually peeled with dry/wet caustic peeling, where sodium hydroxide is applied to soften the peel (Figure 1.25).[121] Although it consumes less water compared with conventional steam peeling, alkaline or salty solid waste is inevitably produced, which leads to severe environmental issues and expensive treatment cost.

(a)   (b)
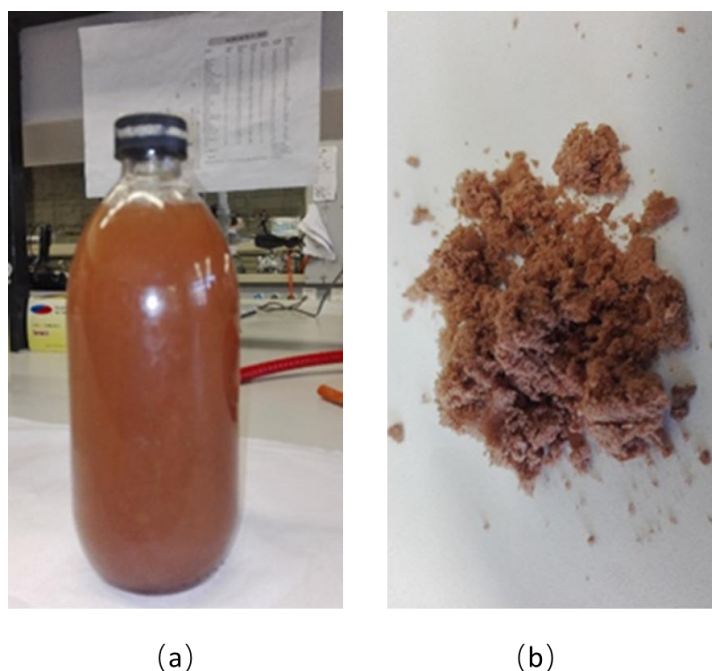
Figure 1.25 Industrial peach peel waste: a). waste stream; b). dried centrifuged pellets from waste steam (original in color)

The recent studies on peach peel mainly focus on its phenolic composition and antioxidant properties. [122,123,124] An exemplar proximate composition of peach peel is given in Table 1.7. The concentration of phenolics compounds, organic acids, flavonoids, hydroxycinnamates and flavonols *etc.* have been reported. Besides, some key coloured compounds (anthocyanins, carotenoids *etc.*) from peach peel have also been studied and Mg-protoporphyrin IX chelatase and pheophorbide a oxygenase (PAO)

Table 1.7 An exemplar proximate composition of peach peel[125]

Component	Content
Dry matter (%)	31.6 ± 0.6
Total phenolic compound (mg GAE/ 100 g dry weight) [a]	1288.4 ± 25.9
Total flavonoid content (mg CE/100 g dery content) [b]	687.5 ± 13.3
Minerals	

K	1330.1 ± 26.4
Ca	81.70 ± 1.57
Mg	100.9 ± 0.2
Mn	0.74 ± 0.1
Fe	6.53 ± 2.7
Zn	0.51 ± 0.05

are reported the key functional proteins associated to these coloured compounds.[126] Apart from its nutrition, peach peel was also reported to be used on synthesis of titanium dioxide (TiO_2) nanoparticles.[127] The size of the nanoparticles was 200 nm, and the size- and dose-dependent antibacterial and antioxidant activities were reported.

In this study, the post caustic peach peeling residues will be explored and compared with manually peeled peach peel as a potential course of pectinaceous-matters. Meanwhile, a simulation of this lye peeling process will be carried out and the resultant peel residue will be studied to explore potential pectic substances and cellulosic content and their properties (Figure 1.25).
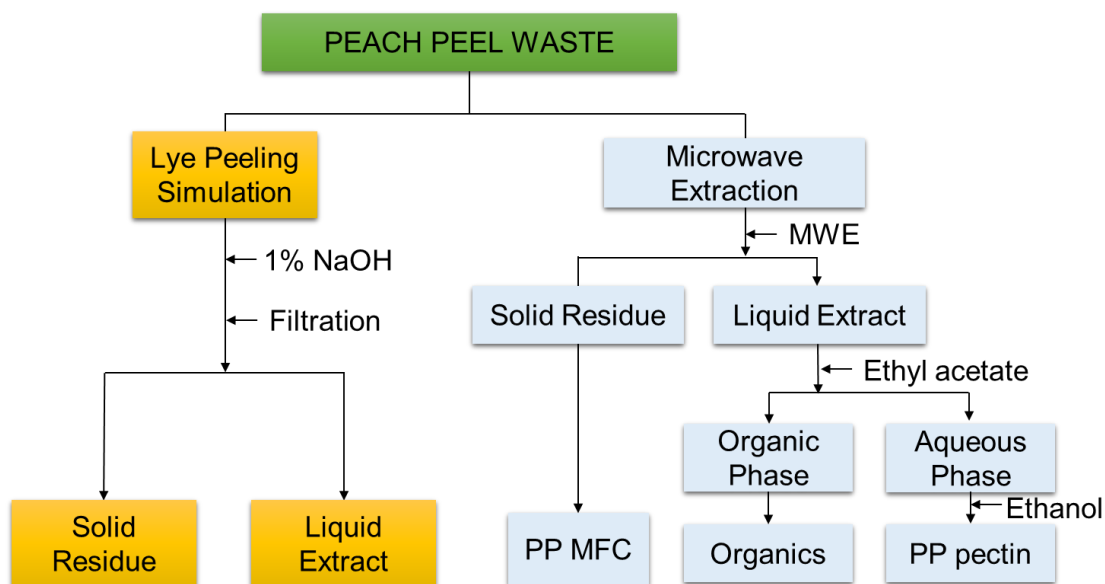
Figure 1.25 Valorisation protocol for peach peel wastes (original in color)

1.4.3 Green Chemistry Contextualisation

The aims of this research highly fit the context of green chemistry, especially the third (less hazardous chemical syntheses), fifth (safer solvents and auxiliaries), sixth (design for energy efficiency) and seventh (use of renewable feedstocks) principles of green chemistry mentioned in chapter 1.2. Firstly, for both microwave and subcritical water extraction, water is used as the sole solvent instead of conventional acids, which significantly reduces the potential hazards and avoids acidic waste stream. Also, for work-up procedures, ethanol was the only chemical used. Thus, "Safer solvent" and "Less hazardous chemical syntheses" were employed throughout the whole experimental process. Secondly, the microwave technique is mainly relevant to "Design for energy efficiency" due to its high heating efficiency, which significantly

reduces the reaction time as well as the energy consumption compared with conventional heating techniques. Finally, all the FSCW used as raw materials in this study were renewable biomass, which conforms to "Use of renewable feedstocks".

Chapter 2 Experimental

2.1 Biomass and Chemicals

Three different mango varieties (*Keitt, Sindhri and Kesar*) were bought from local supermarkets (July 2016). The mangoes were peeled using a stainless-steel knife, and the excess of flesh was removed with the blunt edge of the knife. After that the peel was air dried for about two weeks until constant weight.

Fresh peaches (*Spring Princess* and *Ruby Crest* varieties) were purchased from a local supermarket (December 2017). They were manually peeled using a peeler, and the excess of flesh was removed using a sharp knife and the resultant peel was left air dried until constant weight.

Dried Industrial peel residues were obtained from Langeberg & Ashton, South Africa.

Fresh pea vine waste was supplied by Yorkshire Pea Growers, William Bradley Holdings, York, UK. They were collected at the time of harvest (July 2015) and then dried at 105 °C for 24−48 h and coarsely ground/chopped prior to extraction.

All chemicals and reagents were purchased from standard suppliers (VWR, Fischer Scientific and Sigma-Aldrich).

2.2 Extraction and Work-up

2.2.1 Ethanol/ Heptane Extraction

The air-dried raw materials were chopped into small pieces using a pair of scissors. The chopped feedstock (40 g) in either ethanol or heptane (400 mL) was heated under reflux

for 2 h, slightly cooled and filtered (gravity) whilst still warm. The solid residue remaining on the filtered was dried in vacuum oven until constant weight whilst the filtrate was evaporated to dryness *in vacuo*.

2.2.2 Pectin Isolation: Conventional Acid Extraction (CAE)

The conventional acid extraction (CAE) was carried out as a comparison. Dried raw materials of different biomass were heated at 80 °C in either 0.1 M-aqueous hydrochloric acid or 0.15 M-aqueous citric acid (with a s:l ratio of 1:40) for 2 h. Then the mixture was filtered through a filter paper while it was still hot. The pectin yield was calculated by equation 1:

$$pectin\ yield = \frac{deried\ mass\ extrats\ (g)}{dried\ raw\ materials\ (g)} \times 100\ \%$$

(1)

2.2.3 Microwave Extraction (MWE)

Two different type of microwave were used for the extraction: CEM Discover with a 35 mL of closed vessel and CEM Mars with six 100 mL closed vessel. For both types, dried raw materials were combined with deionized water (s:w ratio = 1:40) and a microwave stirrer bar in the vessel. They were heated to the designed temperatures and held for 15 min. After that they were cooled down until below 60 °C and filtered through a filter paper. The filtrate was treated with twice the volume of ethanol and stirred for 20 min at room temperature, and the ensuing precipitate was isolated by

centrifugation (capacity of 4 large holder, with 6 × 50 mL centrifuge tube each, condition of 3500 rpm, 16 min, acceleration of 9 and deceleration of 6 centrifuge force). The isolated precipitate was first washed with cold ethanol and then hot ethanol; thereafter, it was filtered and dried in a warm air current (40 °C) until constant weight.

2.2.4 Pectin isolation: Acid-free (*pseudo*) Subcritical Water Extraction (SWE)

Acid-free subcritical water extraction (SWE) was carried out by two different systems: flow system and batch systems. For flow system (Figure 2.1), dried raw materials (6-10 g) were loaded into a 50 mL pressurised stainless-steel vessel and heated at designed temperature and flow rate for 15 min. No separation step was needed for flow system. For batch system, the dried raw materials (5 g) were loaded into a 300 mL pressurised stainless-steel vessel with 200 mL deionized water. The mixture was heated at designed temperatures for 15 min and then cooled down until below 60 °C and filtered through a filter paper. The filtrate was treated with twice the volume of ethanol and stirred for 20 min at room temperature, and the ensuing precipitate was isolated by centrifugation (3500 rpm, 16 min, acceleration of 9 and deceleration of 6 centrifuge force). The isolated precipitate was first washed with cold ethanol and then hot ethanol; thereafter, it was filtered and dried in a warm air current (40 °C) until constant weight.
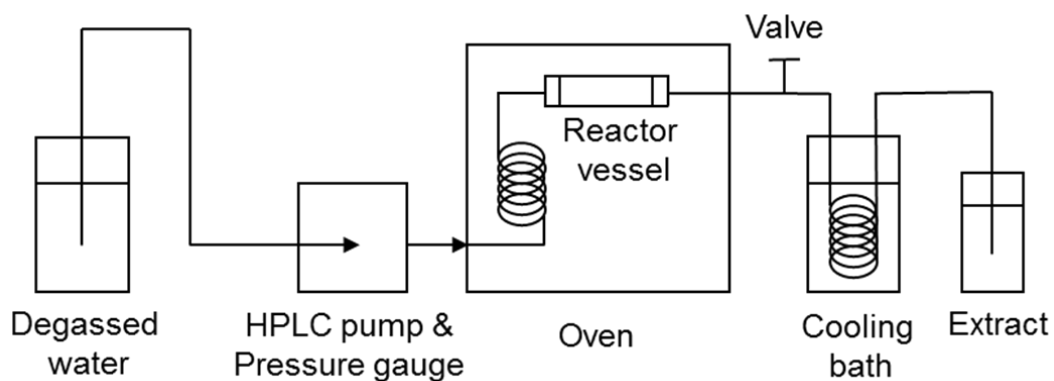
Figure 2.1 Bespoke experimental rig for subcritical water extraction (flow system)

2.2.5 Lye Peeling Simulation (peach peel)

The peaches bought from local supermarket (*Spring Princess* variety) were immersed

hot aqueous NaOH solution (90 °C, 1 wt. %, 250 ml) for 10 – 60 min. Thereafter, the

mixture was filtered (gravity) and the filtrate was processed with the same procedures

as described in 2.2.3.

2.3 Characterisation

2.3.1 ATR-IR Analysis

ATR-IR was performed using a Bruker VERTEX 70 infrared spectrometer including

an ATR probe with a Golden gate attachment. Prior to recording spectra, background

scans were performed for carbon dioxide correction. A sample amount of sample was

placed on the sapphire window and the anvil lightly closed and scanned four times from

4000 and 600 cm^{-1}.

2.3.2 Thermogravimetric Analysis (TGA)

TGA was performed on a PL Thermal Science STA 625. Various samples (9.0−11.0 mg) were weighed accurately into an aluminium pan and analysed against an empty aluminium reference pan under a flow of nitrogen gas, from 20 to 625 °C at a heating rate of 10 °C min^{-1}. Data was acquired using origin for processing.

2.3.3 ^{13}C Solid NMR Cross-polarization Magic Angle Spinning (CP-MAS)

CP-MAS was performed on a 400 MHz Bruker Avance III HD spectrometer equipped with a Bruker 4 mm H(F)/X/Y triple-resonance probe and 9.4T Ascend superconducting magnet. The CP experiments employed a 1 ms linearly ramped contact pulse, spinning rates of 12000 ± 2 Hz, optimized recycle delays of 3 s, spinal- 64 heteronuclear decoupling (at νrf =85 kHz) and are a sum of 600 − 800 co-added transients. Chemical shifts were referenced using adamantane (29.5 ppm) as an external secondary reference.

2.3.4 GC-MS Analysis

GC-MS analyses were performed on a PerkinElmer Clarus 500 Gas chromatography and Clarus 560S mass spectrometer equipped with a DB5-HT column (30 m, 0.25 m, 0.25 μm) and autosampler. The oven was programmed to maintain the temperature at 60 °C for 1 min followed by heating at 8 °C min^{-1} up to 630 °C and held for 10 min. The identified compounds were indicated by comparison with the NIST library of

compounds.

2.3.5 HPLC Analysis

HPLC analyses were performed to analyse the sugar content in the extracts using a HP1100 instrument, equipped with a 100-sample autosampler, quad-pump and both diode array (DAD) and evaporating light scattering (ELSD) detectors. Standard samples of levoglucosan, rhamnose, xylose, fructose, glucose, and sucrose were used to prepare the calibration curve (see Appendix I).

2.3.6 Elemental Analysis (CHN)

EA was performed by Dr Graeme McAllistair, Department of Chemistry, University of York, on an Exeter Analytical CE-440 analyzer in conjunction with a Sartorius SE2 analytical balance. The analysis was performed in triplicate. The mean values are reported.

2.3.7 Calorific Value (CV)

Calorific values were determined using a Parr 6200 Bomb Calorimeter with a standard 1108 Oxygen Bomb. A bucket with 2 L of water was placed in the calorimeter. Approximately 0.70 g of sample was loaded into the bomb. The ignition wires were attached to the bomb head and then the bomb was lowered into the bucket to start the test.

The analysis was performed in duplicate.

2.3.8 Degree of Esterification (DE)

The DE was determined by both titrimetry and NMR method. The titrimetry was carried out according to Mizote *et al.*[128]. Pectin (2 g) was added to 200 mL mixture of water – concentrated hydrochloric acid – 2-propanol (90 + 10 + 100) with stirring for 15 min. It was then filtered and washed with aqueous 2-propanol (65%) until the filtrate was free of chloride. The pectin was then dried in an oven until constant weight. The dried pectin (0.5 g) was loaded into a conical flask, moistened with small amount of aqueous 2- propanol and then dissolved in 100 mL distilled water. The solution was titrated with 0.1 M NaOH solution to neutral and the volume was recorded as V1. Then 30.0 mL of 0.1 M NaOH was added into the flask with stirring for 30 min. After that, an equivalent amount of 0.1 M HCl solution was added and the mixture was titrated again with 0.1 M NaOH. The volume of NaOH consumed was recorded as V2. The degree of esterification is calculated according to equation 2:

$$DE = \frac{V_2}{V_1 + V_2} \times 100\%$$

(2)

The analysis was performed in duplicate.

For NMR method, the DE was calculated from 13C solid NMR spectra, according to equation 3[110]:

$$DE = \frac{I(\text{esterified carboxyl group})}{I(\text{esterified carboxyl group}) + I(non-\text{esterified carboxyl group})}$$

(3)

2.3.9 Scanning Electron Microscopy (SEM)

SEM images were generated using a JEOL JSM-7600F SEM instrument. A diluted suspension of the sample (*ca.* 0.2% w/v) was either, directly air-dried on the SEM grid or freeze-dried. When freeze-dried, a small amount of the gel or suspension was placed on a copper shim and excess of liquid was removed with filter paper. The sample was then frozen in liquid nitrogen slush (-210 °C so it does not bubble, achieving better cooling rate and better preserving the original structure of the material).[129] The shim plus gel was transferred to the cooled Peltier stage in a Polaron coating unit and the air was pumped out. Temperature was kept at ca. -55 °C and the vacuum was maintained around 10^{-4} mBar. After a few hours the sample was warmed to room temperature and the gel was knocked off the shim. The remaining "scraps" of gel were imaged after mounting the shim plus scraps on a stub and coating with gold/palladium (*ca.* 4 nm thick). Analysis was performed by Meg Stark, Dept. of Biology, University of York.

2.3.10 Transmission Electron Microscopy (TEM)

TEM images of structured celluloses were acquired using a TEM Tecnai 12 BioTWIN (manufactured by FEI) coupled to a SIS Megaview 3 camera at an acceleration voltage of 120 kV. Prior to the analysis, diluted samples (0.2 wt.% aqueous) were sonicated for 30 minutes using an ice-cold ultrasound bath (output of 1200 W). Drops of the sample (about 8 μL) were left on the grid for five minutes then negatively stained with 1% uranyl acetate and finally glow discharged. Copper grids with a formvar/carbon support

film were used.

2.3.11 Pectin Gelation

The pectin samples were gelled with the addition of buffer and sucrose. The ratio is pectin: buffer: sucrose = 1: 39: 60 (wt. %). The pectin sample was added into a pH 3 buffer solution with stirring until the solution was homogeneous, where after, half of the sucrose was added and the mixture was heated to its boiling point. After cooling down, another half of sucrose was added and the solution was heated until reaching its boiling point again. Then it was cooled down to room temperature and stored in the fridge overnight.

2.3.12 Cellulose Hydrogel Formation

Cellulose hydrogels were produced at different concentrations (1–3%, w/v) by mixing an adequate amount of MFC (50–150 mg) in deionised water (5 mL). The dispersion was then homogenised using a high-shear homogenisation (Ystral X10/20 E3 homogeniser, 2–3 min. at ~20000 rpm) to afford the hydrogel and refrigerated (4 °C). Gel formation was qualitatively assessed by the tube inversion test, where a sample is placed into a small vial and turn it upside down to check for its flowability.

Chapter 3
Results and Discussion

This chapter is divided in three parts reflecting the aims and objectives as defined earlier (see Section 1.4), namely:

i. Part A: Valorisation of Mango Peel Waste;

ii. Part B: Valorisation of Peach Peel Waste, and;

iii. Part C: Valorisation of Pea Vine Waste.

3.1 Part A: Valorisation of Mango Peel Waste

This part reports a characterisation of pectin and microfibrillated cellulose extracted from waste mango peels by using *pseudo-* subcritical water extraction (SWE) and hydrothermal liquefaction (HL). An ethanol or heptane extraction was carried out prior to SWE and then the mango peel pectin was extracted and analysed with various techniques. In HL, an additional study of MFC was also carried out. The performance of its hydrogels was also explored with respect to their gelling ability (qualitative).

3.1.1 Ethanol/ Heptane Extraction (Minor Study)

The extraction yields following treatment on mangoes (*Keitt*, *Sindhri* and *Kesar*) with boiling ethanol (EE) or boiling heptane (HE) are listed in table 3.1.1. For all three varieties, ethanol extraction (EE) yields were much higher than corresponding yields of heptane extraction (HE). *Keitt* mango peel had the highest EE yield (15.4%) among three varieties. Preliminary GC-MS analysis of the extract (Figure 3.1.1) tentatively suggested some compounds (Table 3.1.2) from partial breakdown of cellulose and

hemicellulose (compounds 13 and 4) and some fatty acids and their esters (compounds 5 and 6). Both DDMP and 5-HMF could come from the partial dehydration of a glucose molecule[130], while compound 2 was most likely from furfural reacting with ethanol during the extraction. However, it must be stressed that these are tentative assignments based on NIST database library matches. Full verification would require running appropriate standards, which was not performed because the extraction study was a minor aspect of the research.

Table 3.1.1 Ethanol/ heptane extraction yield of waste mango peel

| | Yield (wt% on dry basis) | | |
Variety	Keitt	Sindhri	Kesar
Ethanol extraction	15.4	6.4	6.0
Heptane extraction	1.4	1.6	1.7
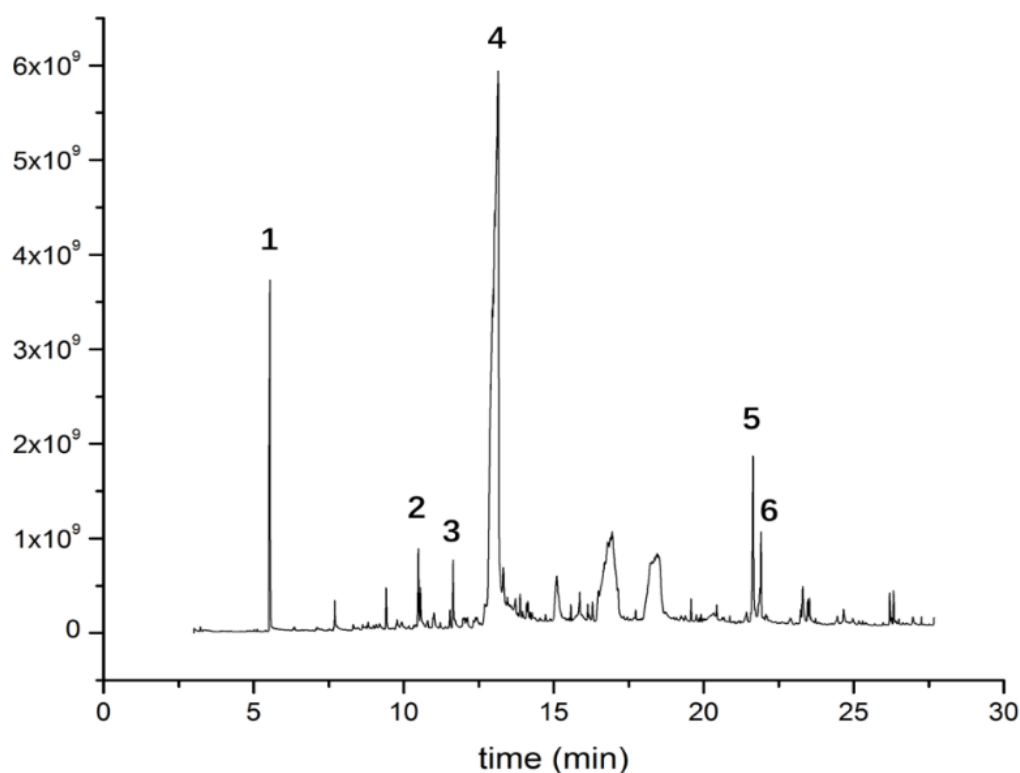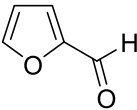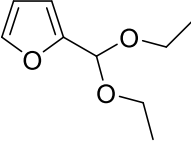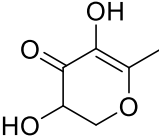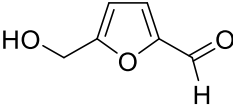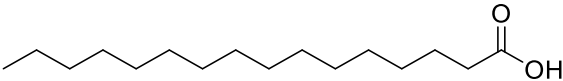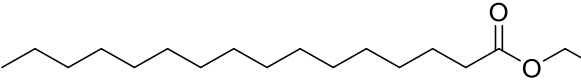
Figure 3.1.1 GC-MS chromatogram of mango peel ethanol extract (*Keitt* variety)

Table 3.1.2 Major components in mango peel ethanol extract (*Keitt* variety)

Peak	Compound	Structure
1	Furfural	
2	2-Furaldehyde diethyl acetal	
3	2,3-Dihydro-3,5-dihydroxy-6-methyl-4H-pyran-4-one (DDMP)	
4	5-Hydroxymethylfurfural	
5	Hexadecanoic acid	
6	Hexadecanoic acid, ethyl ester	

The presence of furfural and 5-HMF is worth noticing as they are supposed to be extracted at harsher condition. For instance, the production of 5-HMF is mainly reported from the dehydration of glucose (Figure 3.1.4) and fructose and normally various catalysts are used to increase the synthesis yield and selectivity (*i.e.* ion exchange resins, minerals and organic acids, zeolites and oxides).[131]

Herein, a control experiment was carried out and 5-HMF was still observed from the spectrum (Figure 3.1.2). This confirms the presence of 5-HMF in ethanol extract. Meanwhile, a ^{1}H NMR analysis of ethanol extract was carried out as well (Figure 3.1.3). The result did not match the spectrum of 5-HMF. The biggest three peaks refer to $CHCl_3$ (7.3 ppm) and ethanol (3.7 and 1.2 ppm) respectively. Apart from those, only some small peaks between 0.8 and 2.4 ppm could be observed, which could be attributed to the the $-CH_2$ and $-CH_3$ groups from fatty acid.[132] The absence of 5-HMF may suggest that compare with ^{1}H NMR, GC-MS is more sensitive to furans as they ionise better.
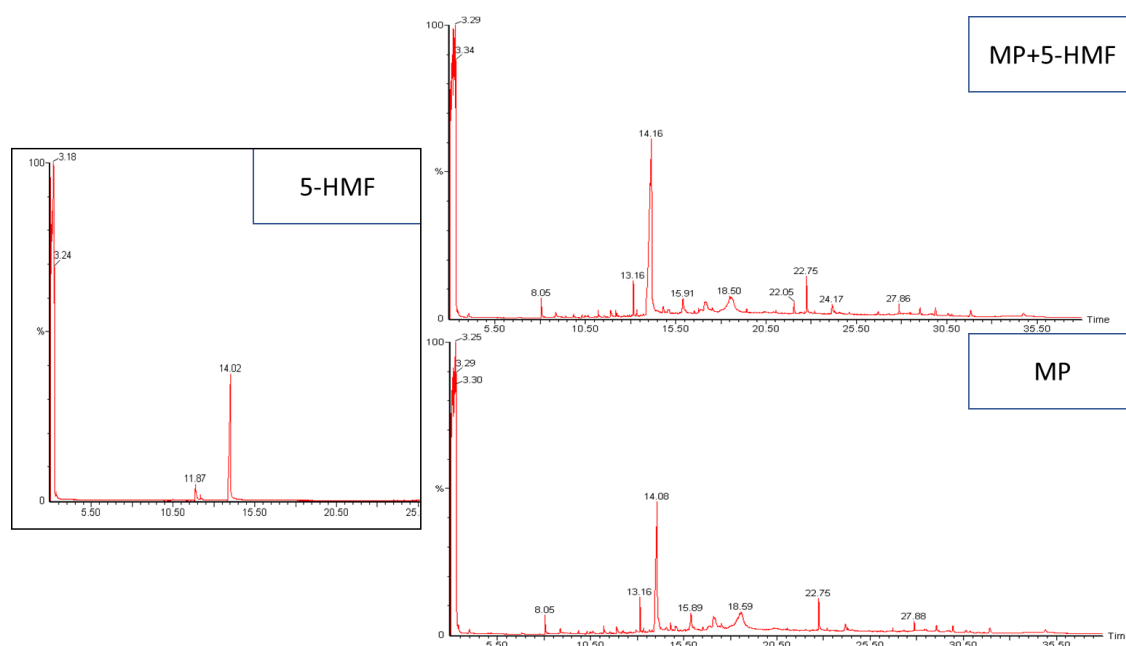
Figure 3.1.2 GC-MS chromatogram of mango peel (MP) ethanol extract with standard 5-HMF (*Keitt* variety) (original in color)

However, only ethanol should not be enough for the decomposition of cellulose so the only explanation could be that the peel (as well as some flesh attached to it) is slightly

acidic and the some compounds described in chapter 1 (such as gallic acid) work as

"catalyst" during the Soxhlet and help form the 5-HMF.
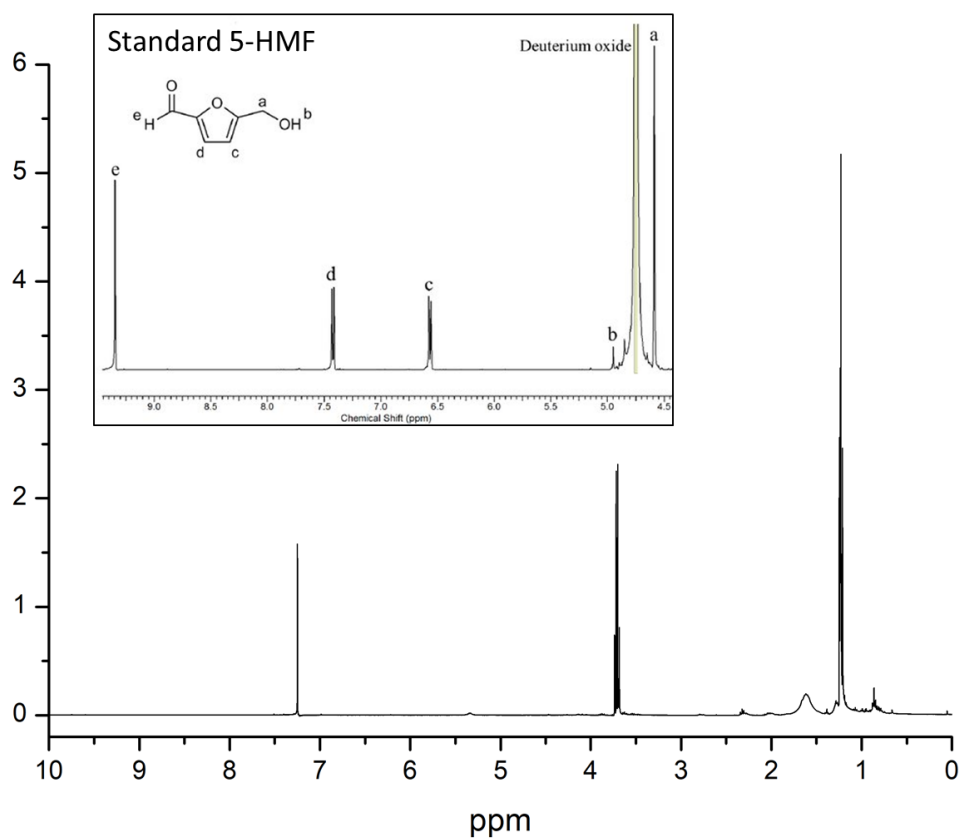
Figure 3.1.3 ^{1}H NMR spectrum of mango peel ethanol extract (*Keitt* variety)[133] (original in color)
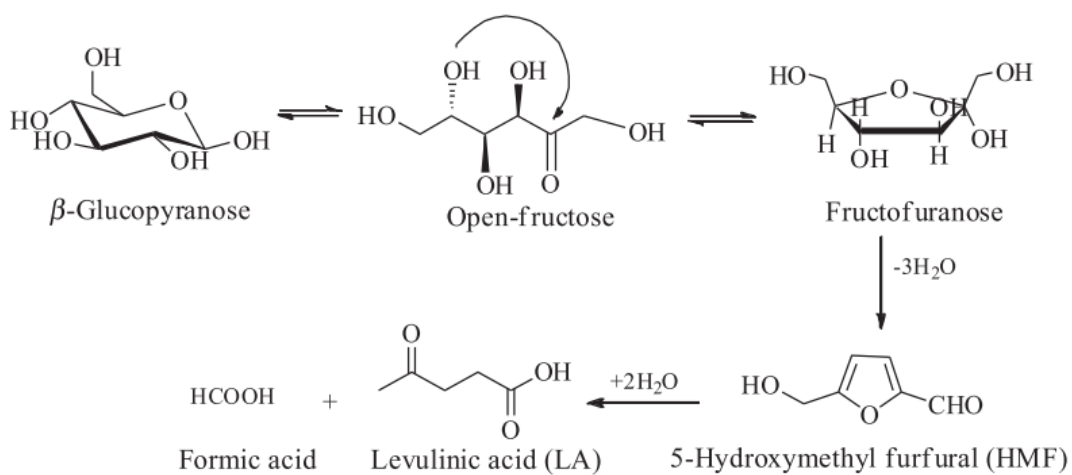
Figure 3.1.4 A typical reaction scheme for HMF production from glucose[134]

3.1.2 Pectin Isolation

Pectin was extracted from three different varieties of mangoes (*Keitt*, *Sindhri* and *Kesar*) by acid-free (pseudo)subcritical water treatment (described in section 2.2.4 earlier). The yield of pectin following acid-free pseudo-SWE with both flow system (all three varieties) are shown in Figure 3.1.5. In flow system, *Kesar* (post EE) and *Keitt* (post HE) afforded the highest yield of pectin, 18.34 % and 18.31 %, respectively. *Sindhri* (post EE) gave the lowest pectin yield (8.11%).   In comparison, conventional acid extraction (*Keitt* variety, HCl, pH 2.5, 80 °C, s-w ratio = 1:40, 2 h) gave a significantly lower pectin yield (4.88 %), which is also much lower than that reported in literature[72,73].
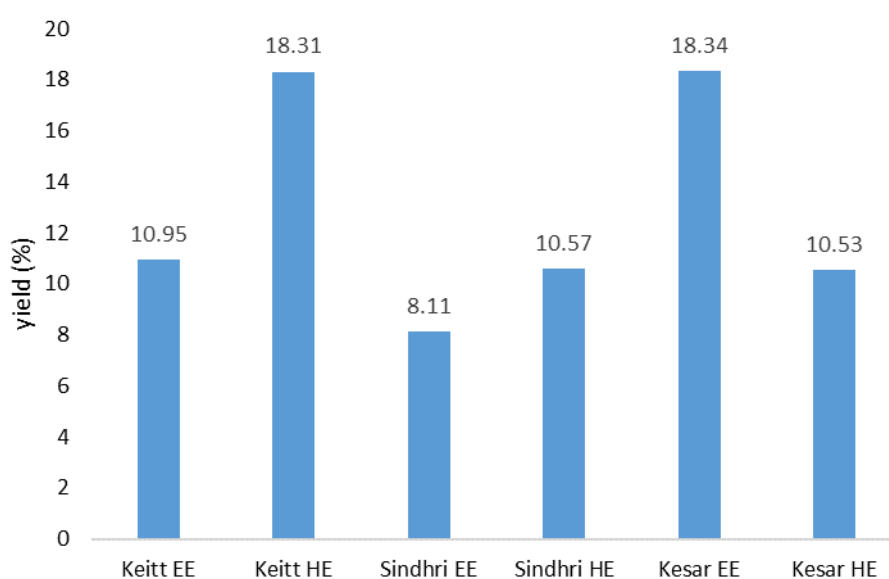
Figure 3.1.5 Mango peel pectin yield (% dry basis) from subcritical water extraction (flow system) (original in color)

Due to feedstock availability, batch-mode (pseudo)SWE of *Sindhri* only was investigated at a range of temperature intervals (75, 100, 125, 150°C). The

corresponding isolated pectin yields are summarised in Figure 3.1.6. Highest pectin yield was achieved at 100 °C (8.68 %), which is slightly higher than that from the flow system. It is noticeable that the yield undergoes significant decrease between 125 and 150 °C, indicating hydrolysis of pectin and/or pectinaceous matter.

Hydrothermal liquefaction was also carried out as a comparison. It is a novel technique mainly used for converting biomass into liquid fuels. It can be considered as wet pyrolysis which normally carried out under 523-647 K of temperature and 4-22 MPa of pressure.[135] In this study, it was attempted at relatively low temperature and thus it could be considered very similar to SWE batch system.

The reaction condition was same as the batch system and the yield was shown in Figure 3.1.7. It can be clearly observed that there was a huge drop between 125 and 150 °C, which confirms the breakdown of pectin under the temperature higher than 125 °C.
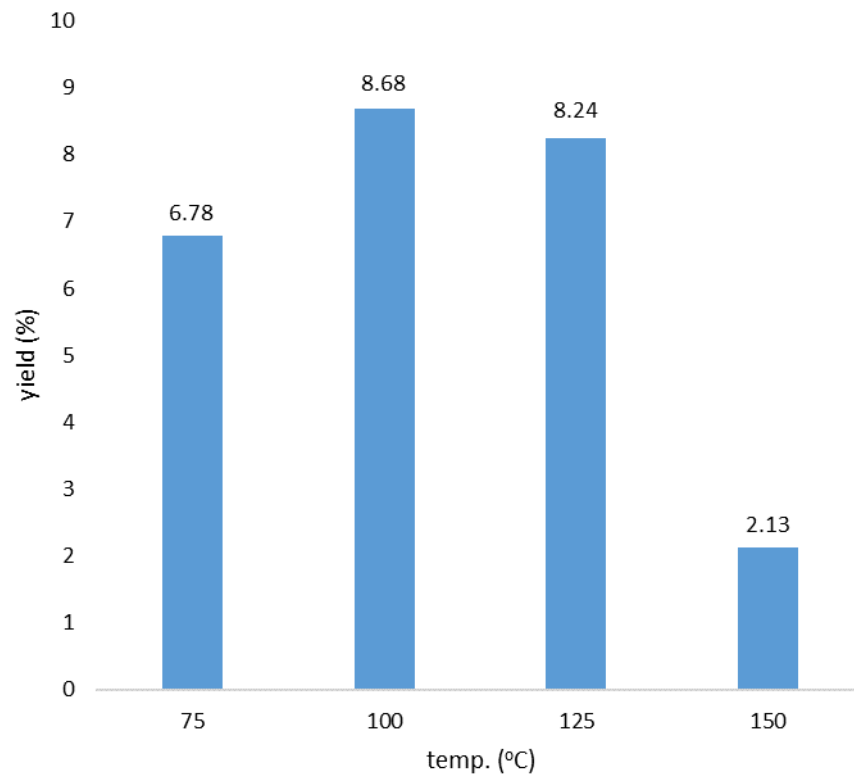
Figure 3.1.6 Mango peel pectin yield (%) from (pseudo)subcritical water extraction batch system (*Sindhri*) (original in color)
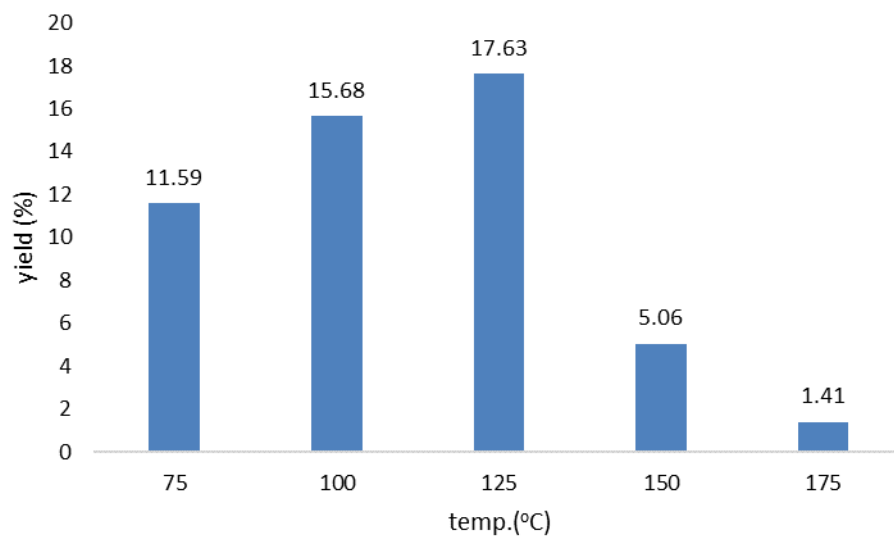
Figure 3.1.7 Mango peel pectin yield (%) from hydrothermal liquefaction extraction (*Keitt*) (original in color)

3.1.3 Pectin Characterisation

3.1.3.1   ATR-IR Analysis

The ATR-IR spectra of mango peel pectin from flow system experiments are shown in Figure 3.1.8. The combination of carbonyl absorption bands at 1730 cm^{-1} (methyl ester) and 1610 cm^{-1} (free carboxylic acid) suggests the presence of pectin, and the ratio of their peak areas indicates the degree of esterification for the pectin. Visually, *Keitt* HE gave the highest degree of esterification while *Sindhri* EE has the lowest. Additionally, the spectra show characteristic absorption peaks associated with the structure of pectin; broad O−H stretch centred at around 3300 cm^{-1} (hydrogen-bonded hydroxyl groups), C−H stretch at approximately 3000 cm^{-1} (-CH- and –CH$_2$-), and intense C−O stretches between 1200 and 1000 cm^{-1} (C-O-C ring and C-O-C ester).
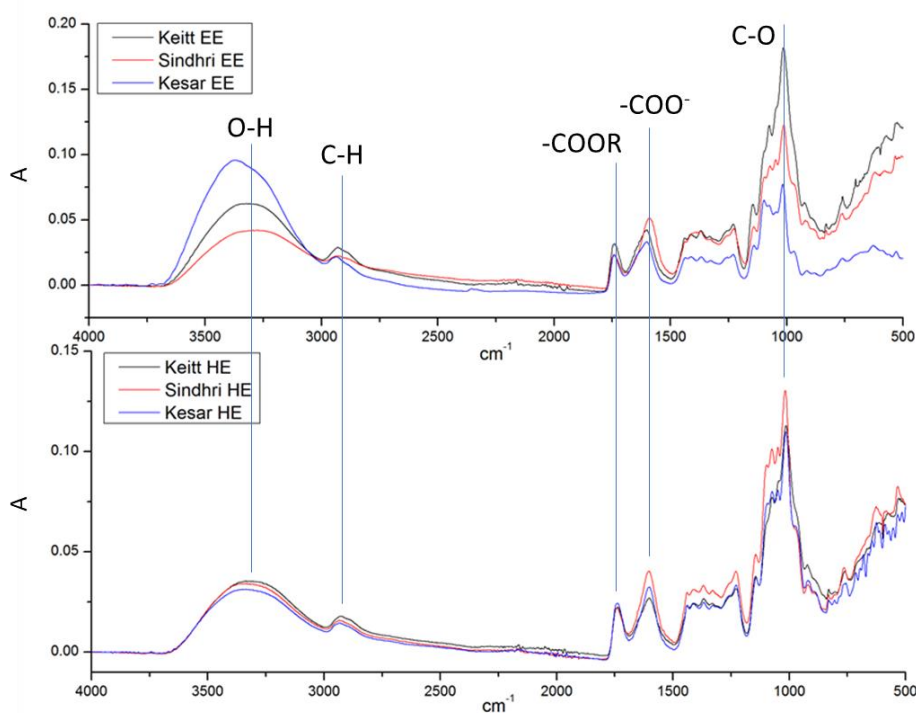
Figure 3.1.8 ATR-IR spectra of mango peel pectin from SWE flow system (175 °C) (original in color)
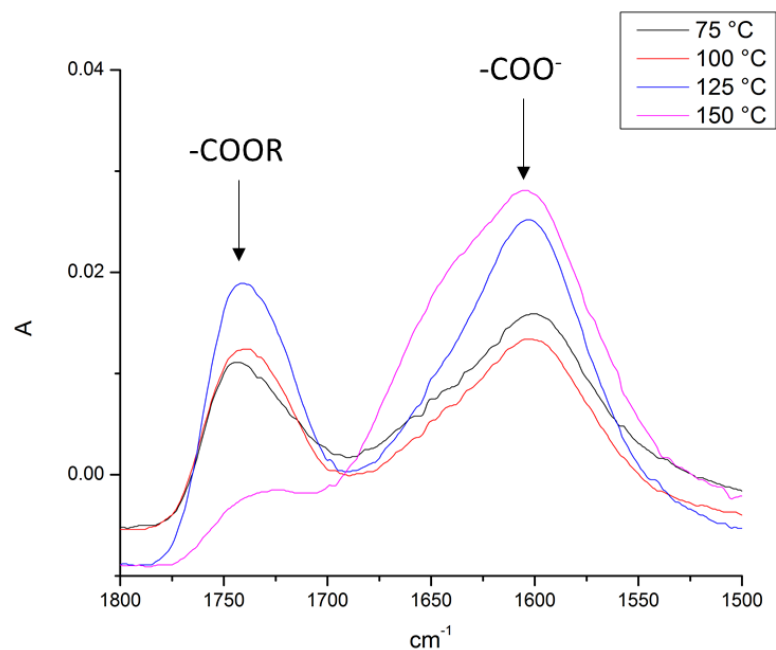
Figure 3.1.9 ATR-IR spectra of mango peel pectin from SWE batch system (original in color)

The ATR-IR spectra of *Sindhri* EE pectin from pseudo SWE batch system are shown in Figure 3.1.9. It can be observed that the intensity of absorption band corresponding to methyl ester group (1730 cm^{-1}) gradually increases as the processing temperature increases from 75 to 125 °C. However, when the temperature reaches 150 °C the intensity of this absorption band dramatically drops indicating pectinaceous matter of very low DE.

The ATR-IR spectra of pectin from hydrothermal liquefaction are shown in Figure 3.1.10. Similarly, the absorption band of methyl ester group (1730 cm^{-1}) increases from 75 to 125 °C and significantly decreases at 150 °C and almost disappears at 175 °C.

Correspondingly, the change in the absorption band of free carboxylic acid group (1600 cm^{-1}) is slightly different from SWE batch system. It gradually increases from 75 to 150 °C but within a very small range, but increases significantly at 175 °C. Meanwhile, it is also noticeable that the ATR-IR spectrum of MP pectin 175 °C has a much stronger absorption band associated at 3300 cm^{-1} (hydrogen-bonded hydroxyl groups). Thus, this sample may still contain water and/or no pectin. In addition, the intensity O-H bond was increased with rising temperature. This was probably because higher extraction temperature would lead to higher acidity of sample, which polarised the O-H bond more and made it absorb more strongly.

3.1.3.2 Thermogravimetric Analysis

The Thermogravimetric Analysis (TGA) and its derivative (dTG) analysis reveals the thermal properties for mango peel pectin samples. The results of flow system are shown in Figure 3.1.11. It can be observed that each sample has three major processes of mass
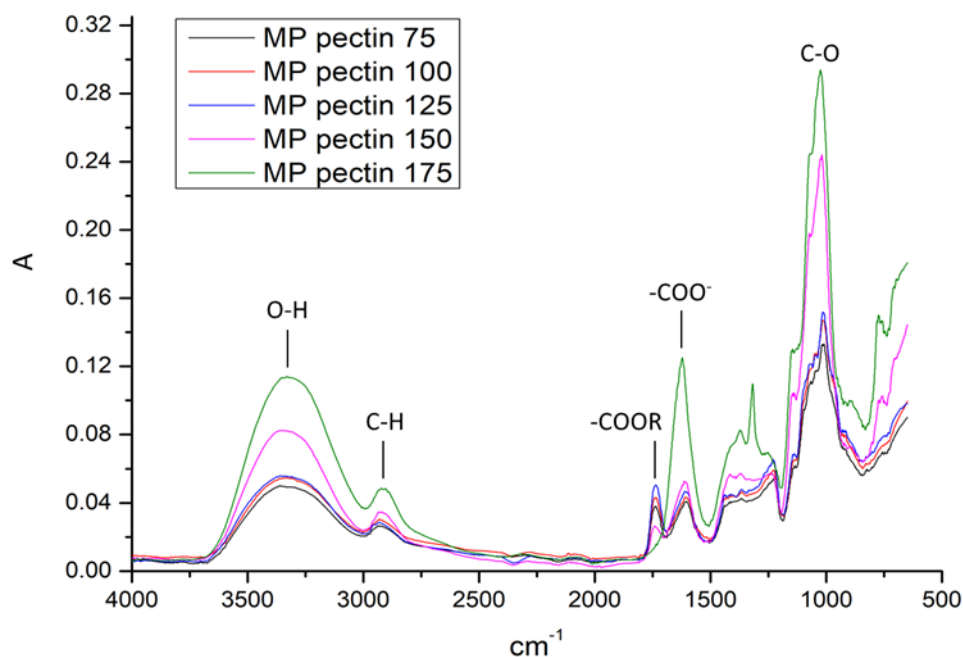
Figure 3.1.10   ATR-IR spectra of mango peel pectin from hydrothermal liquefaction (original in color)

loss. The first ranging from 60 to 120 °C is due to the removal of water followed by the second between 200 and 250 °C is attributed to pectin decomposition. *Kesar* variety has the largest mass loss during this period (32 %), followed by *Sindhri* (26 %) and *Keitt* (20 %). The third main decomposition around 300 °C is probably due to some residual cellulose and/or starch in the samples. A qualitative analysis was carried out to confirm the presence of starch in the sample. A blue-black colouration with respect to iodide solution was observed for certain samples.

The TGA curve of *Sindhri* EE pectin from SWE batch system are shown in Figure 3.1.12. The major mass loss for 100 and 125 °C samples are at around 220 °C which attributes to pectin. They both had a 28 % of mass loss during this period. Meanwhile,

their mass loss around 300 °C, which corresponded to cellulose, were also quite close

(11 % for SWE 100 and 14 % for SWE 125). However, for SWE 150 sample, the

majority of mass loss took place around 305 °C (34 %) and the pectin content (8 %) is

much lower than the other two samples. This suggests that at 150 °C, the pectin in the

extract is even less than it appears in yield.

The TGA curve of pectin from hydrothermal liquefaction are shown in Figure 3.1.13.

Similar to SWE batch system, when it comes to 150 and 175 °C, the mass loss peak of

pectin in dTG not only significantly decreases, but also shifts to around 250 °C.

Meanwhile, the mass of residue higher than 625 °C slightly decreases from 100 to

150 °C but increases again at 175 °C. Also, for 175 °C sample, there is also a small

peak around 490 °C. This indicates that some lignin might be isolated at this

temperature.

The observed cellulose was attempted to be proven by ATR-IR spectra. However,

cellulose and pectin share very similar characteristic peak around 1740 and 1640 cm^{-1},[136] which made it very difficult to confirm the existence of cellulose from ATR-IR

spectra.
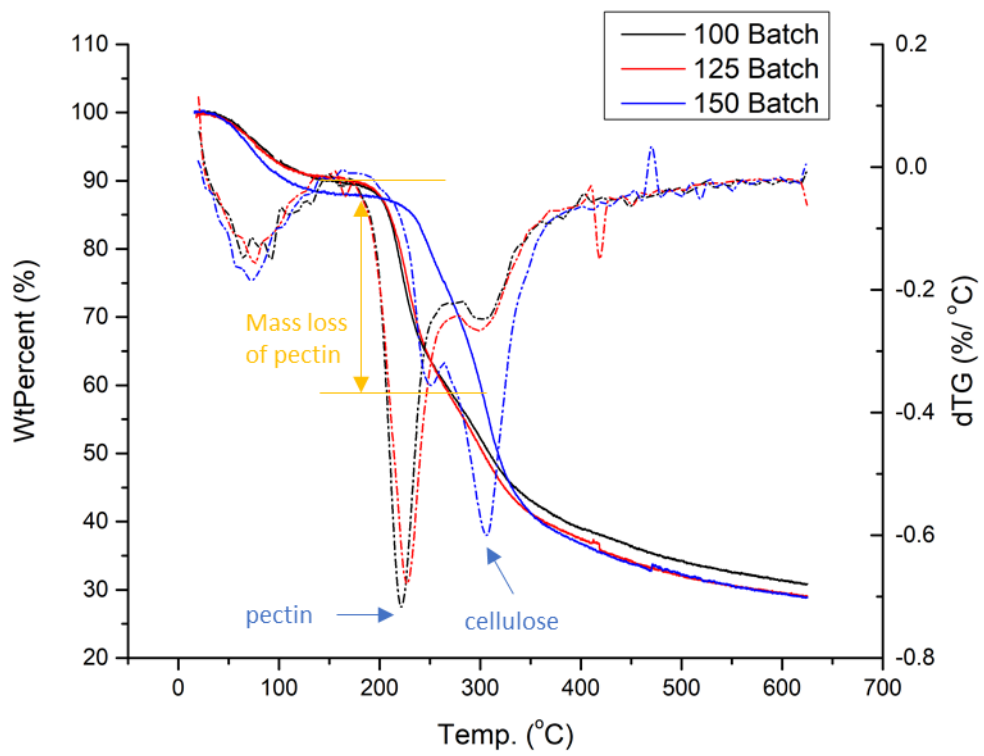
Figure 3.1.12   TGA and DTG traces of mango peel pectin from SWE batch system
(original in color)
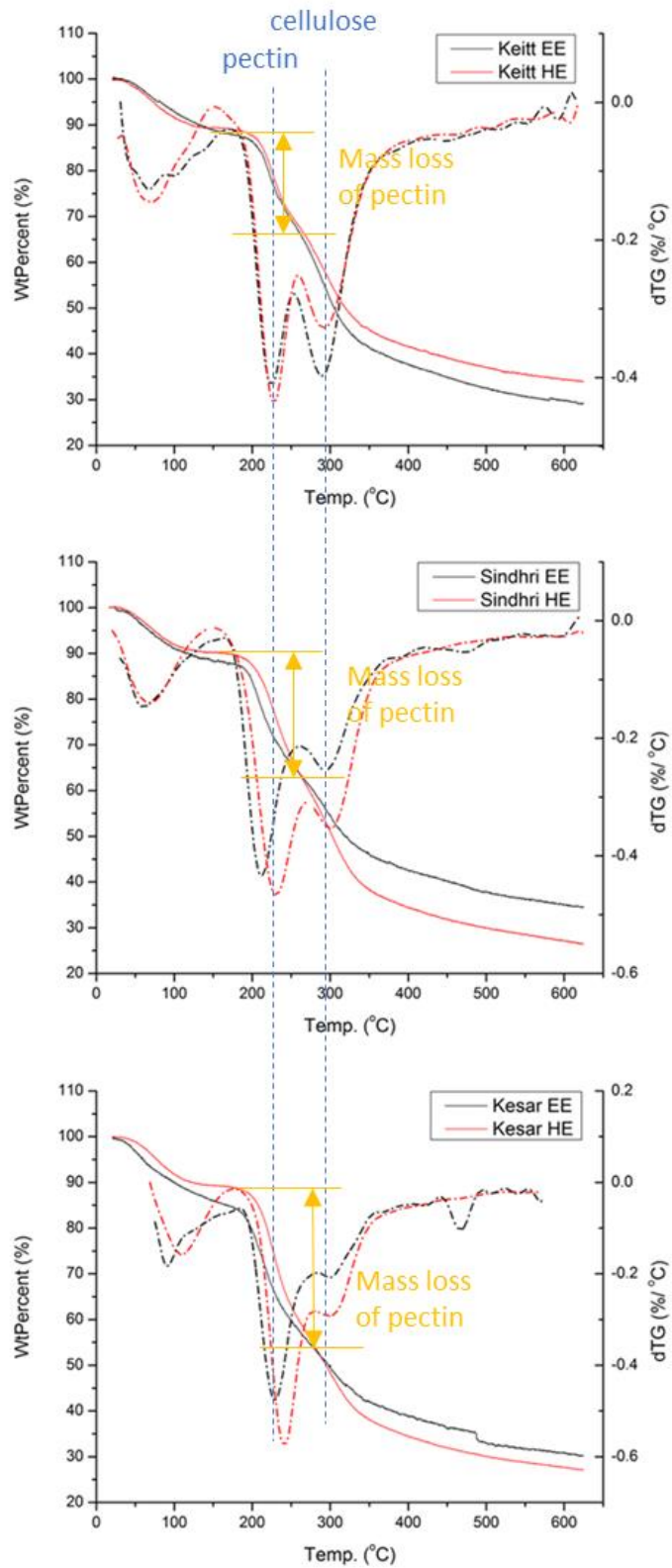
Figure 3.1.11 TGA and DTG traces of mango peel pectin from SWE flow system (original in color)
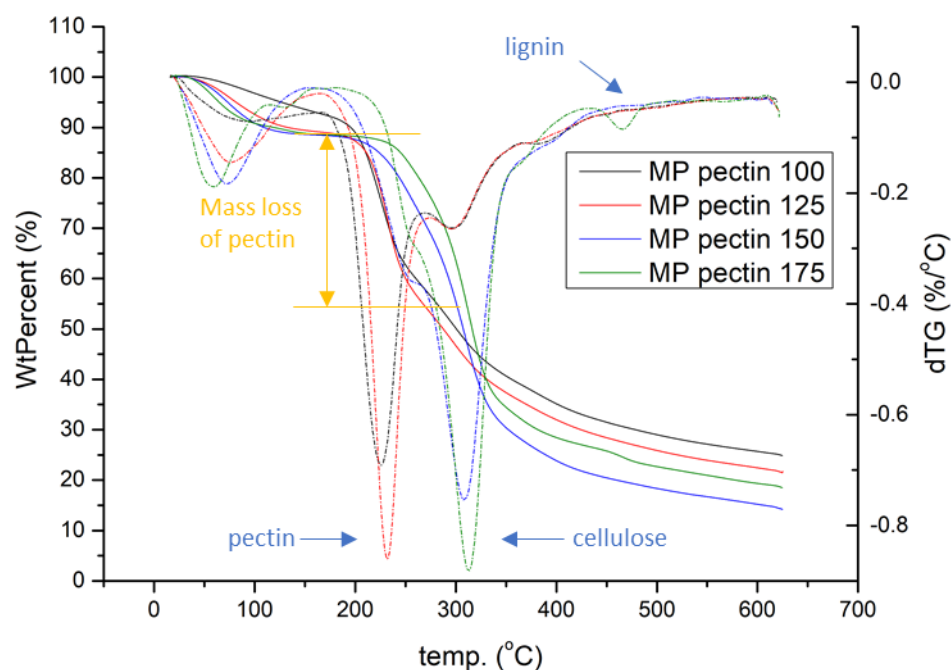
Figure 3.1.13   TGA and DTG traces of mango peel pectin from hydrothermal liquefaction (original in color)
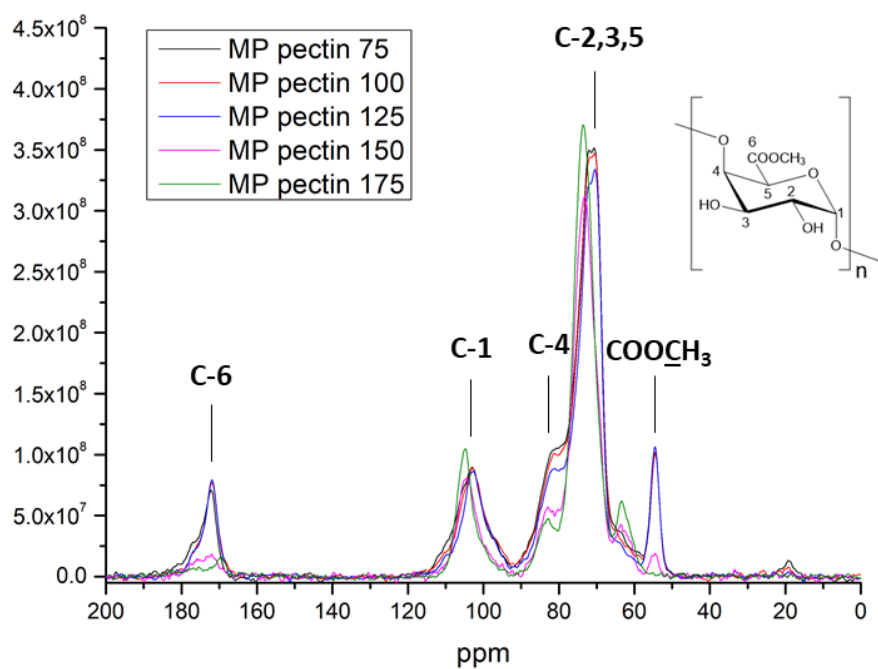
Figure 3.1.14 ^{13}C NMR CP-MAS spectra of mango peel pectin from hydrothermal liquefaction (original in color)

3.1.3.3 ^{13}C Solid NMR Analysis

The solid-state ^{13}C NMR spectra of mango peel pectin from hydrothermal liquefaction
and SWE flow system are shown in Figure 3.1.14 and 3.1.15 respectively. The strong
resonance at 171.08 ppm is attributed to the C-6 carbonyl (ester and carboxylic acid)
carbon of pectin. Similar peak intensity can be observed from 75 to 125 °C, but when
it comes to 150 °C or higher, the resonances almost disappear, indicating the
degradation of pectin at high temperature. The resonances at 102.79 and 81.38 ppm can
be assigned to the anomeric C-1 carbon and C-4 carbon, respectively. Furthermore, the
intense peaks in the region of 60 to 90 ppm are from carbons of pyranoid ring (C-2, 3,
5), while the weak resonance at 53.72 ppm is attributed to the methyl carbons of methyl
ester (COOCH$_3$). It is also worth noticing that there is another resonance at around 63
ppm which is not a characteristic peak for pectin. This resonance could be the C-6 peak
of cellulose,[137] which confirmed the presence of cellulose as suggested in TGA curves.
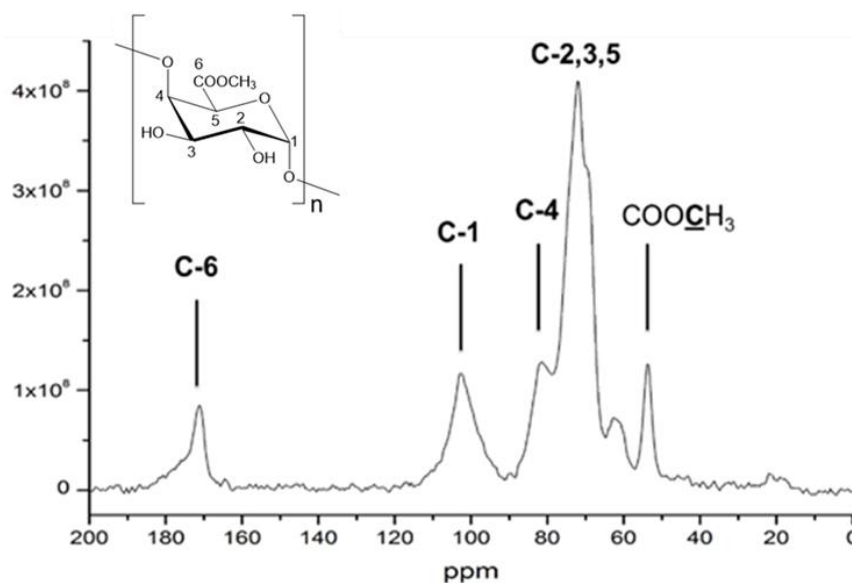
Figure 3.1.15 ^{13}C NMR CP-MAS spectrum of mango peel pectin from flow
system (*Keitt* EE)

3.1.3.4 Degree of Esterification

Table 3.1.3 Degree of esterification (DE) of mango peel pectin (SWE flow system)

Variety	DE (%)	
	titrimetry	NMR
Keitt	76.80 ± 1.6	82.44
Sindhri	70.22 ± 2.5	76.43
Kesar	74.35 ± 3.1	80.66

The degree of esterification of mango peel pectin (SWE flow system) is listed in table 3.1.3. All three varieties have high degree of esterification (DE >50 %). It can be observed that the results from two different methods have a difference for about 6 % but nevertheless are in suitably close agreement.

3.1.4 Sugar Analysis
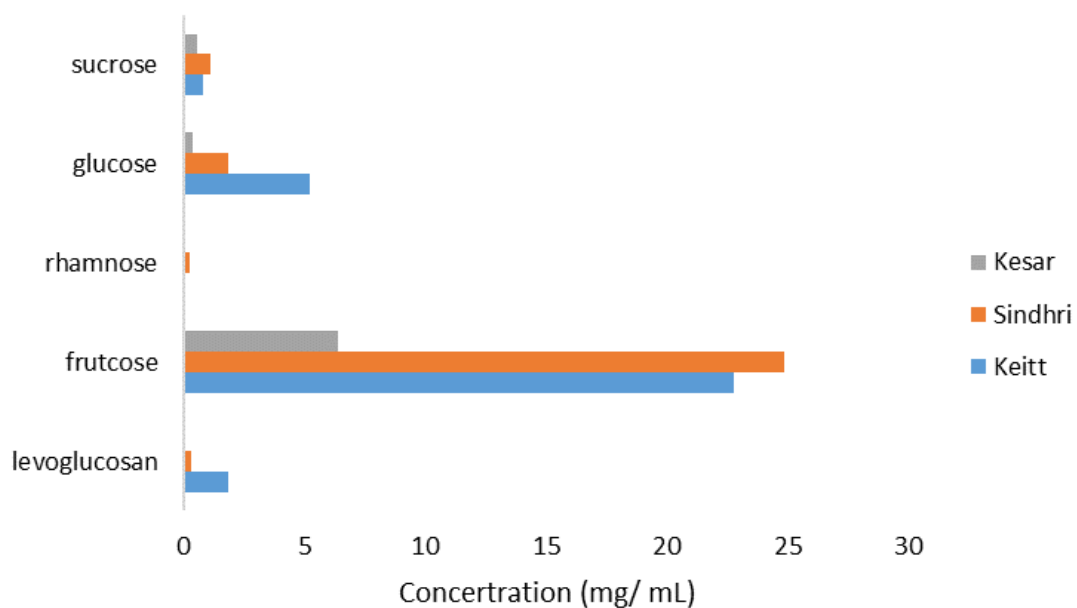
Figure 3.1.16 Sugar content of mango peel ethanol extracts (original in color)

The sugar content in ethanol extract was analysed by HPLC and the result is shown in Figure 3.1.16. Fructose is the most abundant sugar in all three varieties, accounting for at least 75 % of total amount. Interestingly, A. Silva *et al.* reported that sucrose turned out to be the most abundant sugar in ripe *Keitt* mangoes (pulp) instead of fructose.[138] This may suggest that the mango peel appears to keep fructose while most of the sucrose still remains in flesh. Similar result of low sucrose content in mango peel was reported by T. Chaiwarit *et al.* where only 0.76 % (w/w) of sucrose was achieved from residual free sugars content post microwave extraction compared with 10.15 % of fructose (*Nam Dokmai* variety).[139]

It is also noticeable that *Kesar* has much lower sugar concentration than the other two varieties. This exactly accords with their taste (sweetness): *Keitt* and *Sindhri* are both very sweet cultivators while *Kesar* is a bit sour. Meanwhile, *Keitt* has much higher contents of both levoglusosan and glucose compared with the other two varieties, but rhamnose was not detected in it.

3.1.5 MFC XRD

The powder X-Ray diffraction (XRD) spectra of MP MFCs and the respective calculated crystallinity index are presented in Figure 3.1.17. A diffraction pattern typical of semi-crystalline cellulose type-I containing crystalline regions, with main 2θ peaks at ca. 16°, 22° and 34.5°, and an amorphous contribution with a 2θ maximum *ca.* 18° can be observed in all samples.

*signal of sample holder
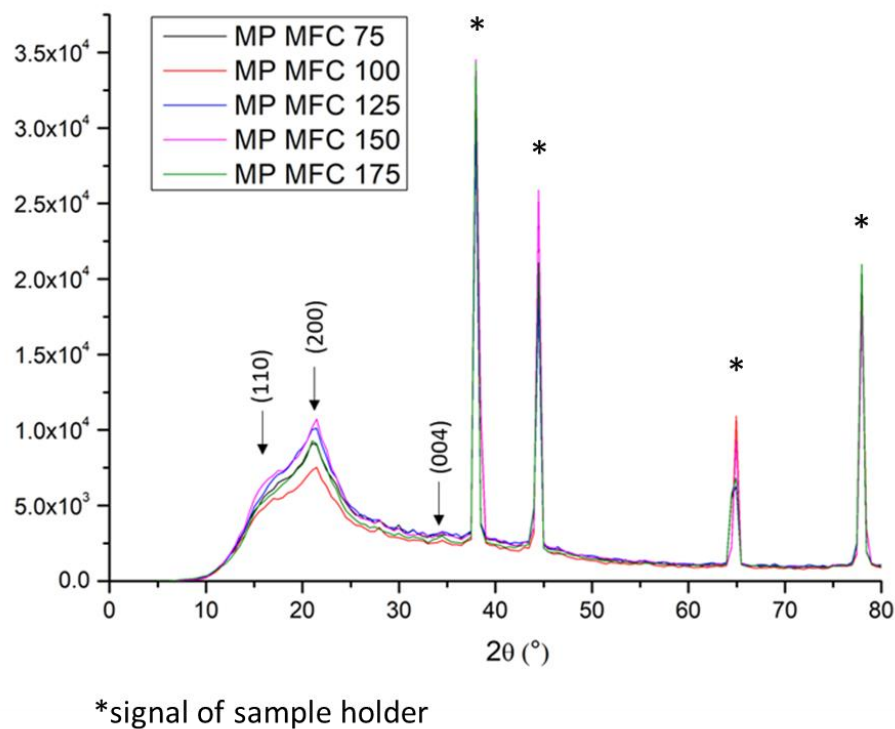
Figure 3.1.17　　XRD spectra of mango peel MFC (original in color)

3.1.6 MFC gels

Hydrogels are structures mainly from biopolymers and/or polyelectrolytes which contain huge amount of water.[140] As discussed earlier, MFC can be used for forming hydrogels simply by physical cross-linking as it has a lot of hydroxy group, which can form hydrogen bonding linked networks with ease.[141] In this study, the MFC hydrogels from mango peel liquefaction hydrolysis are show in Figure 3.1.18. It can be seen the colour of hydrogel changed from light brown to black as HL temperature increased. Due to some favourable properties such as hydrophilicity, biodegradability,

biocompatibility, transparency, low cost, and non-toxicity, cellulose-based hydrogels could have potential applications in tissue engineering, controllable delivery system, agriculture and water purification.[140]
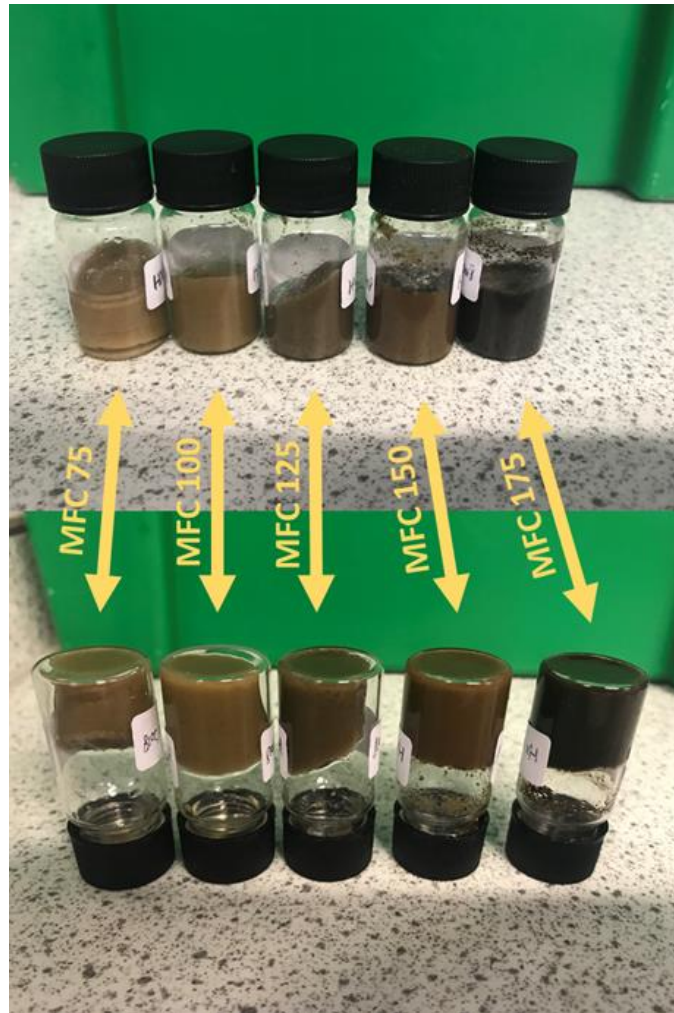
Figure 3.1.18 Mango peel MFC hydrogels (original in color)

Meanwhile, it is also noticeable that they all gelled pretty well even at high hydrolysis temperature. This is probably because of the presence of residual amorphous polysaccharides or amorphous cellulose domains in all samples.

3.1.7 Summary

This part mainly demonstrated subcritical water extraction and hydrothermal liquefaction of pectin from mango peel waste in the absence of any mineral acid. Three different global varieties were studied (*Keitt*, *Sindhri* and *Kesar*) and the highest pectin yield (18.34 %) was achieved at a temperature of 175 °C, flow rate of 3 mL min^{-1} for 15 min from *Kesar* variety post ethanol extraction.

The degree of esterification of pectin was determined by both titrimetry and NMR method and all three varieties have high DE over 70 %. Meanwhile, some other valuable compounds were also explored via ethanol extraction prior to subcritical water extraction. Fructose, glucose and sucrose are the most abundant sugars in mango peel waste. Furfural and HMF, which can be used as potential platform molecules, were also obtained as the major components in ethanol extracts from mango peel.

None of the pectin samples succeeded in gelation test, no matter what technique was used. However, on the other hand, all the MFC samples from hydrothermal liquefaction were able to form hydrogel very quickly and easily even at high temperature, which seems to be quite interesting.

3.2 Part B: Valorisation of Peach Peel Waste

This part is divided into three sub-sections:

i.   A preliminary study of peach peel pectin with different method and comparison with an industrial sample;

ii.   A lab-scale simulation in order to mimic industrial peeling process with sodium hydroxide solution, and;

iii. A study of microwave-assisted hydrolysis of peach peel mainly for extraction of pectin and MFC.

3.2.1 Peach Peel Pectin and Comparison with Industrial Sample

3.2.1.1 Pectin yield and DE of peach peel

Table 3.2.1 Yields of peach peel pectin (%) with different extraction techniques

Technique	Yield/ %	DE/ % (NMR method)
CHE	3.46	72.53
MWE	7.47	77.97
SWE	4.34	54.11

The pectin yield of fresh peach peel is listed in table 3.2.1. MWE gets the highest yield of 7.47 %, which suggest the MW power significantly facilitates the separation of pectin from cell wall compared with conventional heating extraction (HCl, pH 2.5, 80 °C, 2 h) and SWE (batch system, 120 °C, 1 h). Meanwhile, pectin from MWE also results in the highest DE, indicating that it has the best pectin quality among all three

extraction techniques. It is also noticeable that pectin from SWE achieved much lower DE than the other two methods, which may suggest that the condition could be a bit harsh for pectin extraction from peach peel. Lower temperature or shouter extraction time should be explored in future work.

3.2.1.2 ATR-IR Analysis

The ATR-IR spectra of the peach peel pectin are shown in Figure 3.2.1. The combination of carbonyl absorption bands at 1730 cm^{-1} (methyl ester) and 1600 cm^{-1} (free carboxylic acid) suggests the presence of pectin, and the ratio of their peak areas indicates the degree of esterification for the pectin. Visually, CHE and MWE pectin have similar DE and both of them are higher than SWE, which confirms the results shown in table 1. Apart from these two peaks, some other characteristic absorption peaks, such as the broad O–H stretch around 3300 cm^{-1} (hydrogen-bonded hydroxyl
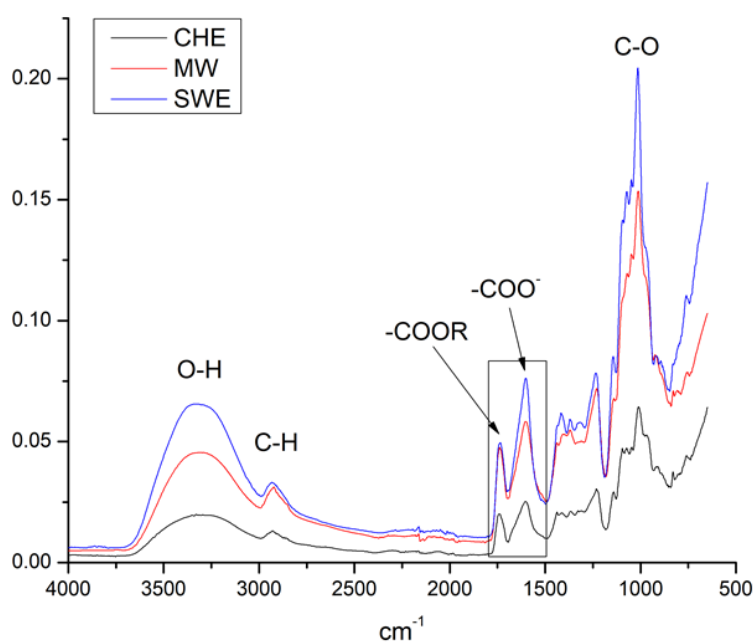
Figure 3.2.1 ATR-IR spectra of peach peel pectin (original in color)

groups), C–H stretch at approximately 3000 cm^{-1} (alkyl groups), and intense C–O

stretches between 1200 and 1000 cm^{-1}, also suggest the existence of pectin.

The IR spectra of post caustic peeling residue and its MW extract are shown in Figure

3.2.2. It can be observed that neither of them shows an obvious absorption peak around

1700 cm^{-1}, which indicates the absence of methyl ester group in both samples.   This is

probably because the sodium hydroxide in the system saponifies the methyl esterified

pectin and dramatically decreases its DE.
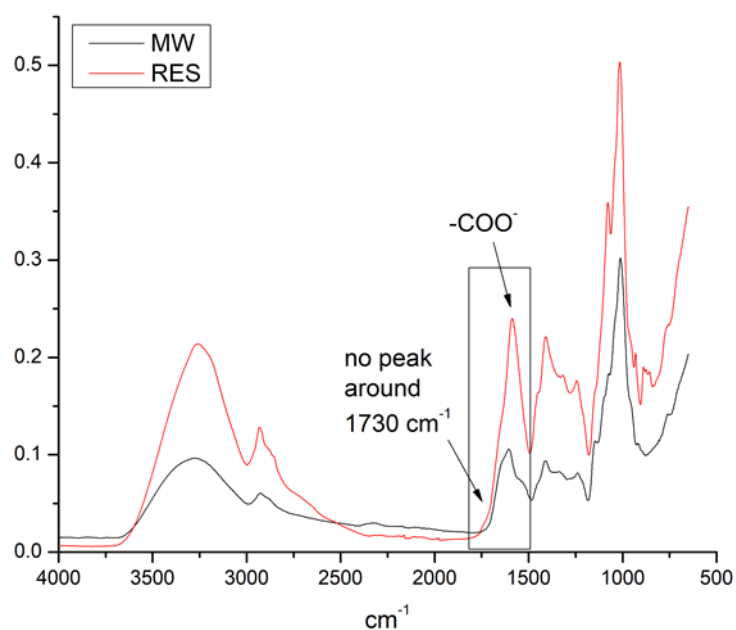
Figure 3.2.2   ATR-IR spectra of post caustic peeling peach residue and its MW
extract (original in color)

3.2.1.3 TGA Analysis

The TGA and DTG analysis of peach peel pectin is shown in Figure 3.2.3. Three major
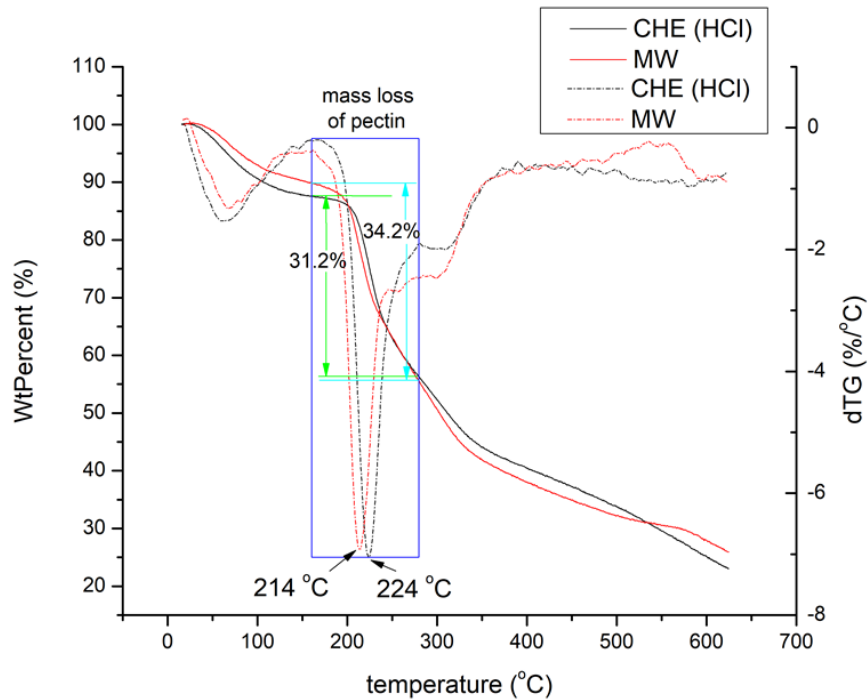
Figure 3.2.3   TGA and DTG curves of peach peel pectin (original in color)

processes of mass loss can be observed for each sample. The first one, ranging from 60

to 120 °C, is due to the removal of moisture in the sample. The second one, between

200 and 250 °C, which is attributed to pectin decomposition. The third main

decomposition process around 300 °C is probably due to some residual cellulose in the

samples.

The TGA and DTG of solid residue post MWE of pectin was also analysed for

comparison (Figure 3.2.4). An obvious mass loss can still be observed from around

210 °C, which indicates that there is still some residual pectin in raw materials that has

not been extracted. Meanwhile, the main mass loss around 330 °C reveals the existence

of large amount of cellulose, which shows the potential for the further nanocellulose

exploration.
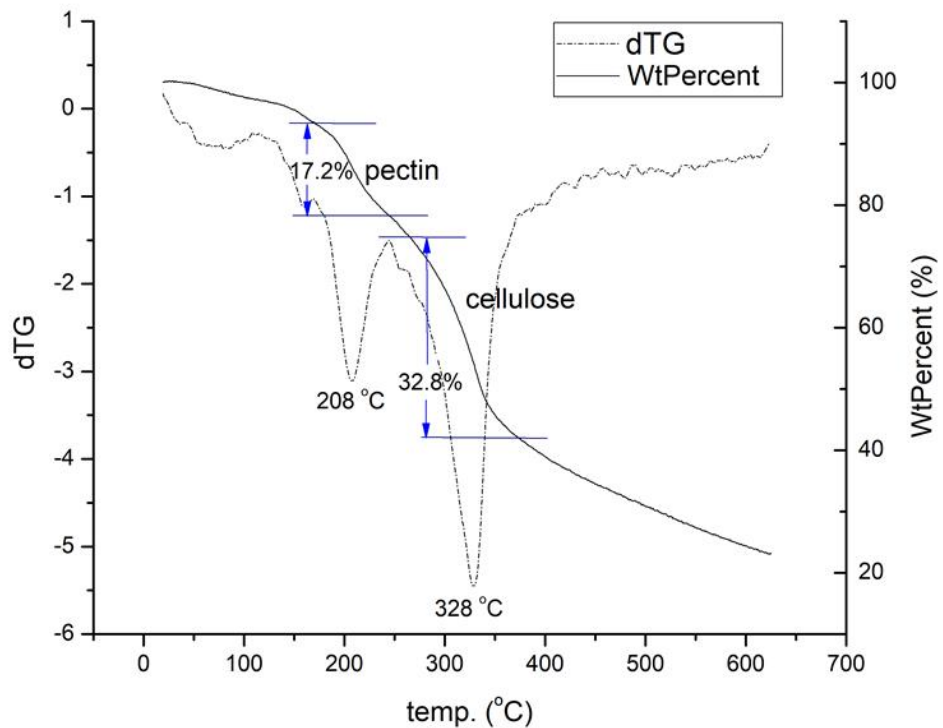
Figure 3.2.4 TGA and DTG curve of solid residue post MWE of peach peel pectin (original in color)

The TGA and DTG analysis of post caustic peeling residue and its MW extract are shown in Figure 3.2.5. The main mass loss period for both samples are between 250 and 350 °C, which is probably attributed to the mixture of cellulose and hemicellulose. Only a small peak can be observed between 200 and 250 °C from both samples which may represent the mass loss of pectin. This suggests either there is a shift of DTG peak for low DE pectin or the pectinaceous -matter contents in both samples are very low.
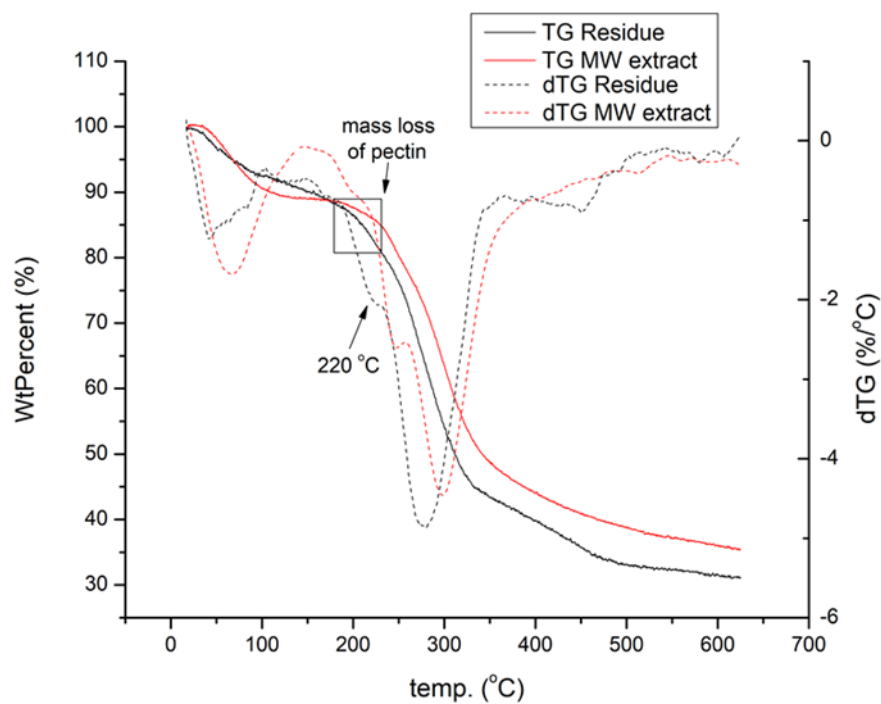
Figure 3.2.5 TGA and DTG curves of post caustic peeling peach residue and its MW extract (original in color)
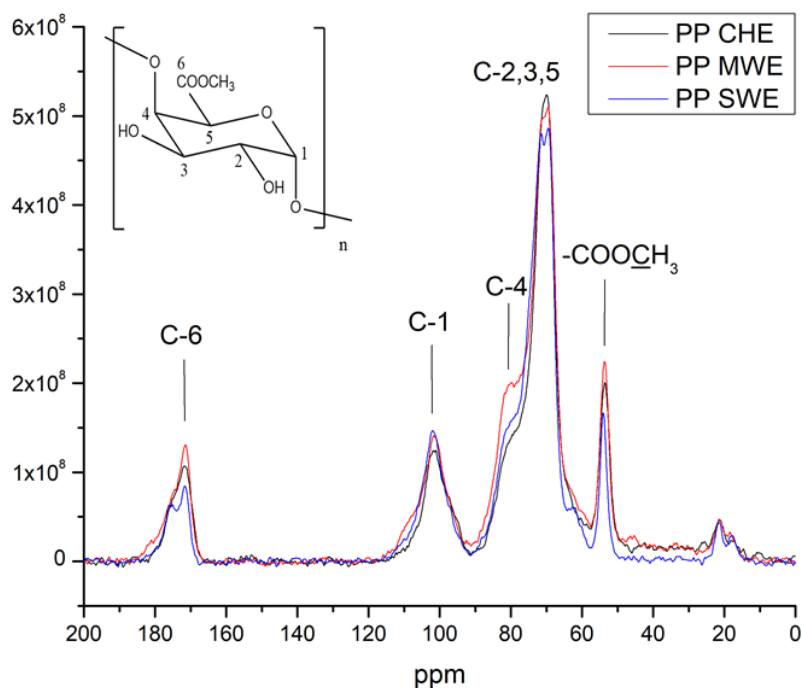
Figure 3.2.6 ^{13}C solid-state NMR spectra of peach peel pectin (original in color)

3.2.1.4 ^{13}C CP-MAS NMR Analysis

The ^{13}C CP-MAS NMR spectrum of the peach peel pectin is shown in Figure 3.2.6. The strong resonance at 171 ppm and weak resonance at 175 ppm are attributed to the esterified carboxyl group and non-esterified carboxyl group of pectin respectively, while the resonances at 103 and 81 ppm can be assigned to the anomeric C-1 carbon and C-4 carbon, respectively. Furthermore, the intense peaks in the region of 60 to 90 ppm are from the carbon atoms of the pyranoid ring (C-2, 3, 5), while the resonance at 54 ppm is attributed to the methyl carbon of the methyl ester (COOC$\underline{H}_3$). It can be observed that the curve of SWE pectin has some slight differences with CHE and MWE pectin as it has a clear peak at 175 ppm which suggests the low degree of esterification and a weak resonance at 62 ppm which suggests the existence of some small amount of cellulose.
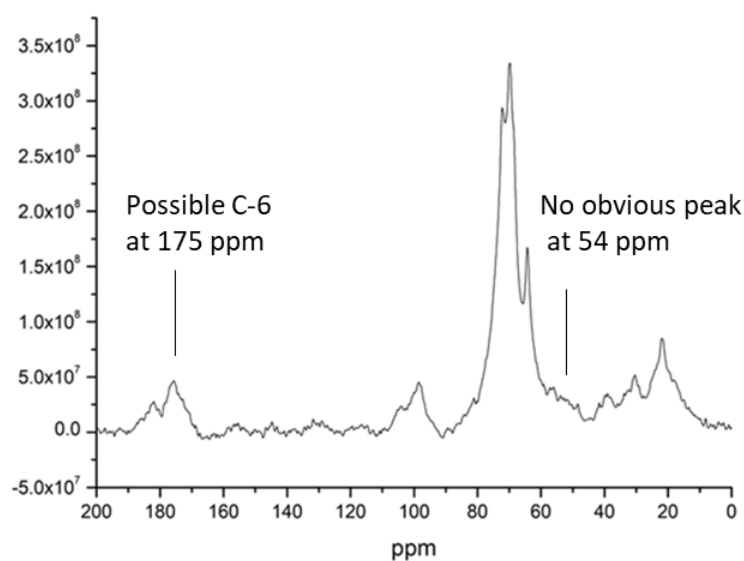
Figure 3.2.7 ^{13}C solid-state NMR spectrum of post caustic peeling peach residue.

The solid-state ^{13}C NMR spectrum of the post caustic peeling residue (Figure 3.2.7) shows a significantly different curve compared with the pectin samples in Figure 3.2.6. However, it is still noticeable that the strong resonance at 175 ppm and weak resonance at 171 ppm indicate the dominance of non-esterified carboxyl group in this sample. Meanwhile, there is no obvious peak observed at 54 ppm, which also confirms the low content of esterified carboxyl group.

3.2.1.5 Pectin Gelation test

The pectin from all extraction techniques (CHE, MWE and SWE) were employed to form the gel with the method described in 2.3.11. Only the pectin from MWE successfully gelled (see Figure 3.2.8) while that from the other two techniques were still in liquid state.
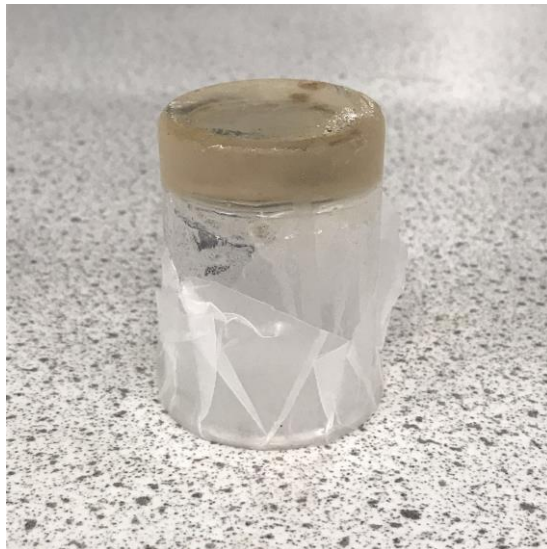
Figure 3.2.8 Pectin gel from peach peel (MWE) (original in color)

3.2.2 Lye Peeling Simulation (LPS)

Due to the lack of industrial samples, a lab-scale lye peeling simulation (LPS) was carried out in order to imitate the industrial peach peeling process and collect the peel residue for analysis. The process of LPS is described in chapter 2.2.5.

3.2.2.1 TGA Analysis

The TGA curves and their derivatives of the extracts from LPS are shown in Figure 3.2.9. A significant mass loss around 230 °C, which could be attributed to pectin. This is interesting as pectin is usually extracted under acidic condition (see Chapter 1.3.1). Meanwhile, other major dTG peaks are responsible for moisture (~ 60 °C), (hemi-)cellulose (~ 280 °C) and lignin (~ 400 °C) respectively. Interestingly, it can be observed that with increased heating time, the peak intensity of pectin starts to decrease while that of (hemi)cellulose start to increase (except for LPS 120 which has the lowest intensity for both peaks harsh condition starts to breakdown the hemicellulose). Meanwhile, the dTG peaks for lignin remains similar. Only that of LPS 120 is slightly lower. It is also noticeable that the solid residue after 600 °C (ash content) seems does not affected too much by heating time as 30 min has much lower ash content than any other samples and 60 min has the highest.
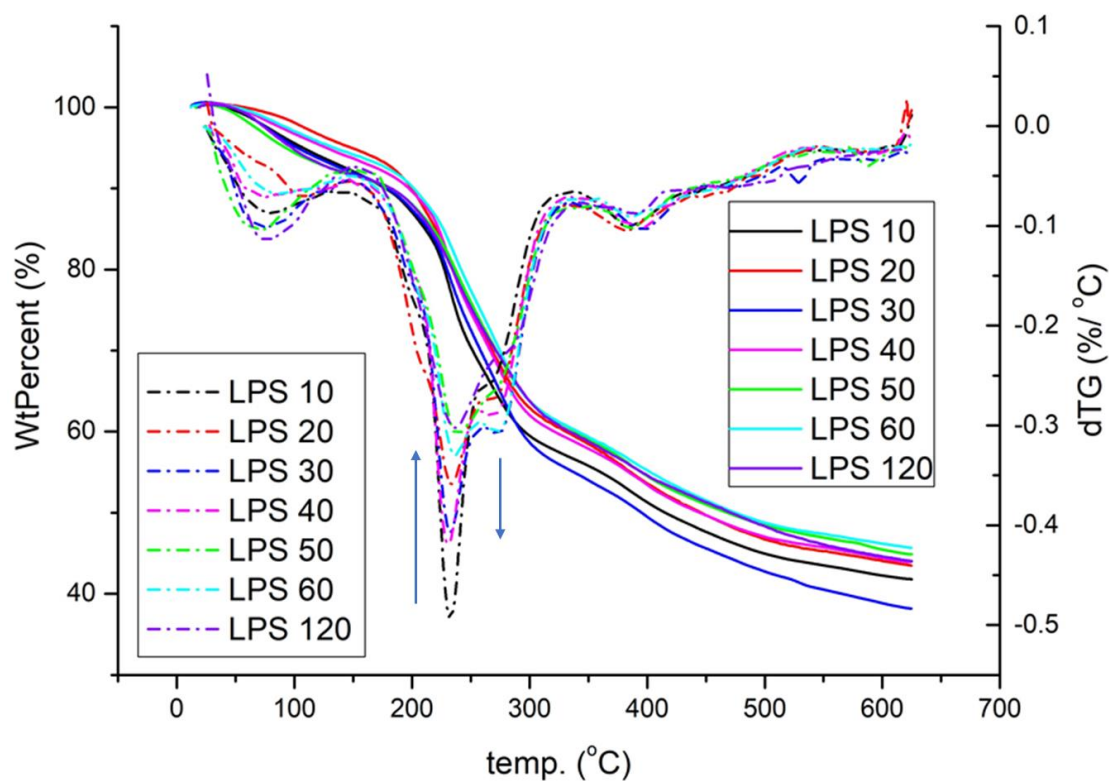
Figure 3.2.9   TGA and DTG curves of LPS biopolymers (original in color)
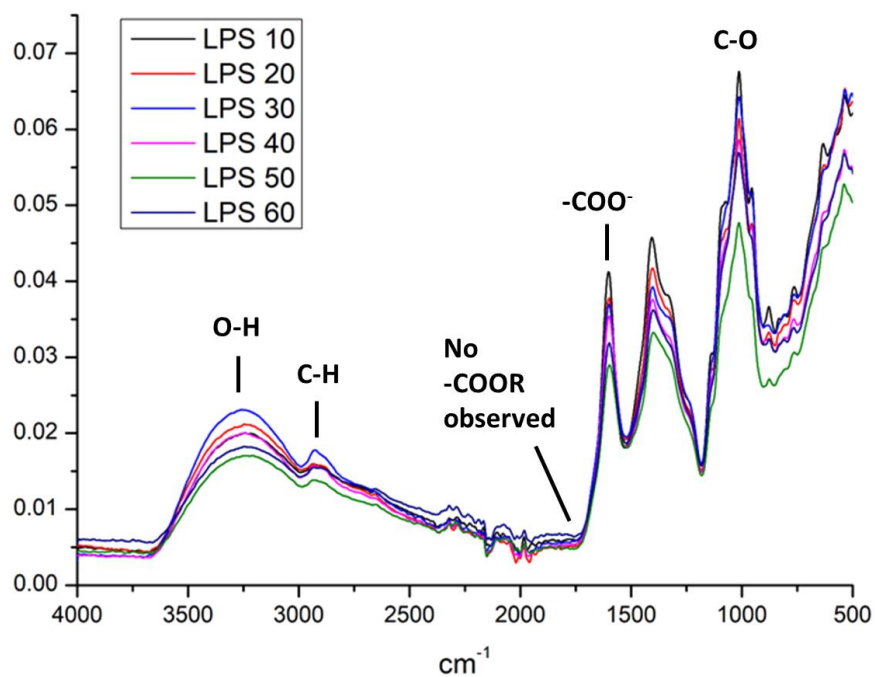
Figure 3.2.10   ATR-IR spectra of LPS biopolymers (original in color)

3.2.2.2 ATR-IR Analysis

The IR spectra of LPS ethanol precipitate are shown in Figure 3.2.10. Generally, the absorption intensity slightly increases as the LPS time increase. The broad O−H stretch centred at around 3300 cm^{-1} is attributed to hydrogen-bonded hydroxyl groups. C−H stretch at approximately 3000 cm^{-1} is attributed to -CH- and –CH_2-, and the intense C−O stretches between 1200 and 1000 cm^{-1} refers C-O-C ring and C-O-C ester. However, only the peak at 1630 cm^{-1} (free carboxylic acid) can be observed as one of the characteristic pectin peaks, while none of the samples show the absorption peak of methyl ester group at 1730 cm^{-1}. This could be explained as that there is either no presence of pectin or the degree of esterification of pectin is almost zero. Based on the TGA results presented before, it seems the later one is more reliable.

3.2.2.3 ^{13}C CP-MAS NMR

Two exemplar solid-state ^{13}C NMR spectra of LPS extract biopolymers are shown in Figure 3.2.11. The resonances at 170 and 176 ppm, which refer to carboxylic acid and ester group of pectin on C-6 respectively, can be observed from both LPS time. This seems indicate the existence of pectin as the resonances of C1-C5 can be seen and all match the spectrum of pectin. But if so, the pectin would be HM pectin as the resonance at 176 is higher than 170 ppm, which is different with what is shown in IR and TGA. However, it is also noticeable that the resonance at 53.72 ppm which is attributed to the methyl carbons of methyl ester ($COOCH_3$) can hardly be observed, so this could be

explained that the resonance at 176 ppm may come from other components in LPS peel residue.
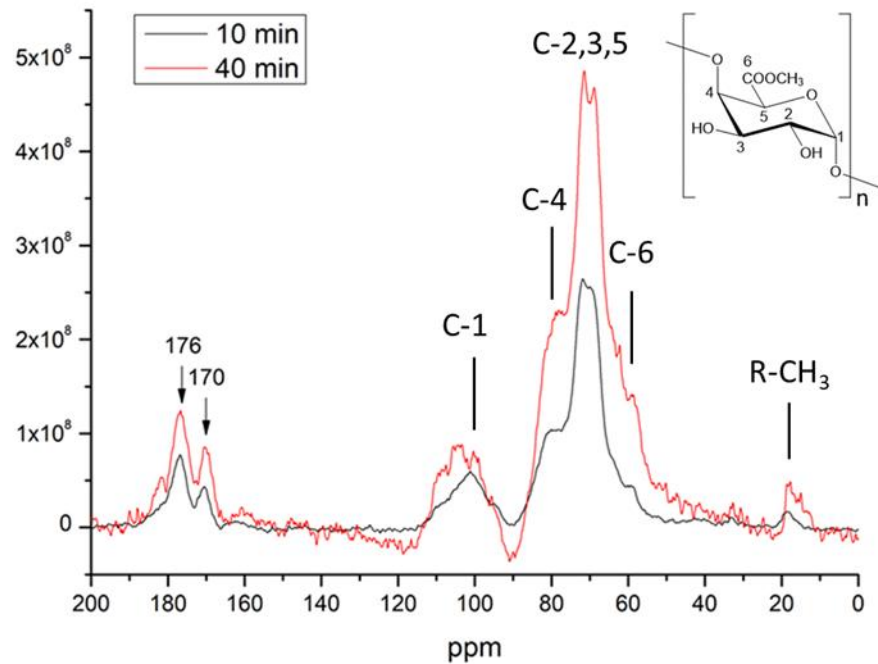
Figure 3.2.11 Exemplar solid-state ^{13}C NMR spectra of LPS extract biopolymers (original in color)

3.2.2.4 Gelation Test

Since almost no DE was observed in all LPS samples, the traditional way of gelation for HM pectin is not suitable in this situation. According to the "Egg-Box Model" theory,[142] Ca^{2+} is required as a "bridge" for LM pectin gelation (see Figure 3.2.12). Therefore, in this study, an exemplar of LPS 10 samples were used for gelation and based on the method described in Chapter 2.3.11, with the addition of Ca^{2+} ($CaCl_2$) in
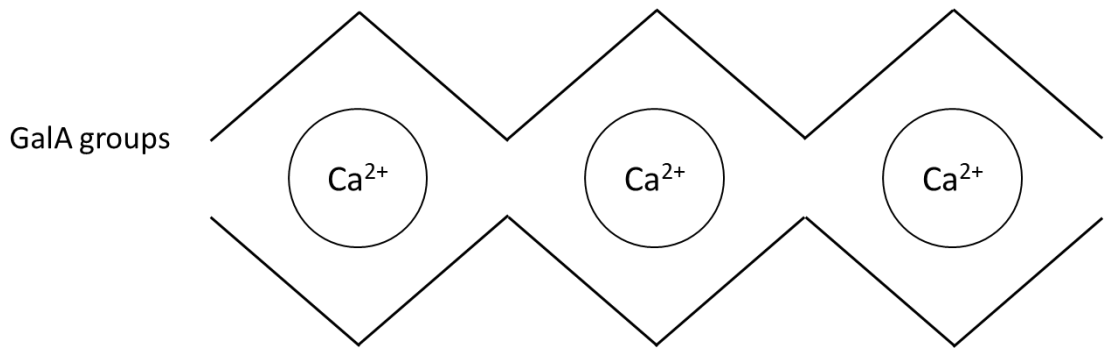
Figure 3.2.12   The "egg box" model of pectin

the process. The results are shown in Figure 3.2.13. It can be observed that the sample

is almost pure liquid with only sugar added. After $CaCl_2$ was added, it became much

more viscous, but still unable to form gels.
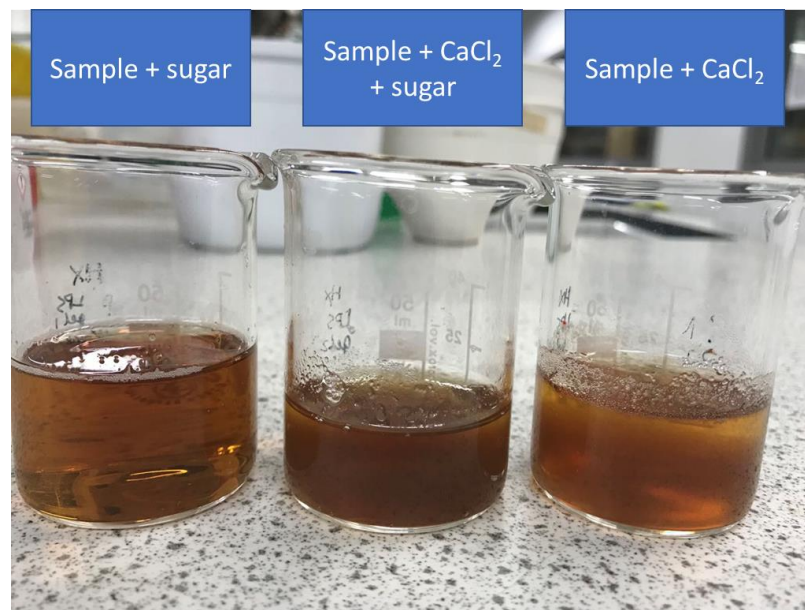
Figure 3.2.13   Gelation test of LPS 10 sample (original in color)

3.2.3 Microwave Hydrolysis of Fresh Peach Peel

The MFC of peach peel are all derived from a two-step microwave hydrolysis. The samples will be labelled as MFC X-X in later discussion, in which X refers to the hydrolysis temperatures.

3.2.3.1 TGA

The fresh peach peel samples were extracted with ethanol under reflux before subjected to microwave hydrolysis. The TGA curves of raw materials and the peel residue post ethanol extraction are shown in Figure 3.2.14. The raw material of peach peel shows a strong mass loss at 209 °C and a weak one at 324 °C which refers to pectin and cellulose
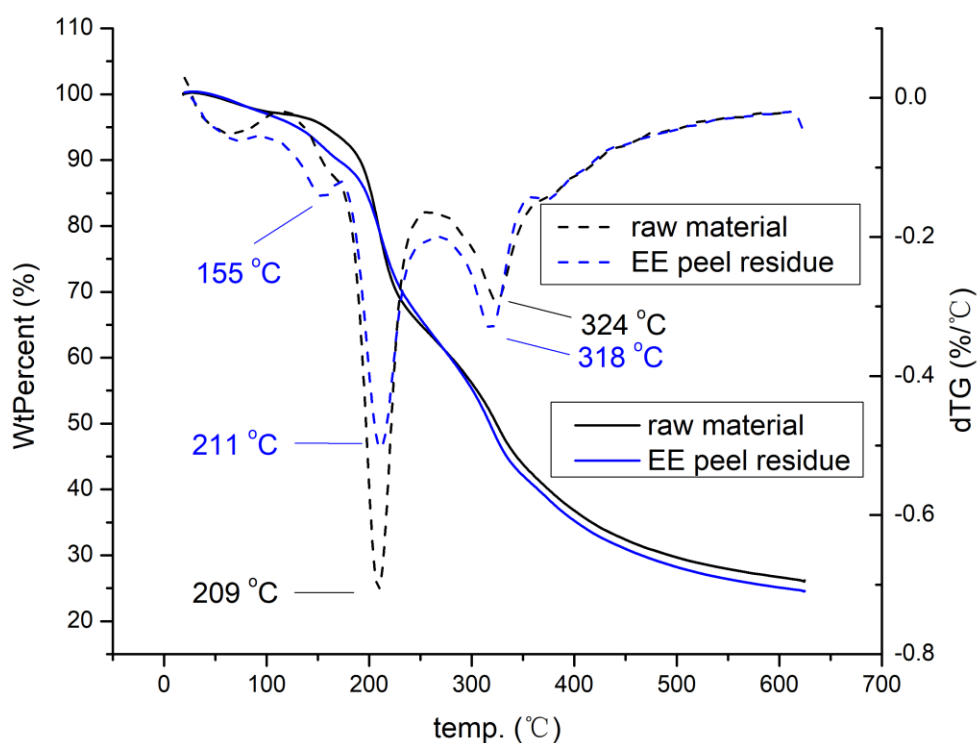
Figure 3.2.14   TGA curves of peach peel raw material and its post ethanol extraction residues (original in color)

respectively. Similar moisture content can be observed from both raw materials and ethanol extract. However, after ethanol extraction, the mass loss of cellulose does not change too much, but it starts to lose mass (decompose) from 110 to 190 earlier than raw material as a dTG peak centred at 155 °C can be observed. This is probably because of the generation of some low molecular weight compounds during the ethanol extraction. (*eg.* on-site of pectin degradation, physiosorbed water).
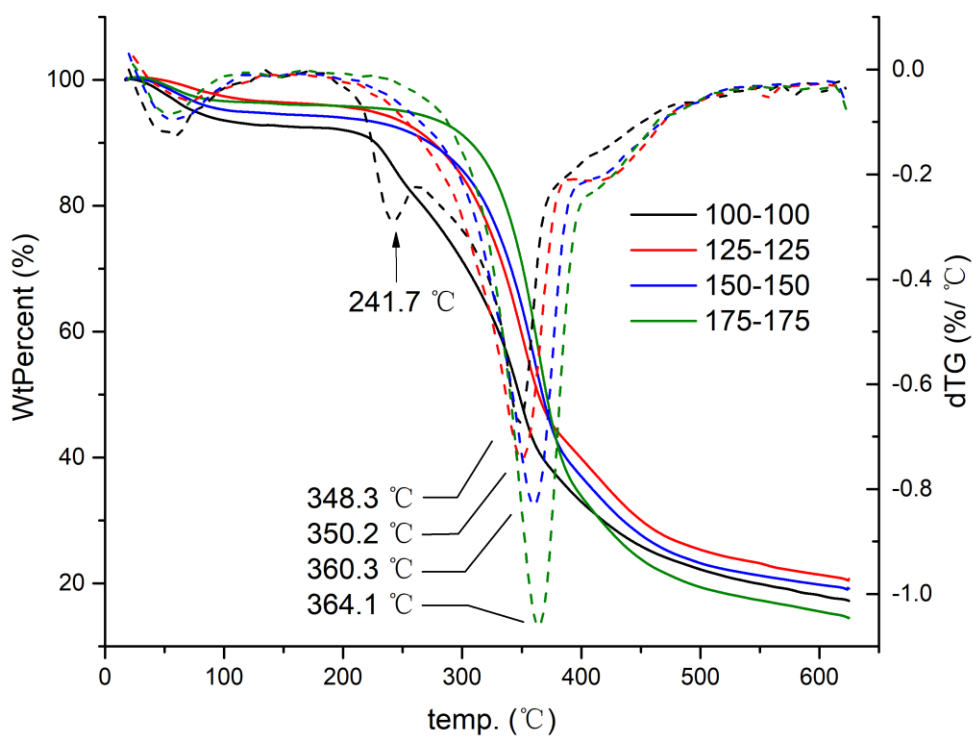
Figure 3.2.15   TGA curves of peach peel MFC (original in color)

The TGA curves of peach peel MFC and their derivatives are shown in Figure 3.2.15. A small amount of mass loss of pectin (at around 240 °C) can be observed only from

MFC 100-100, while the majority mass loss of all samples contributes to MFC, ranging

from 348.3 to 364.1 °C. It is noticeable that the dTG peak intensity and temperature of

MFC increases as elevated temperature. The shifting of the peak temperature can be

explained as the increase of the crystallinity in the samples as they can affect the

thermal property of MFC.[143] Meanwhile, apart from MFC 100-100, all other samples

also have a small mass loss at around 400 °C, which shows the existence of lignin.
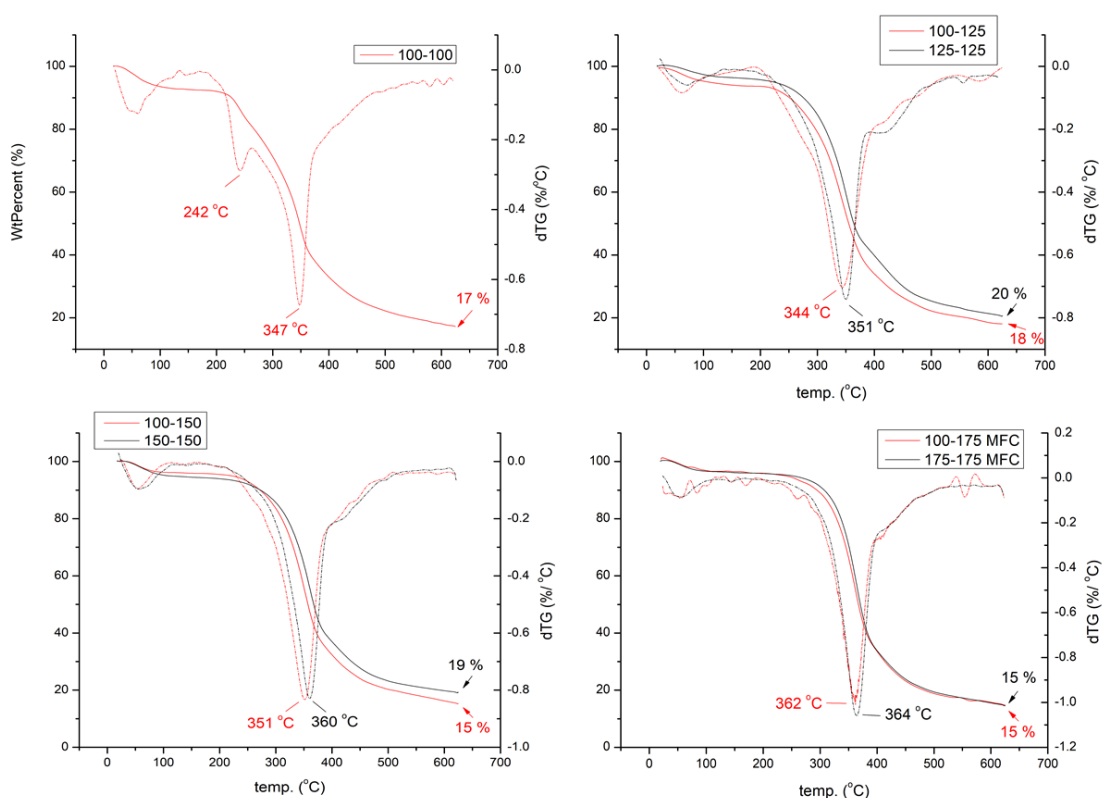
Figure 3.2.16   Comparison of TGA curves of peach peel MFC (X-X and 100-X)
(original in color)

Another set of control experiment has been carried out in which the temperature of first

step microwave hydrolysis maintained at 100 °C, while the second step increased from

125 to 175 °C. The TGA results are presented in Figure 3.2.16. At 175 °C, the two

curves are almost identical, but except for that, the shifting of cellulose peak can still

be observed from the 100-X group (red curves) as elevated temperature, but the

difference is smaller than the X-X group (black curves). Meanwhile, it can also be

observed that the mass of residue (ash content) from 100-X group is lower than that

from X-X group, which suggests that selecting mild temperature (100 °C) as first step

may result in lower degree of crystallinity.

3.2.3.2 ^{13}C CP-MAS NMR

The solid state ^{13}C CP-MAS spectra of peach peel raw material and its post ethanol

extraction peel residue are presented in Figure 3.2.17. The peaks refer to the carbons

on the hexatomic ring (can be responsible for both pectin and cellulose) as labelled in

the Figure can be clearly observed in both samples, and they are quite similar except

for the slight decrease of C-6 peak. Besides, the resonances at 172 and 54 ppm suggest

the presence of pectin. Meanwhile, there are also two resonances can be observed at

around 20 and 30 ppm, which be attributed to R-CH$_3$ and R-CH$_2$ from aliphatic. It can

be seen that the resonance at 20 ppm increase and that at 30 ppm decrease after the

ethanol extraction. The peak at ~ 90 ppm may be related to some sugars, for example,

sucrose.[144]
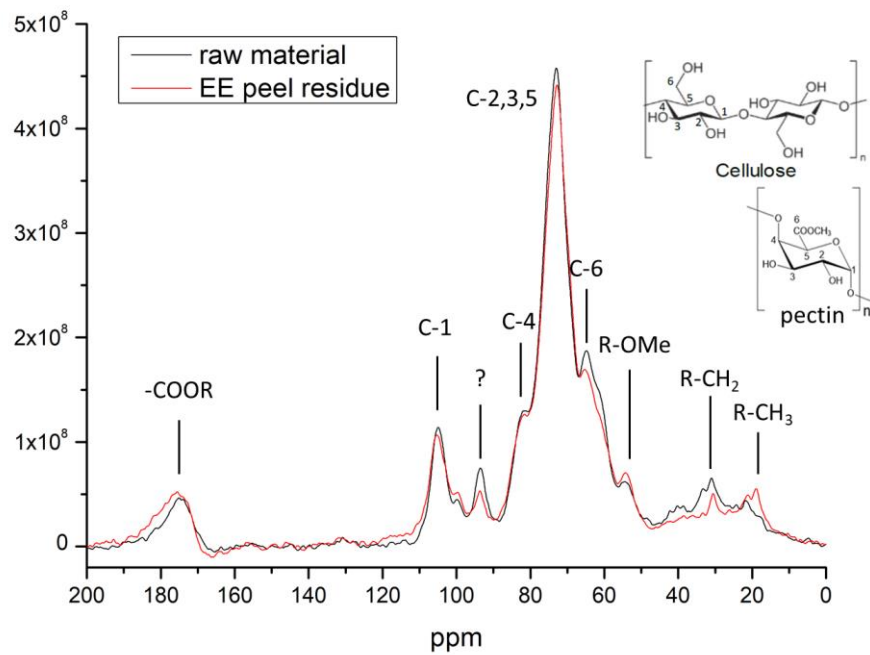
Figure 3.2.17 ^{13}C CP-MAS spectra of peach peel raw material and its post ethanol extraction peel residue (original in color)
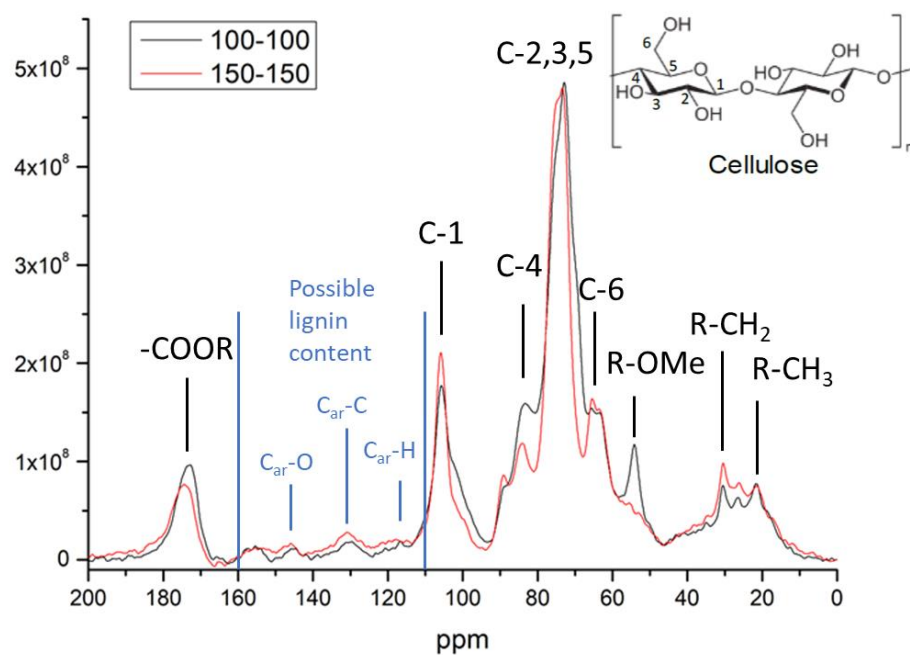
Figure 3.2.18 ^{13}C CP-MAS spectra of peach peel MFC (original in color)

The solid state ^{13}C CP-MAS spectra of peach peel MFC are presented in Figure 3.2.18. The resonances at 170-176 (carbonyls) and 54 ppm (methoxyl) confirm the presence of pectin in MFC 100-100. However, for MFC 150-150, the resonance at 54 ppm can hardly be observed but at 175 ppm it is only slightly lower than MFC 100-100. Interestingly, a change in the ratio of two peaks representing C4 (84 and 89 ppm) and C6 (63 and 65 ppm) respectively can be observed as well (see Figure 3.2.19). This suggests the MFC turns from amorphous into crystalline, which could be due to the removal of amorphous matter such as pectin that makes the material become more homogenous.[145]
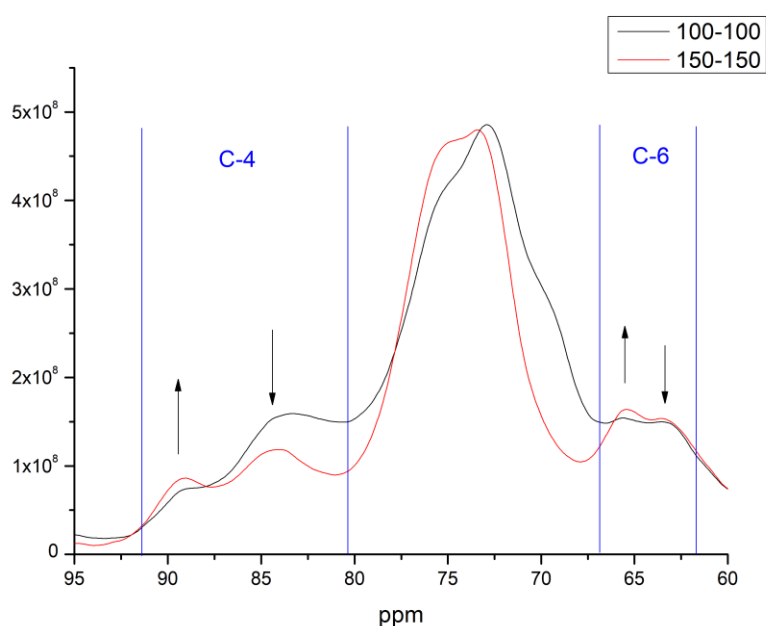
Figure 3.2.19   Changes in the ratio of C4 and C6 peaks from ^{13}C CP-MAS spectra of peach peel MFC (original in color)

According to literature, the Crystallinity Index (CI) of MFC can be calculated based on solid-state ^{13}C NMR spectrum.[146] As mentioned earlier, the C-4 region (80-95 ppm)

has two peaks refer to crystalline and amorphous cellulose, respectively. The CI is calculated by the ration of their peak areas, which is x/(x+y) showed in Figure 3.2.20. In this case, the CI of MFC 100-100 and 150-150 are 0.19 and 0.35 respectively. The increase of the Crystallinity Index confirms the removal of amorphous regions with the increase of the temperature.
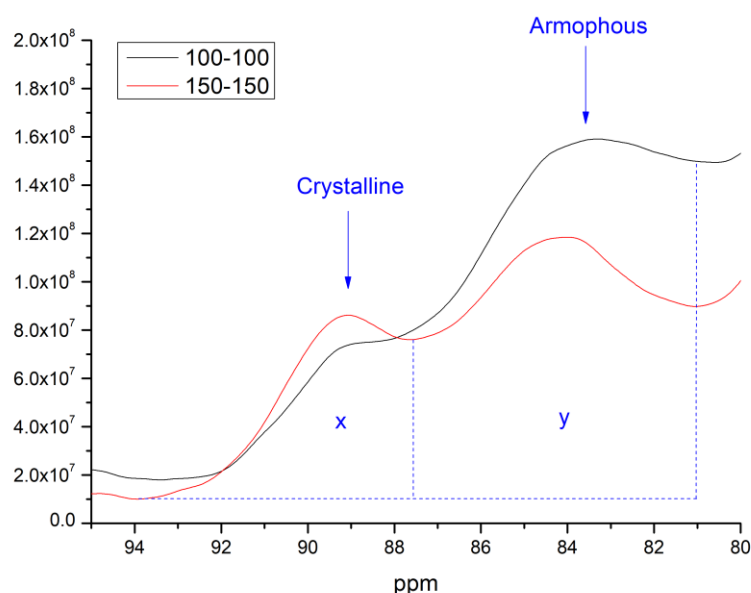
Figure 3.2.20 Sub-spectrum showing peaks assigned to the C4 in peach peel MFC (original in color)

Meanwhile, apart from the C1-C6 from MFC, the two resonances which show in raw material at around 20 ($R-CH_3$) and 30 ppm ($R-CH_2$) can be observed. it is also noticeable that there are also some minor peaks between 120 and 160 ppm. These resonances could be probably attributed to lignin.[147]

3.2.3.3 SEM Analysis

    i.   Drying Method

The influence of different drying method on peach peel residue post pectin isolation (125 °C) was studied and presented in Figure 3.2.21. If just judging from 1000 to 5000 times magnification, there is not much difference between two drying method. However, from the most left-handed figures (100 times magnification), it can be seen that the average particle size of freeze drying MFC is smaller than that from oven drying. This may suggest that freeze drying makes the particles separate more evenly and affected less by aggregation.
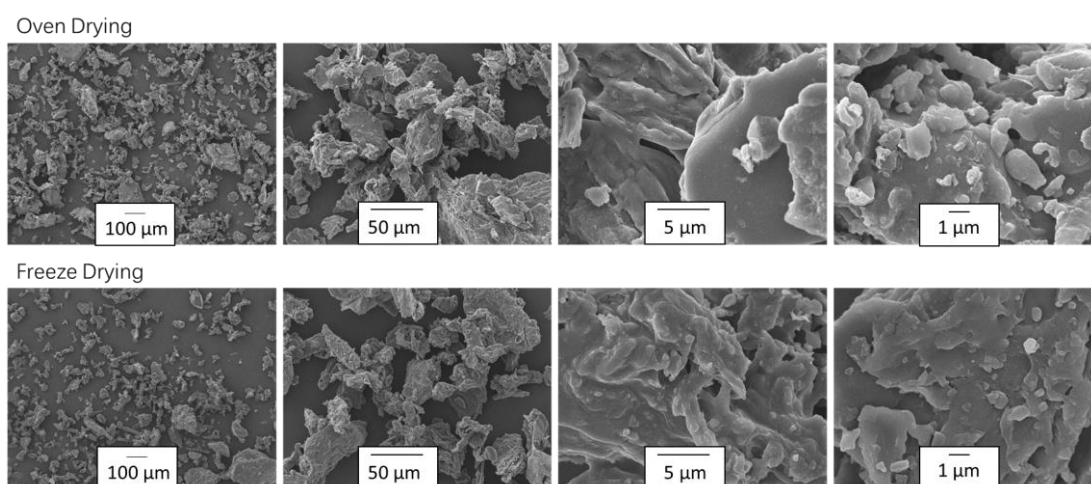
Figure 3.2.21   SEM figures of oven drying and freeze drying on the peach peel MFC isolation

    ii.   Peach peel MFC on difference scale (oven drying)

The SEM of peach peel MFC are shown in Figure 3.2.22. Not much difference can be

told from 100 times magnification. For 1000 times magnification, MFC 100 and 125 still look like a bulk while some small fibrils can be observed from 150 °C (see Appendix II). This is more obvious at 10000 times magnification. The surface of MFC 100 is still very "flat". It starts to wrinkle from 125 ℃ and does not change a lot with increased temperature. However, some porous can be observed from the surface of MFC 175.
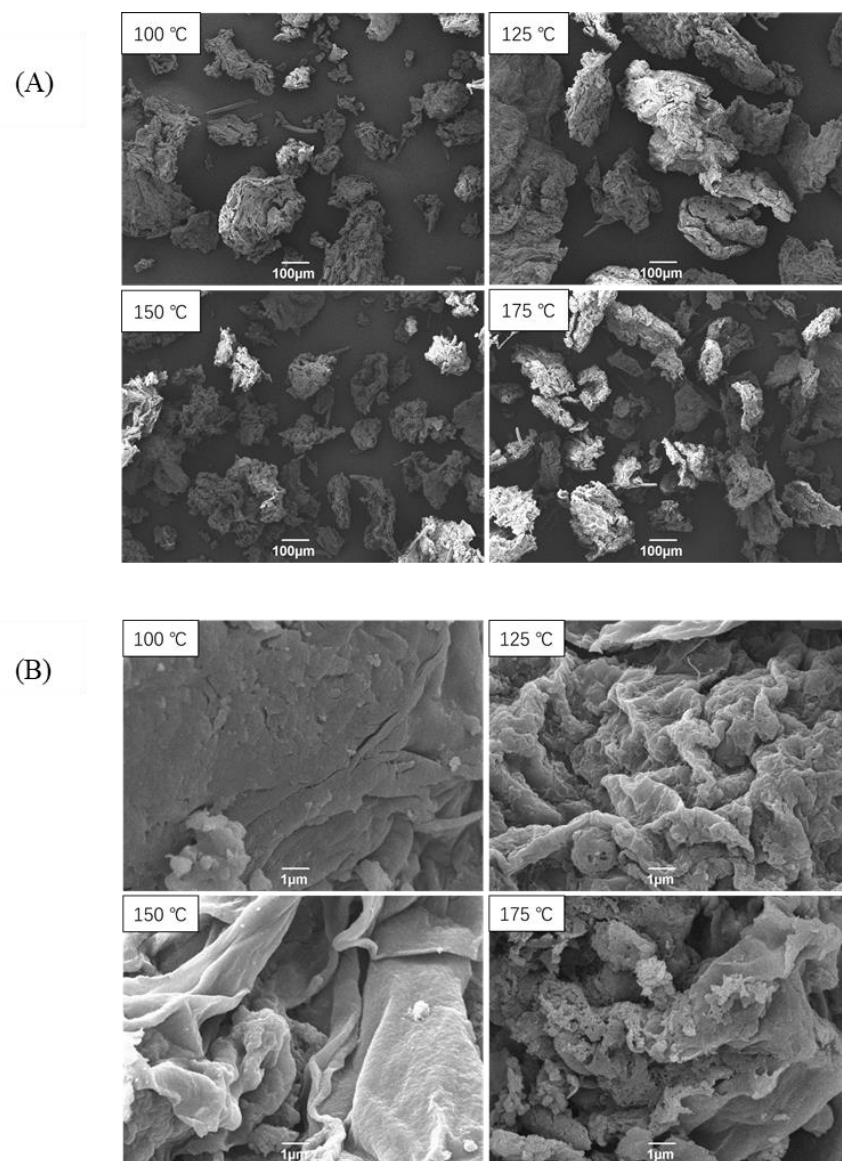
Figure 3.2.22   SEM figures of peach peel MFC: (A) 100 times magnification; (B) 10000 times magnification

iii.　　MFC (semi-)hydrogel

100 °C 3% (semi)gel　　　125 °C 3% gel
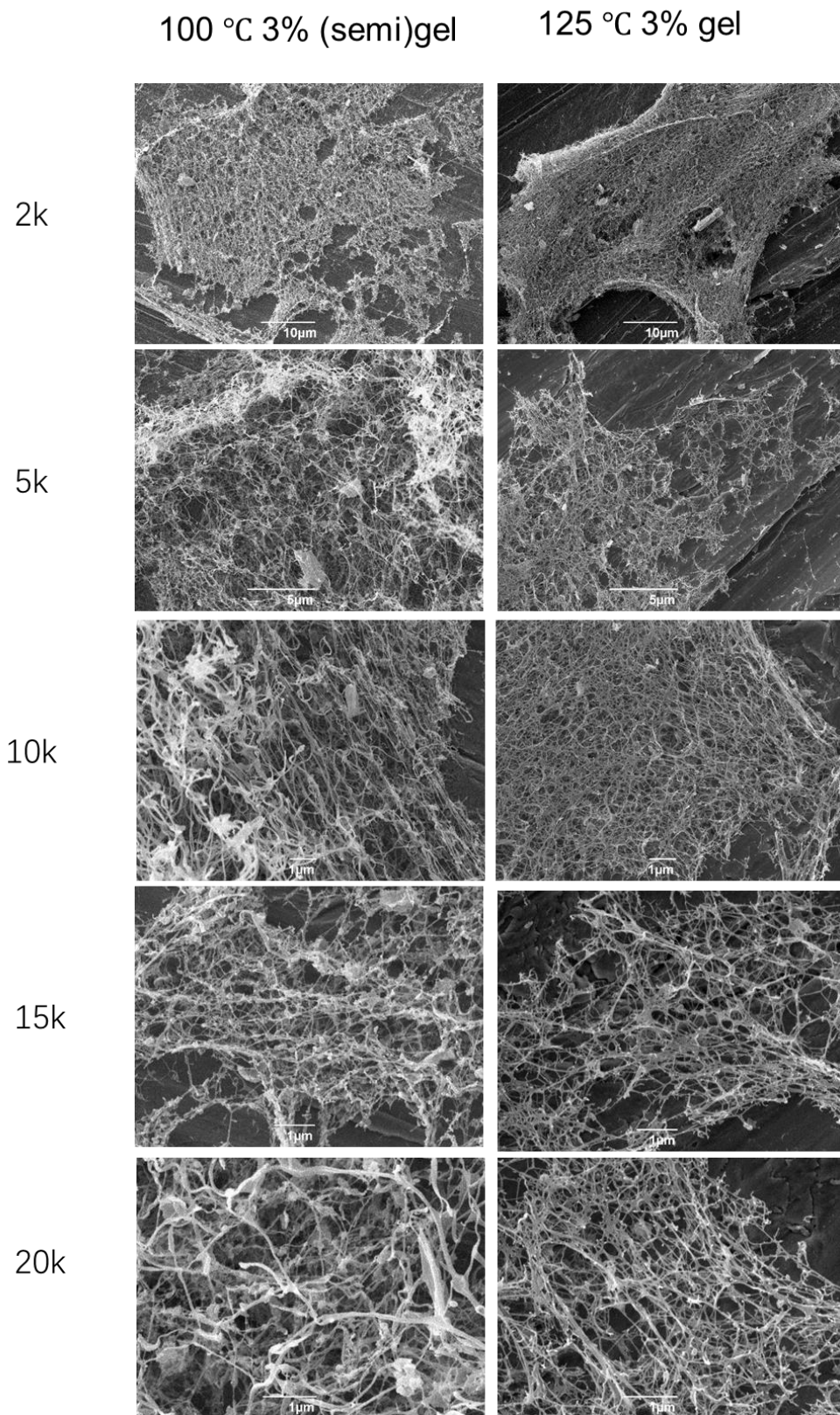
Figure 3.2.23　　SEM figures of peach peel MFC hydrogels

Hydrogels were attempted to be made from peach peel MFC and only MFC 125 formed

the gel at 3 % concentration in water. The SEM of MFC hydrogels (100 and 125 ºC)

were studied and presented in Figure 3.2.23. It can be obviously seen that although

MFC 100 has some network but the one of MFC 125 is much more concentrated. It

seems the bonds of MFC 100 are not strong enough to hold each other tightly. The

fibrils of MFC 100 also looks thicker than MFC 125, which may make it hard to form

gel.

3.2.4 Summary

In this part, a preliminary study of peach peel pectin with different extraction method

was firstly carried out. Microwave extraction resulted in both highest yield (7.47 %)

and DE (77.97 %) compared with CHE and SWE. Meanwhile, pectin from MWE also

succeeded in forming gel, while that from both CHE and SWE failed.

An industrial sample from post caustic peeling residue was received. A potential trace

of pectin/ pectinaceous matter was observed from its TGA result (mass loss at around

220 °C). In order to explore more of its properties, a lab-scale lye peeling simulation

was carried out. A peak around 280 °C was observed from all LPS samples, which

could be attributed to (hemi-)cellulose if not huge shift of pectin. The IR results showed

no absorption peak at 1740 cm^{-1}, which suggested either very low DE or the absence

of pectin. The gelation test (with the addition of Ca^{2+}) also failed. According to

literature, pectin has been successfully extracted from fruit waste with NaOH with

yields up to 19 %. However, they were all carried out under low temperature (32 –

60 °C), which is much lower than the temperature used in industrial peeling.[148] Based

on all these results, it seems unlikely to extract pectin from waste stream of industrial

peach peeling.

Lastly, MWE of peach peel was further studied on its post-extraction residue, which

mainly consist of MFC. TGA curved showed only MFC 100 still contained a small

amount of pectin, while for other samples, there was almost no mass loss between 200

and 250 °C, but instead, a small peak referring to lignin could be observed from all

these samples. The CP-MAS spectra showed the shift of ratio from C-4 and C-6 areas,

which suggested that with temperature increased, the removal of amorphous matter

(like pectin) made the material more homogenous. Unlike mango peel MFC, only MFC

125 successfully formed hydrogels at 3 % concentration. The SEM figures proved its

compact network structure compared with MFC 100 which could only form semi-gel

under same condition.

3.3 Part C: Valorisation of Pea Vine Waste

3.3.1 Preliminary Composition of Ethyl Acetate Extract from SWE.

The GC-MS chromatogram of the ethyl acetate extract (EAE) of SWE is shown in Figure 3.3.1, and the major components are listed in Table 3.3.1. It can be observed that some major components in EAE, such as acetic acid, levoglucosenone, and 5-hydroxymethylfurfural, are characteristic of breakdown of cellulose and hemicellulose in biomass. The peak at 9 min is erroneous (propylene carbonate impurity).
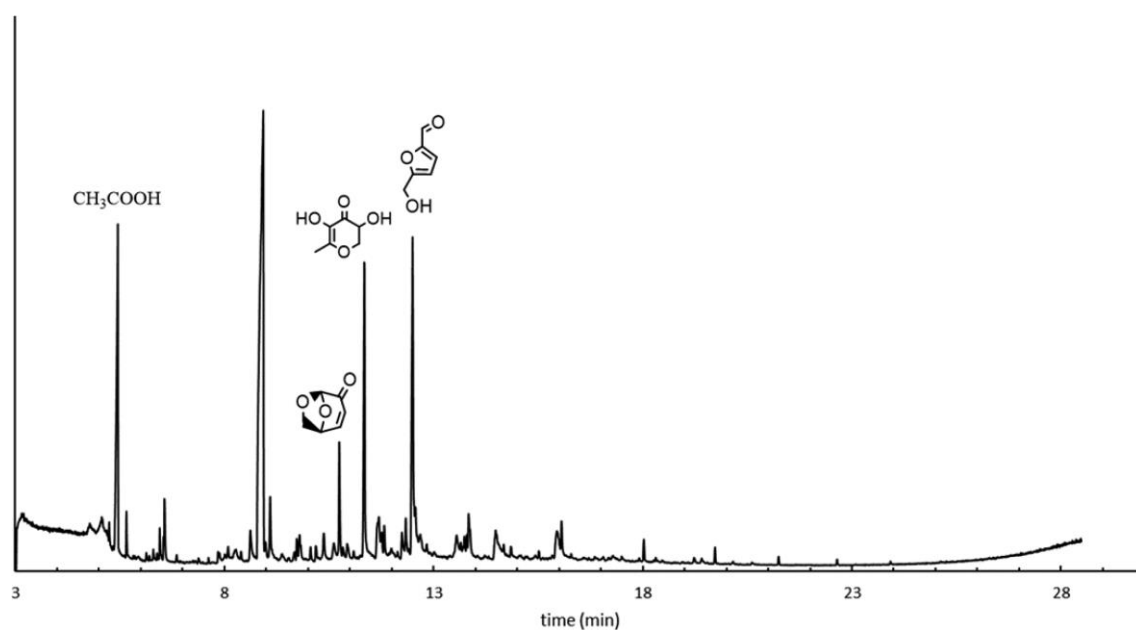
Figure 3.3.1 GC-MS chromatogram of ethyl acetate extract (125 °C SWE extract)

Table 3.3.1 Chemical composition of ethyl acetate extract (EAE)

Compound	Retention time (min)	Formula	Peak area (%)
Acetic acid	5.45	$C_2H_4O_2$	21.47
Levoglucosenone	10.74	$C_6H_6O_3$	4.62
2,3-Dihydro-3,5-dihydroxy-6-methyl-4H-pyran-4-one	11.34	$C_6H_8O_4$	17.60
5-Hydroxymethylfurfural	12.50	$C_6H_6O_3$	25.35

3.3.2 Sugar Analysis

The aqueous SWE liquors were analysed for sugars (Table 3.3.2) revealing the presence of glucose, fructose, sucrose, levoglucosan, rhamnose and xylose dependent on operating temperature. All sugars were obtained at 125 °C and the highest content of glucose, fructose and sucrose was observed at 150 °C. However, xylose was not detected at this temperature. Only levoglucosan, fructose, sucrose and glucose were observed at 175 °C (xylose and rhamnose were not detected).

Table 3.3.2 Sugar content in SWE extracts.

	Sugar Concentration (mg mL^{-1})					
	Levoglucosan	Rhamnose	Xylose	Fructose	Glucose	Sucrose
125 °C extract	5.93×10^{-2}	9.43×10^{-2}	4.98×10^{-3}	7.11	9.40	5.93
150 °C extract	1.03×10^{-1}	1.13×10^{-3}	ND*	8.51	11.41	7.67
175 °C extract	1.18×10^{-1}	ND	ND	6.41	9.12	3.15

*ND = not detected

3.3.3 SWE precipitate (ethanol insoluble biopolymer)

3.3.3.1 Yields

The yields of the pea vine waste precipitate (biopolymer) as a result of subcritical water extraction followed by ethanol precipitation is shown in Figure 3.3.2. The highest yield was achieved at a temperature of 175 $^{\circ}$C and a flow rate of 5 mL min^{-1}. In general, the lowest flow rate (1 mL min^{-1}) gave the lowest yields of precipitate irrespective of temperature except at 125 $^{\circ}$C where yield was marginally higher (6.54%) than 3 mL min^{-1} (6.39%). Similarly, high flow rates (5 mL min^{-1}) gave highest yields irrespective of temperature except at 150 $^{\circ}$C where a flow rate of 3 mL min^{-1} gave the highest yield (10.77%). At high temperature and flow rate (175 $^{\circ}$C and 5 mL min^{-1}) pseudo-subcritical water better penetrates the biomass and ruptures cell walls thus solubilizing more organic matter. Yields of 3.16 % and 2.86 % were achieved from CHE with HCl and citric acid as solvent respectively, which are much lower than the yields from SWE.

3.3.3.2 ATR-IR Analysis

The ATR-IR spectra of pea vine waste precipitates (biopolymers) isolated at different extraction temperatures are shown in Figure 3.3.3. Characteristic absorption bands for hydrogen-bonded hydroxyl groups (broad O-H stretch cantered around 3300 cm^{-1}), alkyl groups (C-H stretch at approximately 3000 cm^{-1}) and carbonyl groups (weak absorption band at approximately 1640 cm^{-1} which shows increasing intensity with increasing temperature). Thereafter, characteristic absorption bands are seen for C-C
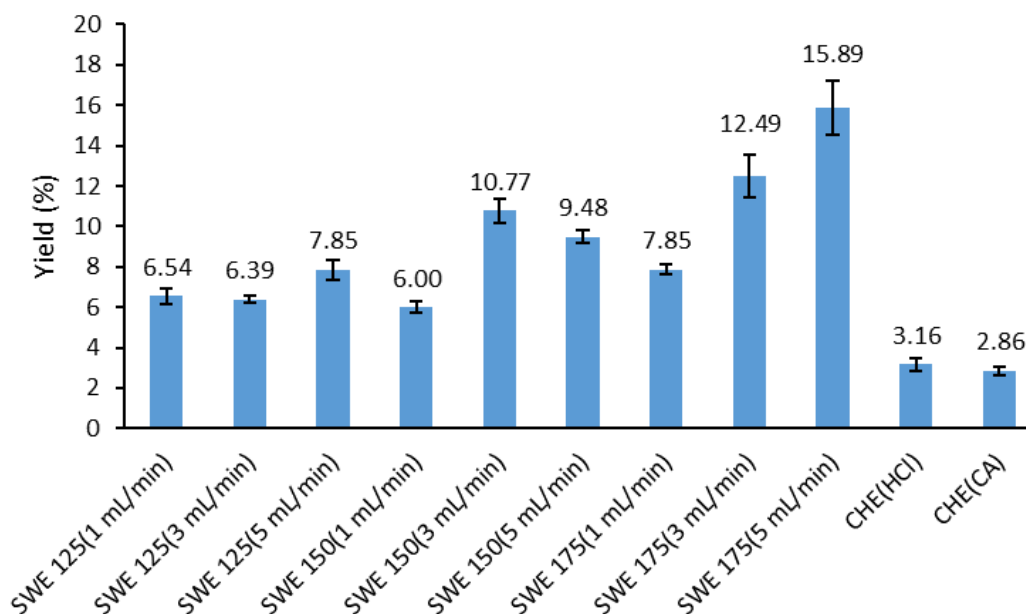
Figure 3.3.2 Yield of pea vine waste precipitates (biopolymer) with respect to extraction technique (original in color)

stretching at approximately 1450 cm^{-1} and intense C-O stretches between 1200 and 1000 cm^{-1} synonymous with a pectinaceous- and starch-like biopolymer.

Interestingly, additional weight is given to a possible pectinaceous-like material through the weak absorption band at 1730 cm^{-1}, detected only for the 150 °C and 175 °C biopolymers, characteristic of the methyl ester of galacturonic acid. The combination of carbonyl absorption bands at 1730 cm^{-1} (methyl ester) and 1640 cm^{-1} (free carboxylic acid) suggests the presence of pectinaceous matter, and the ratio of their peak areas indicates a very low degree of esterification for the pectinaceous matter.[149]
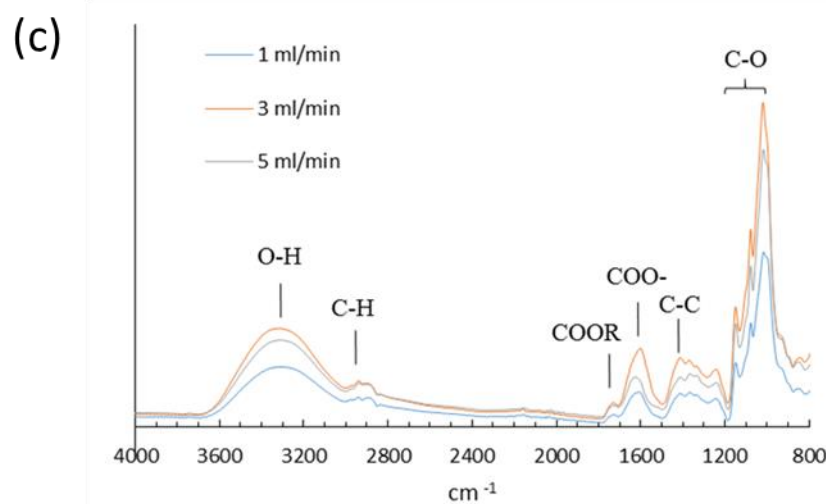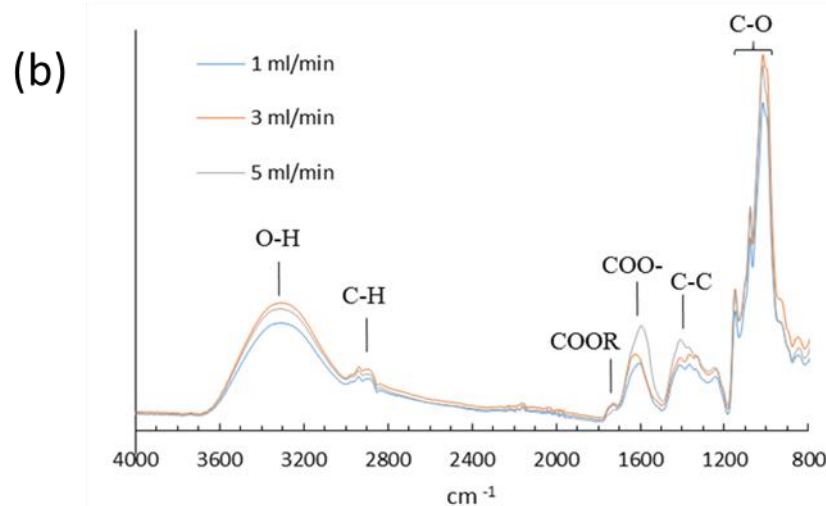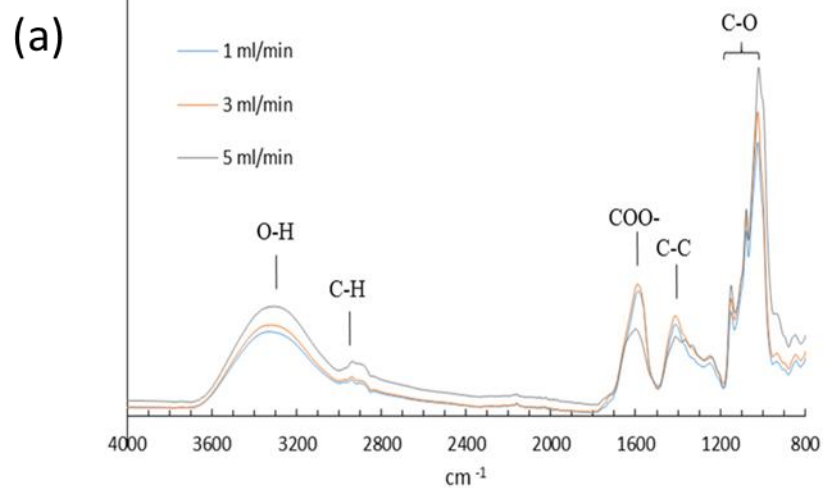
Figure 3.3.3 ATR-IR spectrum of pea vine waste biopolymers: (a) 125 ^{o}C; (b) 150 ^{o}C; (c) 175 ^{o}C. (original in color)

3.3.3.3 Thermogravimetric Analysis

TGA was performed to further ascertain the nature and thermal properties of the pea vine waste precipitate (biopolymer) as shown in Figures 3.3.4 and 3.3.5, respectively. In the absence of any available pea starch a sample of commercial rice starch was also tested for reference.
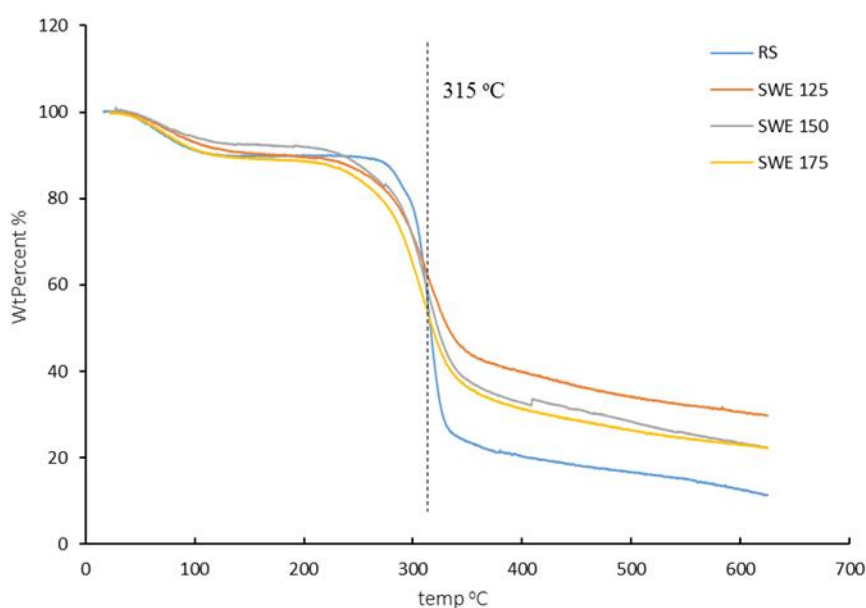
Figure 3.3.4 TGA traces for pea vine waste biopolymers and commercial starch (original in color)

The first mass loss ranging from 60 to 120 °C can be attributed to the removal of physisorbed water in the sample which is characteristic of many carbohydrates (~10 %) and evidenced for rice starch. The decomposition of rice starch (blue line) begins at around 260 °C and the peak decomposition temperature (shown in DTG) is 315 °C. The peak decomposition temperature of pea vine waste precipitate (biopolymer) is similar to that

of rice starch but on closer inspection shows a small shoulder developing from approximately 200 °C to 250 °C characteristic of decomposition of pectinaceous matter (pectin peak decomposition temperature at 250 °C).[150]
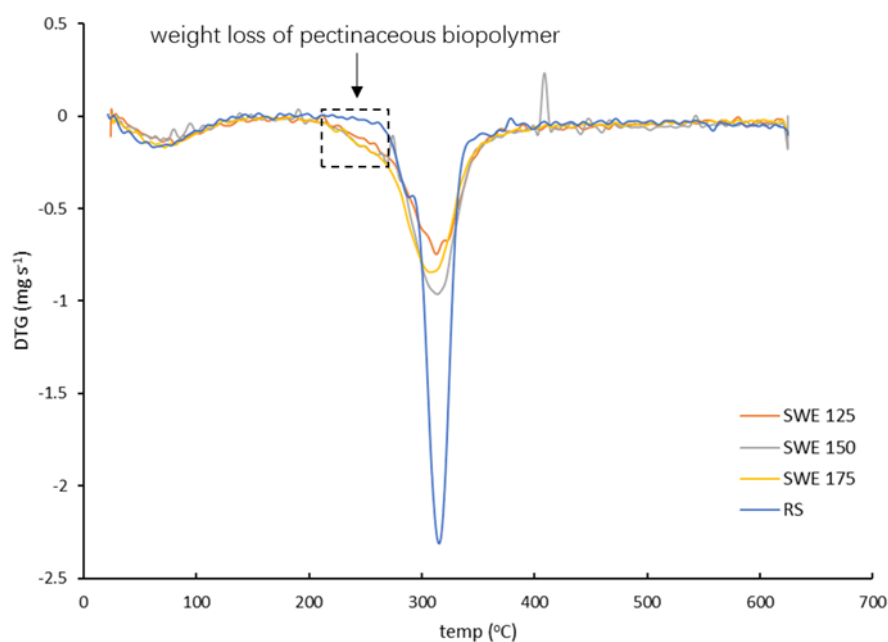
Figure 3.3.5 DTG traces for pea vine waste biopolymers and rice starch (original in color)

3.3.3.4 ^{13}C CP-MAS NMR Analysis

The solid-state ^{13}C CP-MAS NMR of pea vine waste precipitate (Figure 3.3.6) clearly shows a strong resonance at 174.27 ppm synonymous with the C-6 carbonyl (ester and carboxylic acid) carbon of pectinaceous matter. Furthermore, the resonances at 102.97 ppm and 82.21 ppm can be assigned to the anomeric C-1 carbon and C-4 carbon respectively. The intense peaks in the region of 60 to 90 ppm are from carbons of

pyranoid ring (C-2, 3, 5), while the weak resonance at 54.67 ppm is attributed to the methyl carbons of methyl ester (COO$\underline{C}$H$_3$).[151]
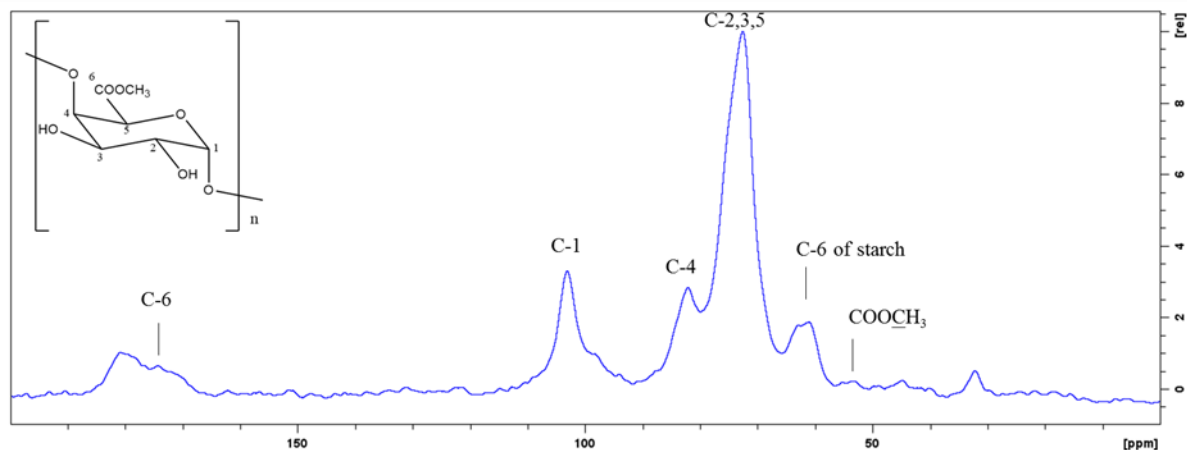
Figure 3.3.6 ^{13}C CP-MAS NMR spectrum of pea vine waste precipitate (175 °C) (original in color)

3.3.3.5 CHN Analysis

The pea vine waste biopolymers were subjected to element analysis and the results are listed in table 5.4. According to the nitrogen-to-protein conversion factor of 4.20[152], a maximum of 4.49 % of protein content is estimated in pea vine waste biopolymer. Therefore, an SDS-PAGE was performed for further analysis of protein. However, there was no clear band observed from the protein gel (see appendix III).

Table 3.3.3 Element and estimated protein content in pea vine waste biopolymers

	C (%)	H (%)	N (%)	Estimated protein (%)
SWE 125	32.49	4.83	1.07	4.49
SWE 150	36.12	5.37	0.88	3.68
SWE 175	36.38	5.31	0.99	4.17

3.3.4 Bio-oil Analysis

The bio-oil produced was analysed by GC-MS (Figure 3.3.7 and table 3.3.4). It can be observed from the chromatogram that most components detected in bio-oil were five-membered cyclic and phenolic-type compounds. The phenolic compounds such as 2-methoxy-phenol and 2,6-dimethoxy phenol are probably due to the decomposition of lignin.[153]
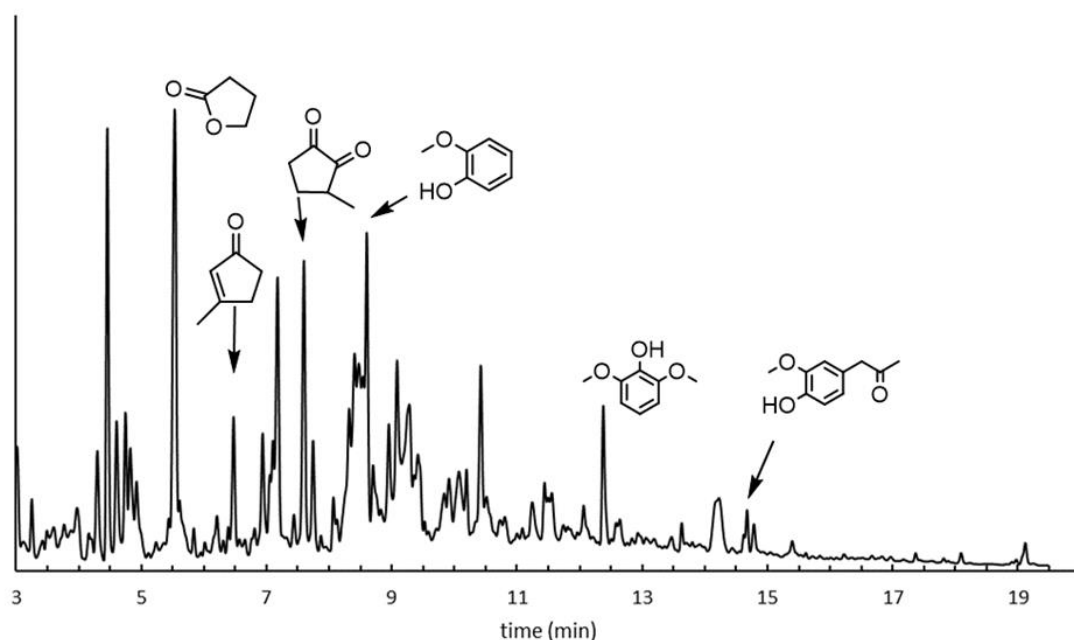
Figure 3.3.7 GC-MS chromatogram of bio-oil

Table 3.3.4 Chemical composition of bio-oil from microwave assisted pyrolysis

Compound	Retention time (min)	Formula	Peak area percent (%)
tetrahydrofuran-2-one	5.54	$C_4H_6O_2$	12.92
3-methylcyclopent-2-en-1-one	6.47	C_6H_8O	2.80
3-methyl-cyclopentane-1,2-dione	7.60	$C_6H_8O_2$	5.46
2-methoxy-phenol	8.60	$C_7H_8O_2$	19.15

| 2,6-dimethoxy phenol | 12.38 | $C_8H_{10}O_3$ | 2.68 |
| 3-(4-hydroxy-3-methoxyphenyl)-2-propanone | 14.67 | $C_{10}H_{12}O_3$ | 3.22 |

3.3.5 Calorific value Analysis

The pea vine waste, SWE solid residue and bio-char from microwave pyrolysis were subjected to calorific value analysis, achieving gross heat values of 16.0, 17.6 and 26.6 MJ kg^{-1} respectively. The gross heat value of pea vine waste bio-char is similar to that of other biomass,[154] and it is higher than many conventional biomass fuels (Figure 3.3.8),[155] which suggests its potential for use as a source of bioenergy.
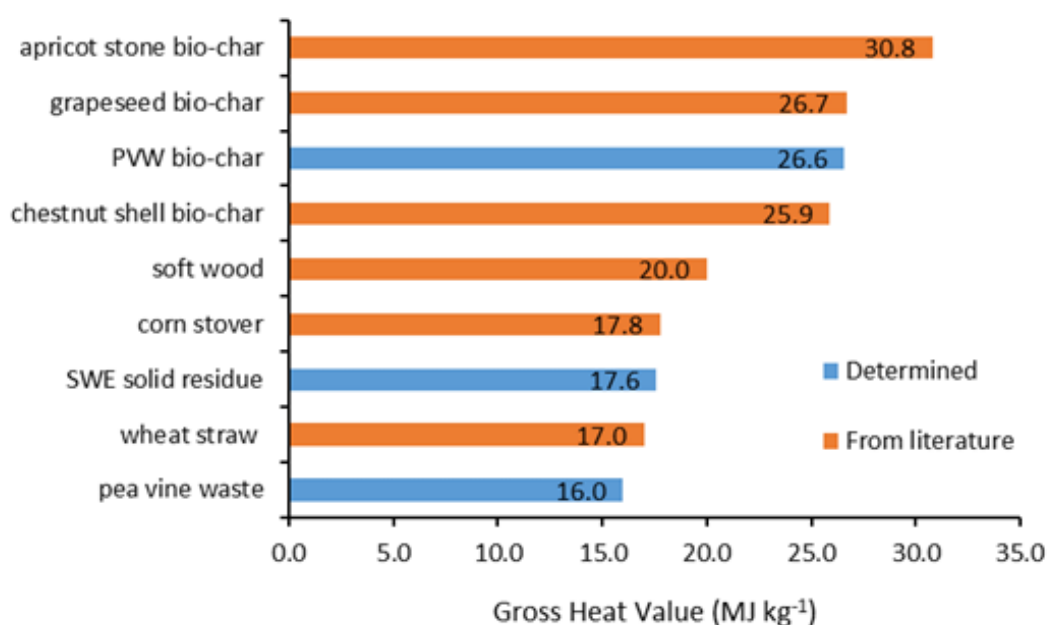
Figure 3.3.8 The gross heat value of pea vine waste, pea vine waste bio-char and comparison of other biomass and biochar (original in color)

3.3.6 Summary

This part explored the potential of pea vine waste as a source of valuable compounds. Subcritical water extraction was used as the primary extraction technique. Glucose, fructose and sucrose are the most abundant sugars in the SWE extract, and the 150 $^{\circ}$C extract gained the highest content of all these sugars with the concentration of 11.41, 8.51 and 7.67 mg mL^{-1} respectively. The major components in the ethyl acetate extract, such as acetic acid and 5-HMF, were predicted to be the decomposition products from cellulose or hemicellulose. The highest yield of pea vine waste biopolymer of 15.89 % was achieved at a temperature of 175 $^{\circ}$C and a flow rate of 5 mL min^{-1}. Starch is the main component of pea vine waste biopolymer, while there were also some small amounts of pectinaceous matter in the 150 $^{\circ}$C and 175 $^{\circ}$C biopolymers. The post SWE solid residue was subjected to microwave pyrolysis in order to produce a bio-oil and a bio-char. The bio-oil mainly consists of phenolic compounds such as 2-methoxy-phenol and 2,6-dimethoxy phenol from the decomposition of lignin, while the bio-char has a gross calorific value of 26.6 MJ kg^{-1}, which is higher than many conventional biomass fuels. Therefore, pea vine waste, as an easily accessible food supply chain waste, has great potential as a source of valuable compounds and bioenergy to achieve valorization within a biorefinery scheme.

Although the valorisation of pea vines wastes represents an exciting opportunity for chemicals, materials and energy many logistical challenges will need to be addressed

beforehand. As pea vine wastes are currently not collected then machinery will need to be developed of modified to collect wastes and transport to a valorisation site prior to decomposition. Alternatively, if the latter is not an immediate option then storage and stabilization of wet biomass will need to be considered which may be costly and/or reduce its chemical value over time.

Chapter 4
Conclusions and Future work

4.1 Greenness Content Assessment

4.1.1 Energy Consumption Assessment (PVW)

The energy consumption from SWE (175 °C) and CHE (80 °C) and their post-extraction work-up procedures was calculated and listed in Table 4.1. As the purifying process for both extraction techniques were same, the main difference of energy consumption between them was the extraction process, in which CHE consumed double energy as SWE did due to its long time of heating. When combined with the yield of biopolymer, it would consume 1.07 kWh for CHE (HCl, 80 °C) to produce 1.00 g of biopolymer, 2.7 times more than that for SWE (0.29 kWh for 175 °C and 3 mL min^{-1}). According to colleague's work (Eduardo Melo), it would consume 0.05 kWh at 120 °C and 0.21 kWh at 180 °C to produce 1.00 g of biopolymer (citrus peel MFC) Therefore, it can be concluded that both microwave extraction and subcritical water extraction have better efficiency for both solvent and energy usage than conventional heating extraction based on lab scale.

Table 4.1 Energy consumption of subcritical water extraction (175 °C) and conventional heating extraction (80 °C)

	SWE (175 °C)		CHE (80 °C)	
	Instrument	Energy consumption (kWh)	Instrument	Energy consumption (kWh)
Extraction	Oven (15 min)	0.12	Hot plate (2 h)	0.24
	Pump (15 min)	<0.01		

Purifying	Centrifuge × 2 (16 min, 3500 rpm)	0.04	Centrifuge × 2 (16 min, 3500 rpm)	0.04
	Hot plate (hot ethanol washing, 10 min)	0.02	Hot plate (hot ethanol washing, 10 min)	0.02
	Stirring	<0.01	Stirring	<0.01
Total		0.22		0.34

4.1.2 E-factor Analysis

E-factor is a concepted which refers to mass of waste/mass of product (usually expressed as kgs/kg in industry). This concept was first published in 1992 and since then it has been widely used for assessing the environmental impact on manufacturing processes.[156] The mass of waste and mass of products (pectin/ pertinacious matter) in this study are concluded in table 4.2.

Table 4.2 E-factor of all studied pectin/ pertinacious matter extraction techniques

Biomass	Extraction technique	Highest yield (mg)	Solvent Waste (g)	E-factor (g/g)
Mango peel	SWE flow system	915	87	95
	SWE batch system	435	331	761
	HL	880	268	305
Peach peel	CHE	175	331	1891
	MWE	375	55	147
	SWE batch	215	331	1539

	system			
Pea vine waste	SWE flow system	795	134	169
	CHE	160	331	2069

The solvent waste here is mainly the ethanol used for precipitating/ washing after the extraction. The hydrolysate (liquid residue after wash) did not count as waste here as it may be considered as the source for the extraction/ production of other chemicals. It can be seen from the chart that the SWE flow system has the lowest E-factor. MWE was also low in E-factor as it required least ethanol for washing process. The SWE batch system although achieved similar yield (%) with flow system, but it consumed much more solvent in work-up procedures. CHE had highest E-factor in all cases. It not only had huge solvent waste, but also resulted in lower yield compared with other extraction techniques. Therefore, from the perspective of greenness, SWE flow system and MWE are highly suggested rather than SWE batch system and CHE as extraction techniques for pectin from biomass.

4.2 Conclusion Based on the Obtained Results

4.2.1 Comparison of Three Biomass

4.2.1.1 Pectin

The pectin/ pectinaceous matter yields from all three biomass are summarised in table 4.3. Mango peel has the highest overall yield of pectin while peach peel has the lowest.

This is probably because of the difference of the thickness of peels between these two biomasses. Pea vine waste is much complicated compared with other two biomass as it is a combination of agricultural residues rather than just peels. Although decent amount of biopolymer was extracted with same method, the products were more like starch than pectin. As for degree of esterification, all the determined samples were all quite similar except the SWE batch system from peach peel. This may indicate that the condition is a bit too harsh for thin skin fruit. However, all the samples still had more than 50 % of DE which means pectin from peach peel and mango peel can both be considered as HM pectin.

The gelation test was also carried out for all three biomasses. Unfortunately, only pectin from peach peel (MWE) succeeded to form gel, while all the other samples were still semi-liquid.

Table 4.3 Yields and DE of pectin/ pectinaceous matter from all studied biomass and extraction techniques

Biomass	Extraction technique	Highest yield (%)	DE (%)
Mango peel	SWE flow system	8.1-18.3	76.4-82.4
	SWE batch system	2.1-8.7	/
	HL	1.4-17.6	/
Peach peel	CHE	3.5	72.5
	MWE	7.5	78.0
	SWE batch system	4.3	54.1
Pea vine waste	SWE flow system	6.0-15.9	/
	CHE	2.9-3.2	/

4.2.2.2 MFC

The main difference of MFC between mango peel and peach peel are the property of their hydrogel. For mango peel MFC, samples from all extraction temperature succeeded to form gel within very short time of stirring, while for peach peel MFC, only one sample was able to form gel even with the pretreatment for ultrasound (125 ºC). Such difference can also be found in their SEM/TEM figures. The SEM of peach peel MFC clearly showed the network structure of its hydrogel, while the TEM mango peel MFC (see appendix IV) was very blurry.

4.3 Limitations and Future Work

4.3.1 Regarding Subcritical water extraction

The flow system of subcritical water extraction is still in development and thus there might be some limitations that influence the quality of the products. For instance, the system would not pump the water into the reactor until it reached set temperature, which means especially under high extraction temperature, the raw materials in the reactor had undergone "pyrolysis" process for several minutes before they got in touch with water. This will probably degrade/ decompose some of the components in raw materials which may thus lead to the low yield of pectin. Meanwhile, compared with microwave extraction, the ramping time and cooling time cannot be precisely

controlled, which means the real processing time for high temperature extraction could be much longer compared with low temperature extraction. Another drawback of flow system was that the raw materials could not be milled too fine, otherwise it would go through the filter of the reactor and block the coil (system).

The batch system did not have the first problem as the raw materials were mixed in water all the time. But when it comes to ramping time, it took even long timer time to reach the set temperature (30 min to 175 $^\circ$C). This might explain why very little extracts yielded at extraction temperature higher than 150 $^\circ$C.

4.3.2 Regarding peach peel extraction

The simulation of lye peeling was carried out in order to mimic the industrial peeling process. The peel/ flesh started to turn into dark color very fast (within 30 s) although only 1 wt% of sodium hydroxide was used (see appendix V).

4.3.3 Regarding pea vine extraction

Pea vine waste was barely reported when the study started, so did the subcritical water extraction. The lack of enough background knowledge made it difficult the judge the property of the products although several characterisations were carried out. it turned out to be more like starch than pectin for the main extract, which made it less valuable depending on the market price. However, the calorific value of its biochar seemed to be quite good. Therefore, the study should probably focus a bit more on its pyrolysis

properties rather than extraction value.

4.3.4 Regarding Drying Method

Drying method is also an important issue that impact the quality of both pectin and MFC. The air drying is the easiest way and consumes the least energy, but it's very efficient as high amount of water could often be found in TGA data from air drying samples. Vacuum oven drying was very effective in removing water from samples, but it consumes much more energy. It can also be seen from SEM figures from peach peel MFC that even it was carried out under low temperature (<40 $^{\circ}$C), it still caused the aggregation of MFC samples, which made it much less porous. Freeze drying is the best method in theory, but it also has high energy consumption.

4.3.5 Future Work

The limitations mentioned in Chapter 4.3 also motivate future work. A lot of issues, from equipment to method, are worth considering for improvements.

Firstly, the equipment for SWE extraction needs to be improved. A more efficient heating source is recommended for both systems to shorten the ramping time. For flow system, a proper particle size of raw material is suggested to investigate while for batch system, the ratio of raw materials and water is suggested to explored in order the minimized the solvent consumption used for precipitating/ washing. Scaling-up issues should also be considered especially for the flow system, but it may also lead to more

water/ ethanol consumption. The efficiency and e-factor should be carefully considered.

For the pectin extracted from all biomass in this study, the gelation test did not result well as only MWE from peach peel pectin succeeded to form gels. It was noticeable that all the pectin samples in this study were (dark) brown when heating with sugar and buffer. Meanwhile, orange peel (a common source of industrial pectin) are usually (light) yellow under same condition. Therefore, it is suggested to investigate whether it is the pigment or other impurities in mango/ peach peel pectin that affected its gelation, or if the gelation method itself needed to be improved.

As for MFC, a lot of works can be considered to carried out in the future. As mentioned earlier, the TEM of mango peel MFC was very blurry but still all the samples formed hydrogels really well compared with peach peel, which only one of the samples barely form gel but clearly showed the network structure on its SEM figures. Some more characterisations, such as N_2 adsorption porosimetry, gel permeation chromatography and rheology study of hydrogels are highly recommended to investigate the reason of such difference. Meanwhile, apart from hydrogel, other potential applications of MFC, such as films and supercapacitors (mentioned in chapter 1.3.2), should also be explored.

Last but not least, FSCW valorisation should not be limited extraction of pectin/ MFC only. Many other by-products should also be explored during the whole valorisation process. Therefore, a more efficient overall proposal for FSCW biorefinery is designed and showed in Figure 4.1. This aims to achieve a real "zero-waste" valorisation. Thus,

waste to landfill is minimised, resource is recovered and re-used promoting a future

circular economy and is commensurate with UN Sustainable Development Goals.
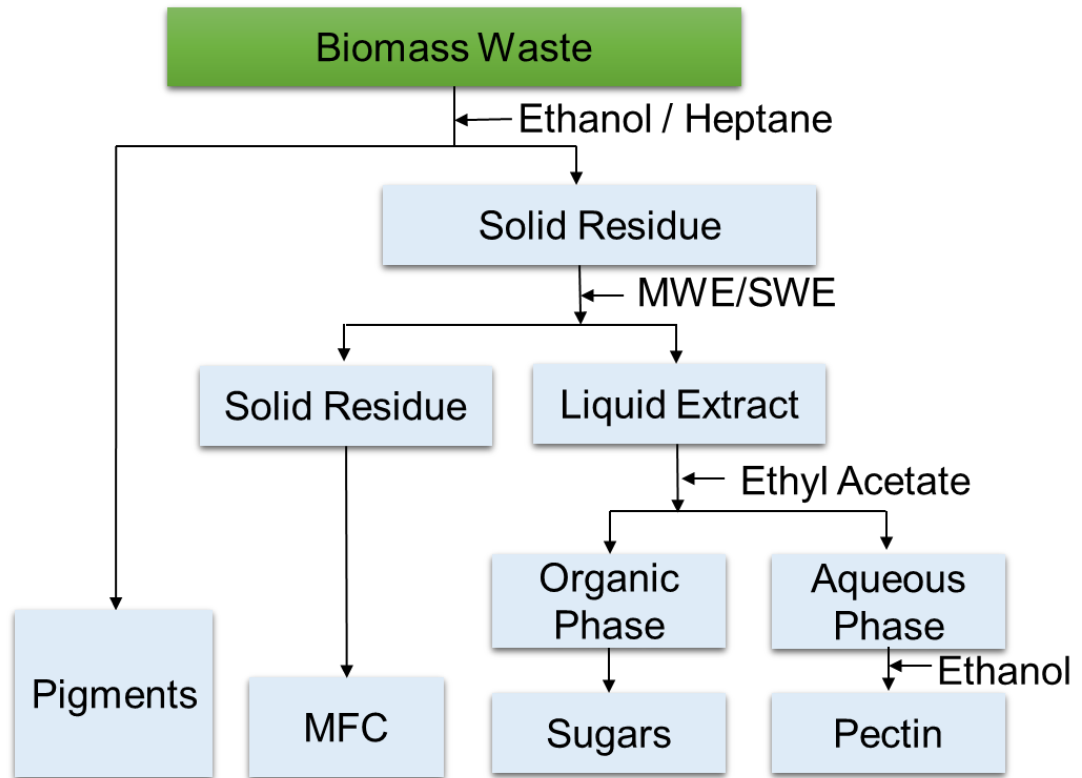
Figure 4.1   A proposed model for a more efficient zero-waste biomass biorefinery
(original in color)

Reference

1   C. Tortajada and A. K. Biswas, *Int. J. Water Resour. Dev.*, 2018, **34**, 147–149.

2   A. Zabaniotou, *J. Clean. Prod.*, 2018, **177**, 197–206.

3   P. Morone, A. Koutinas, N. Gathergood, M. Arshadi and A. Matharu, *J. Clean. Prod.*, 2019, **221**, 10–16.

4   M. B. Cole, M. A. Augustin, M. J. Robertson and J. M. Manners, *npj Sci. Food*, 2018, **14**, 1–8.

5   The General Assembly, Transforming our world : the 2030 Agenda for Sustainable Development, https://www.un.org/ga/search/view_doc.asp?symbol =A/RES/70/1&Lang=E, (accessed 23 January 2020).

6   J. Blesh, L. Hoey, A. D. Jones, H. Friedmann and I. Perfecto, *World Dev.*, 2019, **118**, 1–14.

7   S. Corrado, C. Caldeira, M. Eriksson, O. J. Hanssen, H. E. Hauser, F. van Holsteijn, G. Liu, K. Östergren, A. Parry, L. Secondi, Å. Stenmarck and S. Sala, *Glob. Food Sec.*, 2019, **20**, 93–100.

8   K. H. Olsen, F. Bakhtiari, V. K. Duggal and J. V. Fenhann, *Int. Environ. Agreements Polit. Law Econ.*, 2019, **19**, 225–251.

9   L. A. Pfaltzgraff, M. De Bruyn, E. C. Cooper, V. Budarin and J. H. Clark, *Green Chem.*, 2013, **15**, 307–314.

10   L. a Pfaltzgraff, M. De bruyn, E. C. Cooper, V. Budarin and J. H. Clark, *Green Chem.*, 2013, **15**, 307–314.

11   J. Webb, T. H. Misselbrook and T. Tscharntke, *Foresight. The Future of Food and Farming: Challenges and choices for global sustainability*, 2011, vol. 149.

12   Food and Agriculture Organization of the United Nations (FAO), *Food wastage footprint*, 2013.

13   Food and Agriculture Organization of the United Nations (FAO), *Food wastage footprint & Climate Change Global food loss and waste*, 2015.

14   F. and R. A. C. House of Commons, Environment, *House of Commons*.

15   WRAP, Food Surplus and Waste in the UK – key facts, http://www.wrap.org.uk/sites/files/wrap/Food_surplus_and_waste_in_the_UK_ key_facts_Jan_2020.pdf, (accessed 23 January 2020).

16   F. Cherubini, *Energy Convers. Manag.*, 2010, **51**, 1412–1421.

17   J. T. Keränen and E. A. Retulainen, *BioResources*, 2016, **11**, 10625–10653.

18   W. Wardencki, J. Curyło and J. Namiesśnik, *Polish J. Environ. Stud.*

19   P. T. Anastas and J. C. Warner, *Green chemistry: theory and practice*, Oxford university press, 2000.

20   C. S. K. Lin, L. A. Pfaltzgraff, L. Herrero-Davila, E. B. Mubofu, S. Abderrahim, J. H. Clark, A. A. Koutinas, N. Kopsahelis, K. Stamatelatou, F. Dickson, S. Thankappan, Z. Mohamed, R. Brocklesby and R. Luque, *Energy Environ. Sci.*, 2013, **6**, 426–464.

21   P. Sriamornsak, *Silpakorn Univ. Int. J.*, 2003, **3**, 206–228.

22   D. Mohnen, *Curr. Opin. Plant Biol.*, 2008, **11**, 266–277.

23   D. B. Pedrolli, A. C. Monteiro, E. Gomes and E. C. Carmona, *Open Biotechnol. J.*, 2009, **3**, 9–18.

24   B. L. Ridley, M. A. O'Neill and D. Mohnen, *Phytochemistry*, 2001, **57**, 929–967.

25   J. Harholt, A. Suttangkakul and H. V. Scheller, *Plant Physiol.*, 2010, **153**, 384–395.

26   A. A. Sundar Raj, S. Rubila, R. Jayabalan and T. V Ranganathan, *Sci. Rep.*, 2012, **1**, 550–551.

27   G. D. Manrique and F. M. Lajolo, *Postharvest Biol. Technol.*, 2002, **25**, 99–107.

28   C. D. May, *Carbohydr. Polym.*, 1990, **12**, 79–99.

29   B. R. Thakur, R. K. Singh, A. K. Handa and M. A. Rao, *Crit. Rev. Food Sci. Nutr.*, 1997, **37**, 47–73.

30   U. Einhorn-Stoll, *Food Hydrocoll.*, 2018, **78**, 109–119.

31   Y. Xu, L. Zhang, Y. Bailina, Z. Ge, T. Ding, X. Ye and D. Liu, *J. Food Eng.*, 2014, **126**, 72–81.

32   A. Rehman, T. Ahmad, R. M. Aadil, M. J. Spotti, A. M. Bakry, I. M. Khan, L. Zhao, T. Riaz and Q. Tong, *Trends Food Sci. Technol.*, 2019, **90**, 35–46.

33   T. Vanitha and M. Khan, in *Pectins - Extraction, Purification, Characterization and Applications [Working Title]*, IntechOpen, 2019, pp. 1–21.

34   A. N. Grassino, F. J. Barba, M. Brnčić, J. M. Lorenzo, L. Lucini and S. R. Brnčić, *Food Chem.*, 2018, **266**, 47–55.

35   Global Info Research, Global Pectin Market by Manufacturers, Regions, Type

and Application, Forecast to 2021, https://bit.ly/2VrN0nM.

36   B. B. Koubala, G. Kansci, L. I. Mbome, M.-J. Crépeau, J.-F. Thibault and M.-C. Ralet, *Food Hydrocoll.*, 2008, **22**, 1345–1351.

37   J. Pagan, A. Ibarz, M. Llorca, A. Pagan and G. V Barbosa-Cánovas, *Food Res. Int.*, 2001, **34**, 605–612.

38   I. M. D. A. Silva, L. V Gonzaga, E. R. Amante, R. F. Teófilo, M. M. C. Ferreira, R. D. M. C. Amboni and others, *Bioresour. Technol.*, 2008, **99**, 5561–5566.

39   B. M. Yapo, C. Robert, I. Etienne, B. Wathelet and M. Paquot, *Food Chem.*, 2007, **100**, 1356–1364.

40   M. L. Fishman, P. Cooke, B. Levaj, D. T. Gillespie, S. M. Sondey and R. Scorza, *Arch. Biochem. Biophys.*, 1992, **294**, 253–260.

41   X. Q. Shi, K. C. Chang, J. G. Schwarz, D. P. Wiesenborn and M. C. Shih, *Bioresour. Technol.*, 1996, **58**, 291–297.

42   Y. Wandee, D. Uttapap and P. Mischnick, *Food Hydrocoll.*, 2019, **87**, 237–244.

43   X. Yang, T. Nisar, D. Liang, Y. Hou, L. Sun and Y. Guo, *Food Hydrocoll.*, 2018, **79**, 560–571.

44   S. S. Hosseini, F. Khodaiyan, M. Kazemi and Z. Najari, *Int. J. Biol. Macromol.*, 2019, **125**, 621–629.

45   A. N. Grassino, M. Brnčić, D. Vikić-Topić, S. Roca, M. Dent and S. R. Brnčić, *Food Chem.*, 2016, **198**, 93–100.

46   Y. Liu, J. Shi and T. A. G. Langrish, *Chem. Eng. J.*, 2006, **120**, 203–209.

47   J. P. Maran, K. Swathi, P. Jeevitha, J. Jayalakshmi and G. Ashvini, *Carbohydr. Polym.*, 2015, **123**, 67–71.

48   M. Kazemi, F. Khodaiyan, M. Labbafi, S. Saeid Hosseini and M. Hojjati, *Food Chem.*, 2019, **271**, 663–672.

49   M. L. Fishman, H. K. Chau, P. D. Hoagland and A. T. Hotchkiss, *Food Hydrocoll.*, 2006, **20**, 1170–1177.

50   M. L. Fishman, H. K. Chau, A. T. Hotchkiss, A. White, R. A. Garcia and P. H. Cooke, *Food Hydrocoll.*, 2019, **92**, 104–116.

51   X. Wang, Q. Chen and X. Lü, *Food Hydrocoll.*, 2014, **38**, 129–137.

52   H. Ueno, M. Tanaka, M. Hosino, M. Sasaki and M. Goto, *Sep. Purif. Technol.*, 2008, **62**, 513–516.

53   S. Q. Liew, W. H. Teoh, C. K. Tan, R. Yusoff and G. C. Ngoh, *Int. J. Biol. Macromol.*, 2018, **116**, 128–135.

54   W. J. Li, Z. G. Fan, Y. Y. Wu, Z. G. Jiang and R. C. Shi, *J. Sci. Food Agric.*, , DOI:10.1002/jsfa.9729.

55   M. Poletto, H. L. Ornaghi Júnior and A. J. Zattera, *Materials (Basel).*, 2014, **7**, 6105–6119.

56   M. Ioelovich, *BioResources*, 2008, **3**, 1403–1418.

57   Y. Habibi, L. A. Lucia and O. J. Rojas, *Chem. Rev.*, 2010, **110**, 3479–3500.

58   G. Chinga-Carrasco, *Nanoscale Res. Lett.*, 2011, **6**, 1–7.

59   I. Siró and D. Plackett, *Cellulose*, 2010, **17**, 459–494.

60   S. H. Osong, S. Norgren and P. Engstrand, *Cellulose*, 2016, **23**, 93–123.

61   O. Nechyporchuk, M. N. Belgacem and J. Bras, *Ind. Crops Prod.*, 2016, **93**, 2–25.

62   M. N. F. Norrrahim, H. Ariffin, T. A. T. Yasim-Anuar, F. Ghaemi, M. A. Hassan, N. A. Ibrahim, J. L. H. Ngee and W. M. Z. W. Yunus, *Cellulose*, 2018, **25**, 3853–3859.

63   C. Holland, A. Perzon, P. R. C. Cassland, J. P. Jensen, B. Langebeck, O. B. Sørensen, E. Whale, D. Hepworth, R. Plaice-Inglis, Ø. Moestrup, P. Ulvskov and B. Jørgensen, *Biomacromolecules*, 2019, **20**, 443–453.

64   M. Jonoobi, R. Oladi, Y. Davoudpour, K. Oksman, A. Dufresne, Y. Hamzeh and R. Davoodi, *Cellulose*, 2015, **22**, 935–969.

65   A. M. Adel, A. A. El-Gendy, M. A. Diab, R. E. Abou-Zeid, W. K. El-Zawawy and A. Dufresne, *Ind. Crops Prod.*, 2016, **93**, 161–174.

66   C. Gómez H., A. Serpa, J. Velásquez-Cock, P. Gañán, C. Castro, L. Vélez and R. Zuluaga, *Food Hydrocoll.*, 2016, **57**, 178–186.

67   S. Hindi, *Nanosci. Nanotechnol. Res.*, 2017, **4**, 17–24.

68   Ç. Meriçer, M. Minelli, M. G. D. Angelis, M. Giacinti Baschetti, A. Stancampiano, R. Laurita, M. Gherardi, V. Colombo, J. Trifol, P. Szabo and T. Lindström, *Ind. Crops Prod.*, 2016, **93**, 235–243.

69   M. M. Pérez-Madrigal, M. G. Edo and C. Alemán, *Green Chem.*, 2016, **18**, 5930–5956.

70   N. Grishkewich, N. Mohammed, J. Tang and K. C. Tam, *Curr. Opin. Colloid Interface Sci.*, 2017, **29**, 32–45.

71   Markets and Markets, *Global Nanocellulose Market - Forecast until 2019*, 2015.

72   L. Axelsson, M. Franzén, M. Ostwald, G. Berndes, G. Lakshmi and N. H. Ravindranath, *Biofuels, Bioprod. Biorefining*, 2012, **6**, 246–256.

73   R. Kapoore, T. Butler, J. Pandhal and S. Vaidyanathan, *Biology (Basel).*, 2018, **7**, 18.

74   W. Routray and V. Orsat, *Food Bioprocess Technol.*, 2012, **5**, 409–424.

75   K. E. Haque, *Int. J. Miner. Process.*, 1999, **57**, 1–24.

76   F. Chemat, N. Rombaut, A. Meullemiestre, M. Turk, S. Perino, A. S. Fabiano-Tixier and M. Abert-Vian, *Innov. Food Sci. Emerg. Technol.*, 2017, **41**, 357–377.

77   D. A. Jones, T. P. Lelyveld, S. D. Mavrofidis, S. W. Kingman and N. J. Miles, *Resour. Conserv. Recycl.*, 2002, **34**, 75–90.

78   S. Périno, J. T. Pierson, K. Ruiz, G. Cravotto and F. Chemat, *Food Chem.*, 2016, **204**, 108–114.

79   A. Filly, X. Fernandez, M. Minuti, F. Visinoni, G. Cravotto and F. Chemat, *Food Chem.*, 2014, **150**, 193–198.

80   G. Garcia-Garcia, S. Rahimifard, A. S. Matharu and T. I. J. Dugmore, *ACS Sustain. Chem. Eng.*, 2019, **7**, 5167–5175.

81   A. G. Carr, R. Mammucari and N. R. Foster, *Chem. Eng. J.*, 2011, **172**, 1–17.

82   A. H. Asl and M. Khajenoori, in *Mass Transfer - Advances in Sustainable Energy*

and Environment Oriented Numerical Modeling, 2013, pp. 459–487.

83   P. Bocchiaro and A. Zamperini, in *Mass Transfer—Advances in Sustainable Energy and Environment Oriented Numerical Modeling*, ed. N. Hironori, 2013.

84   M. J. Ko, H. L. Kwon and M. S. Chung, *Innov. Food Sci. Emerg. Technol.*, 2016, **38**, 175–181.

85   H. L. Kwon and M. S. Chung, *Food Chem.*, 2015, **185**, 58–64.

86   B. K. Tiwari, *TrAC - Trends Anal. Chem.*, 2015, **71**, 100–109.

87   F. Chemat, N. Rombaut, A. G. Sicaire, A. Meullemiestre, A. S. Fabiano-Tixier and M. Abert-Vian, *Ultrason. Sonochem.*, 2017, **34**, 540–560.

88   W. Sitzmann, E. Vorobiev and N. Lebovka, 2016, **37**, 302–311.

89   F. J. Barba, O. Parniakov, A. Pereira, A. Wiktor, N. Grimi, N. Boussetta, J. A. Saraiva, J. Raso, O. Martin-belloso, D. Witrowa-rajchert, N. Lebovka and E. Vorobiev, 2015, **77**, 773–798.

90   F. J. Barba, Z. Zhu, M. Koubaa and A. S. Sant, *Trends Food Sci. Technol.*, 2016, **49**, 96–109.

91   S. Toepfl, *Ital. Oral Surg.*, 2011, **1**, 776–779.

92   N. Berardini, M. Knödler, A. Schieber and R. Carle, *Innov. Food Sci. Emerg. Technol.*, 2005, **6**, 442–452.

93   A. J. Perea-Moreno, M. Á. Perea-Moreno, M. P. Dorado and F. Manzano-Agugliaro, *J. Clean. Prod.*, 2018, **190**, 53–62.

94   C. M. Ajila, K. A. Naidu, S. G. Bhat and U. J. S. P. Rao, *Food Chem.*, 2007, **105**,

982–988.

95   M. H. A. Jahurul, I. S. M. Zaidul, K. Ghafoor, F. Y. Al-Juhaimi, K. L. Nyam, N. A. N. Norulaini, F. Sahena and A. K. Mohd Omar, *Food Chem.*, 2015, **183**, 173–180.

96   H. Castro-Vargas, D. Ballesteros Vivas, J. Ortega Barbosa, S. Morantes Medina, F. Aristizabal Gutiérrez and F. Parada-Alfonso, *Antioxidants*, 2019, **8**, 41.

97   C. M. Ajila, K. Leelavathi and U. J. S. Prasada Rao, *J. Cereal Sci.*, 2008, **48**, 319–326.

98   C. D. G. Sampaio, J. Gaspar, A. E. Silva, E. S. De Brito, H. Becker, M. Teresa, S. Trevisan, R. W. Owen, R. W. Owen and H. Becker, *J. Exp. Agric. Int.*, 2019, **26**, 5588–5600.

99   A. Haq, M. Saeed, M. Usman and M. Yameen, *Green Process. Synth.*, 2019, **8**, 337–347.

100   L. S. Silva, E. H. Mizobutsi, G. P. Mizobutsi, D. F. De Oliveira, V. Aparecida, C. Campos, F. P. Monção, R. Cássia, F. Ribeiro, M. Paz, S. Câmara, M. Luísa and M. Rodrigues, *J. Exp. Agric. Int.*, 2019, **32**, 1–8.

101   E. M. Coelho, M. Eduardo, A. Olinda, L. Claudio, L. Cavalcanti, D. Azev and S. Lima, *Antioxidants*, 2019, **8**, 1–11.

102   W. H. S. Z.U. Rehman, A.M. Salariya, F. Habib, *Jour.Chem.Soc.Pak.*, 2004, **26**, 73–76.

103   N. Berardini, R. Fezer, J. Conrad, U. Beifuss, R. Carl and A. Schieber, *J. Agric.*

Food Chem., 2005, **53**, 1563–1570.

104   D. V. Sudhakar and S. B. Maini, *J. Food Process. Preserv.*, 2000, **24**, 209–227.

105   B. B. Koubala, G. Kansci, L. I. Mbome, M. J. Cr??peau, J. F. Thibault and M. C. Ralet, *Food Hydrocoll.*, 2008, **22**, 1345–1351.

106   Z. Jamsazzadeh Kermani, A. Shpigelman, H. T. T. Pham, A. M. Van Loey and M. E. Hendrickx, *Food Hydrocoll.*, 2015, **44**, 424–434.

107   M. Wang, B. Huang, C. Fan, K. Zhao, H. Hu, X. Xu, S. Pan and F. Liu, *Int. J. Biol. Macromol.*, 2016, **91**, 794–803.

108   J. P. Maran, K. Swathi, P. Jeevitha, J. Jayalakshmi and G. Ashvini, *Carbohydr. Polym.*, 2015, **123**, 67–71.

109   J. Banerjee, R. Singh, R. Vijayaraghavan, D. MacFarlane, A. F. Patti and A. Arora, *Food Hydrocoll.*, 2018, **77**, 142–151.

110   A. S. Matharu, J. A. Houghton, C. Lucas-Torres and A. Moreno, *Green Chem.*, 2016, **337**, 695–699.

111   U. In, C. Production, U. Solid and S. Cultivation, 2011, **6**, 1505–1519.

112   R. Affairs, T. S. Government, A. Directorate and W. A. Government, .

113   O. Santana-Méridas, A. González-Coloma and R. Sánchez-Vioque, *Phytochem. Rev.*, 2012, 11, 447–466.

114   Feedipedia, Pea Forage, https://www.feedipedia.org/node/7047#description, (accessed 23 January 2020).

115   A. Torcello-Gómez, M. A. Gedi, R. Ibbett, K. Nawaz Husain, R. Briars and D.

Gray, *Food Chem.*, 2019, **272**, 18–25.

116   P. R. Nimbalkar, M. A. Khedkar, P. V. Chavan and S. B. Bankar, *Renew. Energy*, 2018, **117**, 520–529.

117   I. Mateos-aparicio and A. Redondo-cuenca, *LWT - Food Sci. Technol.*, 2010, **43**, 1467–1470.

118   J. Anwar, U. Shafique, M. Salman, Z. Hussain, M. Saleem, N. Shahid, S. Mahboob, M. Akram, R. Rehman, N. Jamil, J. Anwar, U. Shafique and M. Salman, , DOI:10.1080/17518251003730833.

119   T. A. Khan, R. Rahman, I. Ali, E. A. Khan and A. Amer, *Toxicol. Environ. Chem.*, 2014, **96**, 569–578.

120   FAO,   Global   Peach   Prduction   2017, http://www.fao.org/faostat/en/#data/QC/visualize, (accessed 23 January 2020).

121   G. G. Santonja, P. Karlis, K. R. Stubdrup, T. Brinkmann and S. Roudier, *Best Available Techniques Reference document on food, drink and milk industries*, 2019.

122   X. Zhao, W. Zhang, X. Yin, M. Su, C. Sun, X. Li and K. Chen, *Int. J. Mol. Sci.*, 2015, **16**, 5762–5778.

123   F. Muradoğlu and O. Küçük, *J. Anim. Plant Sci.*, 2018, **28**, 533–538.

124   B. T. Stojanovic, S. S. Mitic, G. S. Stojanovic, M. N. Mitic, D. A. Kostic, D. D. Paunovic and B. B. Arsic, *Not. Bot. Horti Agrobot. Cluj-Napoca*, 2016, **44**, 175–182.

125   M. Manzoor, F. Anwar, Z. Mahmood, U. Rashid and M. Ashraf, *Molecules*, 2012, **17**, 6491–6506.

126   H. Zhou, Z. Yu and Z. Ye, *Sci. Hortic. (Amsterdam).*, 2018, **239**, 123–132.

127   N. Ajmal, K. Saraswat, M. A. Bakht, Y. Riadi, M. J. Ahsan and M. Noushad, *Green Chem. Lett. Rev.*, 2019, **12**, 244–254.

128   A. Mizote, H. Odagiri, K. Toei and K. Tanaka, *Analyst*, 1975, **100**, 822–826.

129   A. K. Pathan, J. Bond and R. E. Gaskin, *Mater. Today*, 2009, **12**, 32–43.

130   H. Li, X. Y. Tang, C. J. Wu and S. J. Yu, *LWT - Food Sci. Technol.*, 2019, **105**, 156–163.

131   F. C. De Melo, R. F. De Souza, P. L. A. Coutinhob and M. O. De Souza, *J. Braz. Chem. Soc.*, 2014, **25**, 2378–2384.

132   Magritek, *Characterizing Fatty Acids with advanced multinuclear NMR methods*, 2018, vol. 6.

133   P. Bhaumik and P. L. Dhepe, *RSC Adv.*, 2013, **3**, 17156–17165.

134   F. R. Tao, C. Zhuang, Y. Z. Cui and J. Xu, *Chinese Chem. Lett.*, 2014, **25**, 757–761.

135   A. R. K. Gollakota, N. Kishore and S. Gu, *Renew. Sustain. Energy Rev.*, 2018, **81**, 1378–1392.

136   B. Abderrahim, E. Abderrahman, A. Mohamed, T. Fatima, T. Abdesselam and O. Krim, *World J. Environ. Eng. Vol. 3, 2015, Pages 95-110*, 2015, **3**, 95–110.

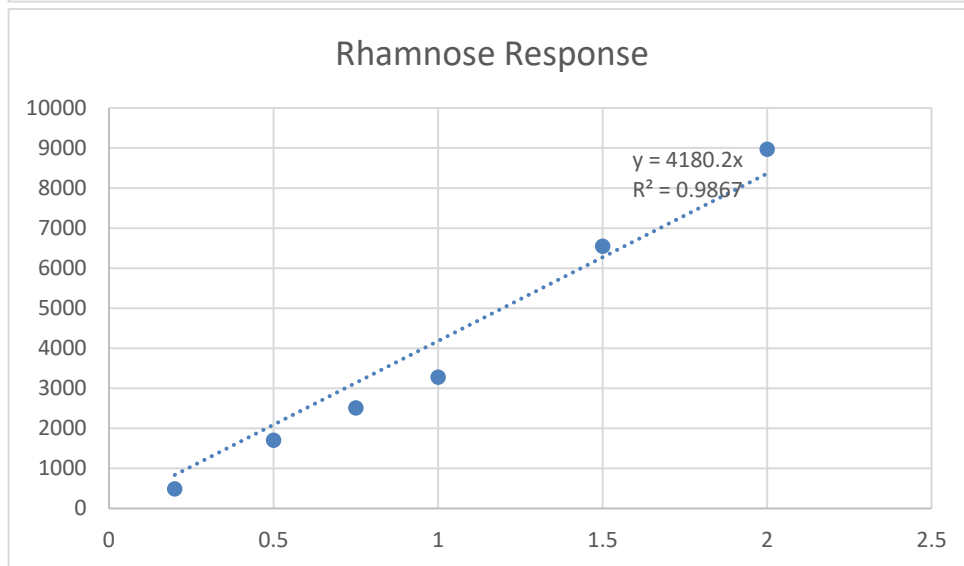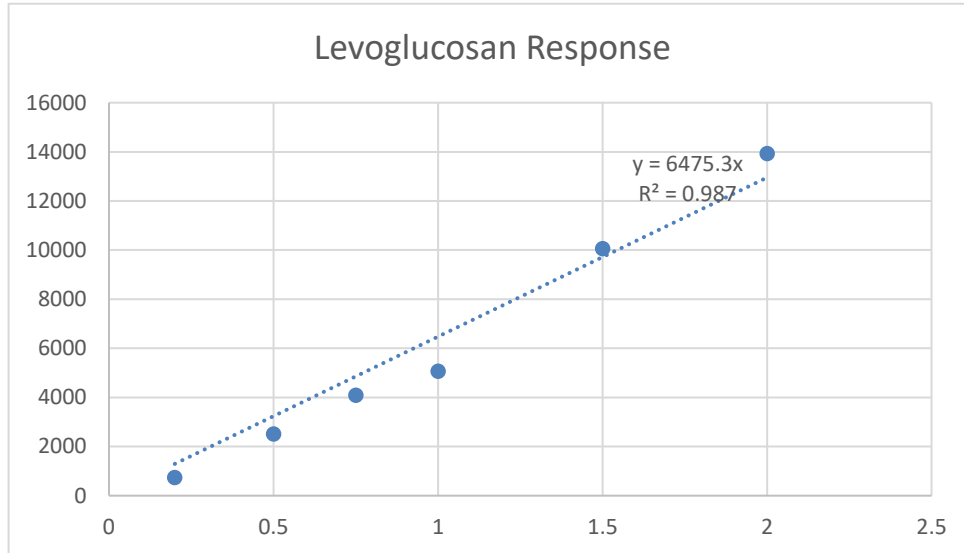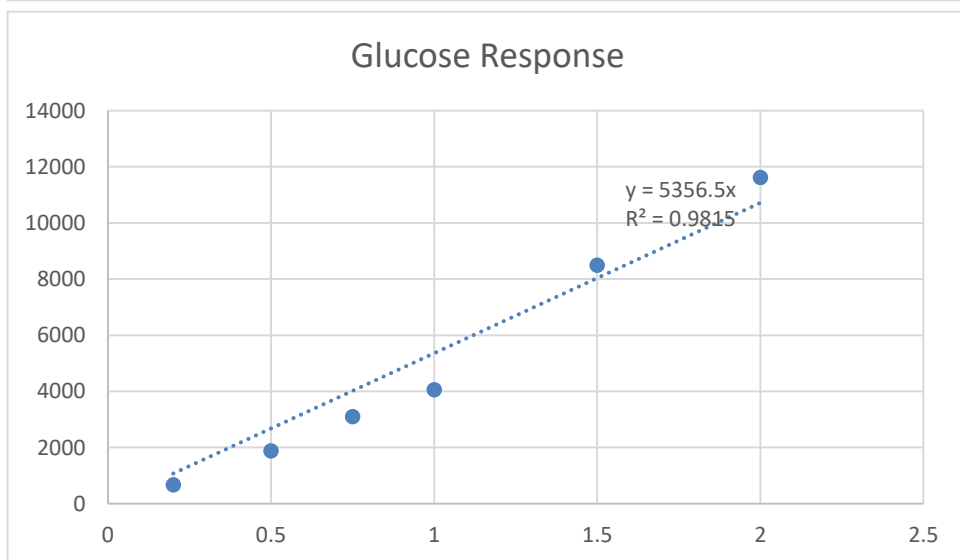137   K. Okushita, T. Komatsu, E. Chikayama and J. Kikuchi, *Polym. J.*, 2012, **44**,
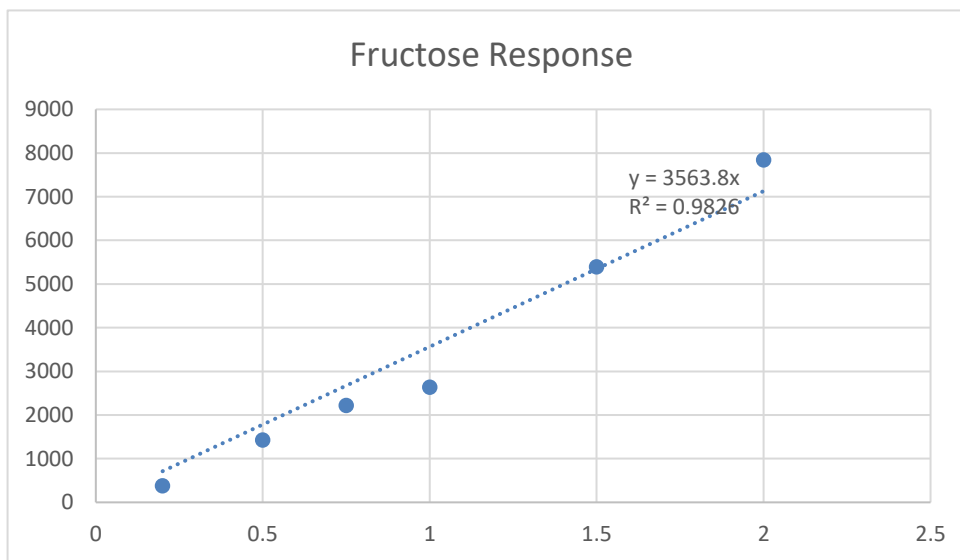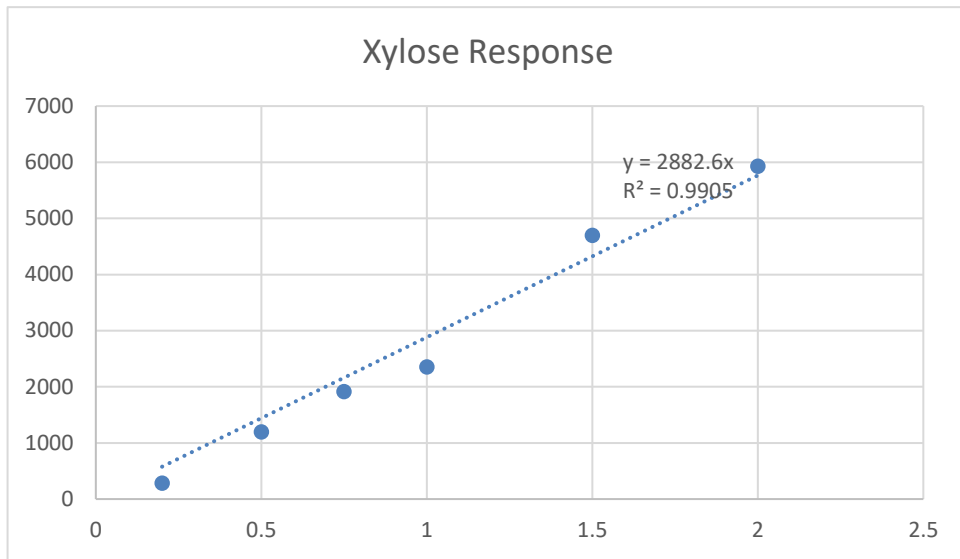
895–900.

138   A. P. F. B. Silva, J. R. O. Do Nascimento, F. M. Lajolo and B. R. Cordenunsi, *J. Food Biochem.*, 2008, **32**, 384–395.

139   T. Chaiwarit, S. Masavang, J. Mahe, S. Sommano, W. Ruksiriwanich, C. H. Brachais, O. Chambin and P. Jantrawut, *Food Hydrocoll.*, , DOI:10.1016/j.foodhyd.2019.105611.

140   C. Chang and L. Zhang, *Carbohydr. Polym.*, 2011, **84**, 40–53.

141   H. Dong, J. F. Snyder, D. T. Tran and J. L. Leadore, *Carbohydr. Polym.*, 2013, **95**, 760–767.

142   I. Braccini and S. Pérez, *Biomacromolecules*, 2001, **2**, 1089–1096.

143   S. Xiao, R. Gao, Y. Lu, J. Li and Q. Sun, *Carbohydr. Polym.*, 2015, **119**, 202–209.

144   R. Lefort, P. Bordat, A. Cesaro and M. Descamps, *J. Chem. Phys.*, 2007, **126**, 014510.

145   A. Idström, H. Brelid, M. Nydén and L. Nordstierna, *Carbohydr. Polym.*, 2013, **92**, 881–884.

146   S. Park, J. O. Baker, M. E. Himmel, P. A. Parilla and D. K. Johnson, *Biotechnol. Biofuels*, 2010, **3**, 1–10.

147   B. Shrestha, Y. Le Brech, T. Ghislain, S. Leclerc, V. Carré, F. Aubriet, S. Hoppe, P. Marchal, S. Pontvianne, N. Brosse and A. Dufour, *ACS Sustain. Chem. Eng.*, 2017, **5**, 6940–6949.

148   G. Mao, D. Wu, C. Wei, W. Tao, X. Ye, R. J. Linhardt, C. Orfila and S. Chen, *Trends Food Sci. Technol.*, 2019, **94**, 65–78.

149   A. K. Chatjigakis, C. Pappas, N. Proxenia, O. Kalantzi, P. Rodis and M. Polissiou, 1998, **37**, 395–408.

150   U. Einhorn-Stoll and H. Kunzek, *Food Hydrocoll.*, 2009, **23**, 40–52.

151   A. Sinitsya, J. Copiková and H. Pavliková, *J. Carbohyd. Chem.*, 1998, **17**, 279–292.

152   S. Fujihara, A. Kasuga and Y. Aoyagi, *J. Food Sci.*, 2001, **66**, 412–415.

153   C. A. Mullen and A. A. Boateng, *Fuel Process. Technol.*, 2010, **91**, 1446–1458.

154   D. Özçimen and A. Ersoy-Meriçboyu, *Renew. Energy*, 2010, **35**, 1319–1324.

155   A. Demirbas, *Energy Sources, Part A Recover. Util. Environ. Eff.*, 2016, **38**, 2693–2697.
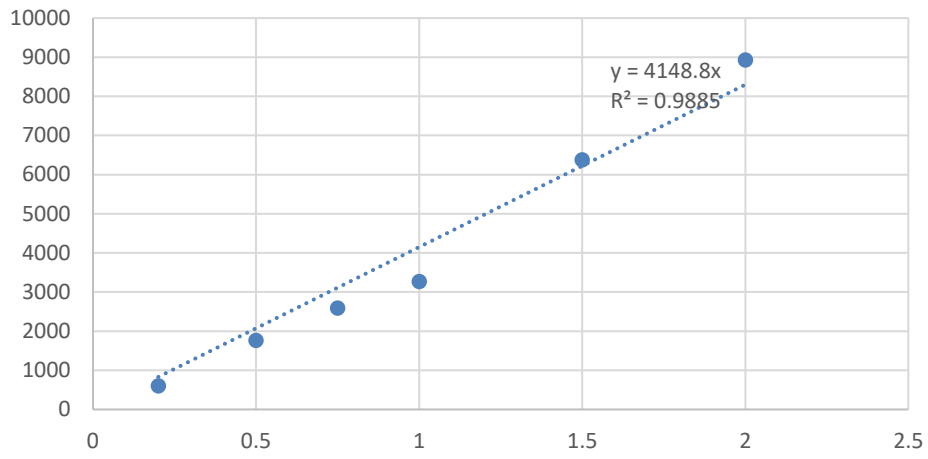
156   R. A. Sheldon, *Green Chem.*, 2017, **19**, 18–43.
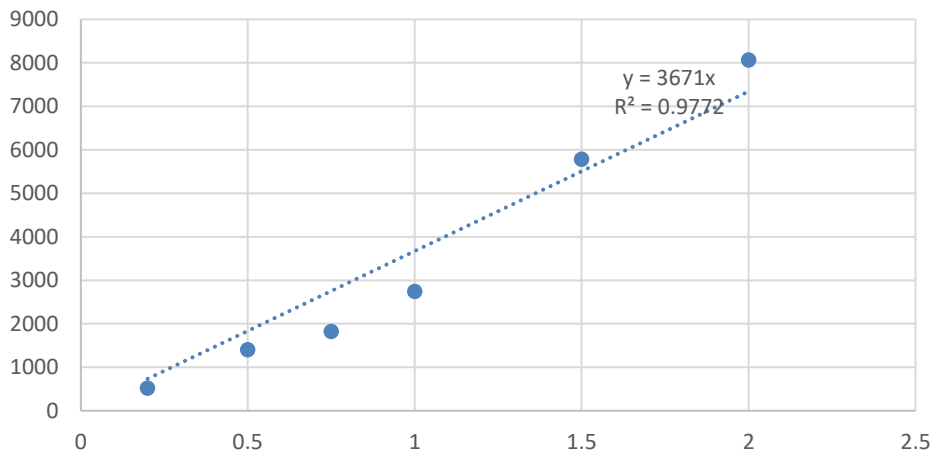
Appendix I

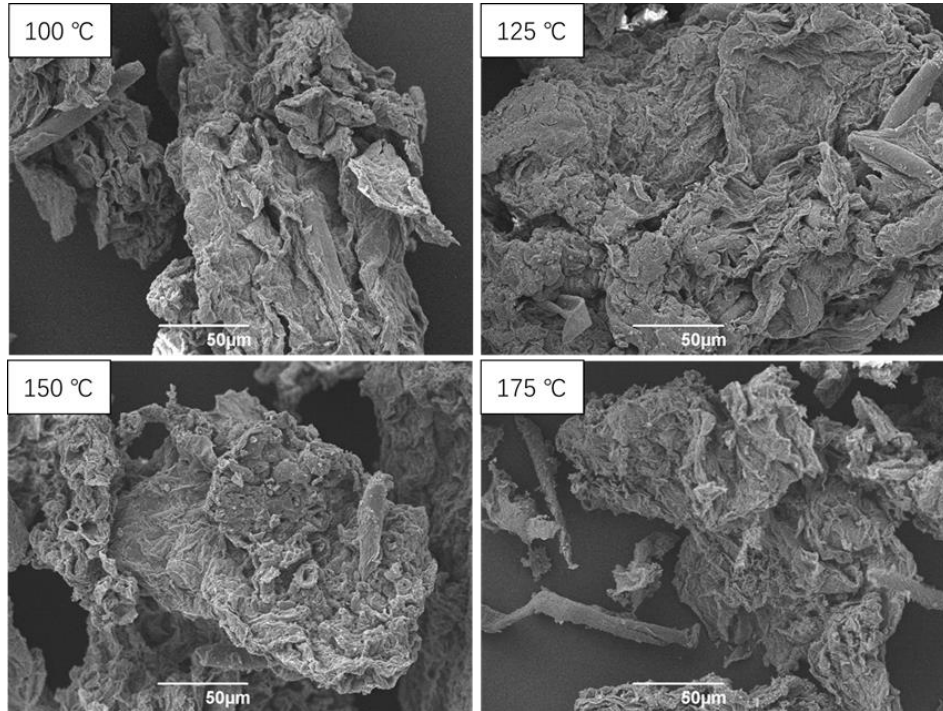HPLC standard sugars

Xylose Response

y = 2882.6x
R² = 0.9905

Fructose Response

y = 3563.8x
R² = 0.9826

Glucose Response

y = 5356.5x
R² = 0.9815

Sucrose Response
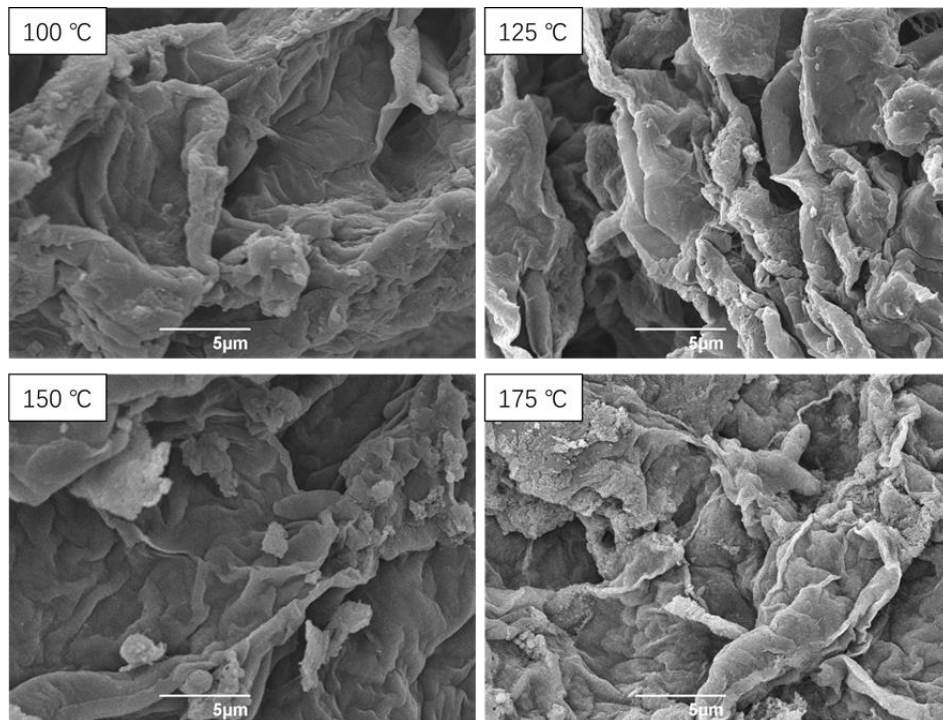
y = 4148.8x
R² = 0.9885

Cellobiose Response

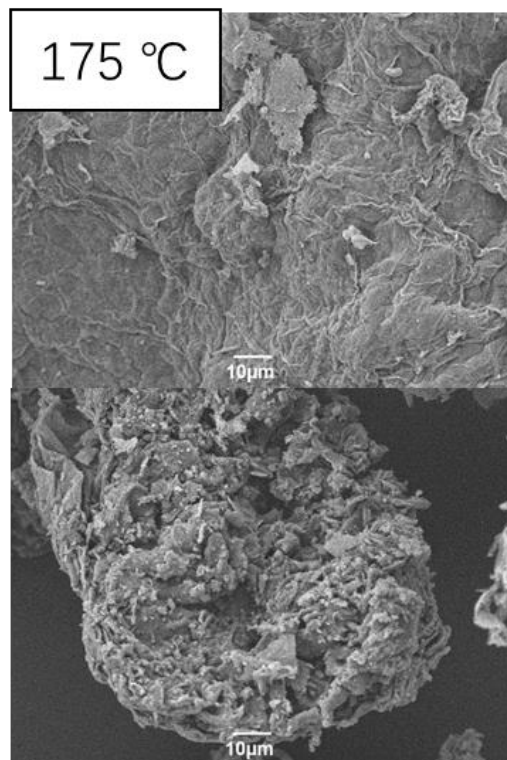y = 3671x
R² = 0.9772

Appendix II

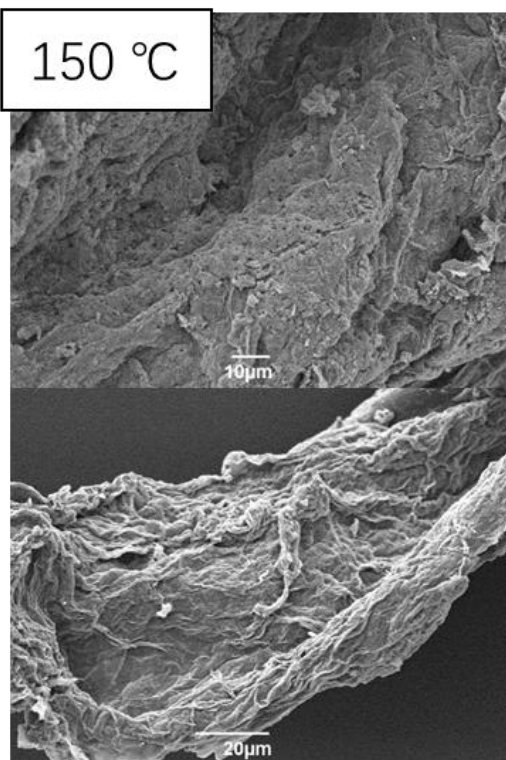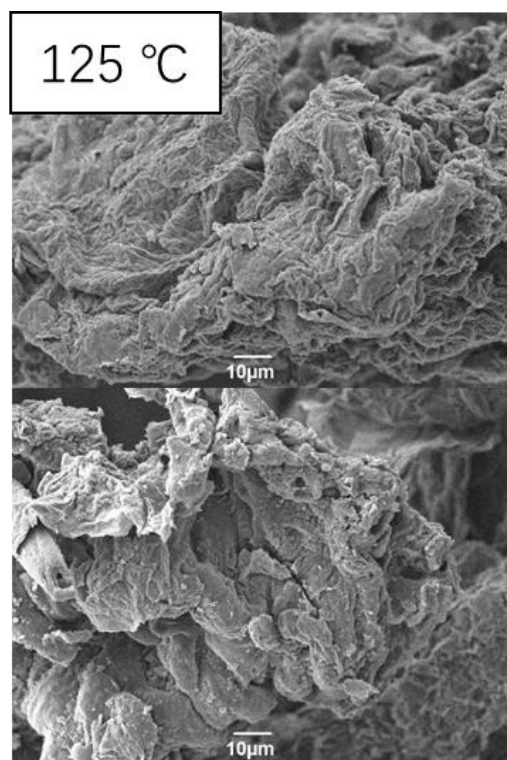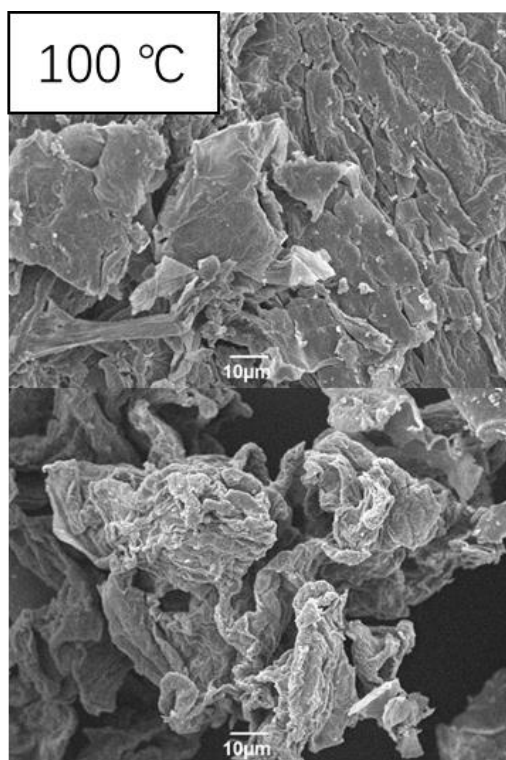SEM figures of peach peel MFC

500 times

5000 times

1000 times

Appendix III

Sodium Dodecyl Sulfate Polyacrylamide Gel Electropho-resis (SDS-PAGE) test of pea vine waste


SDS-PAGE was carried out on an XCell SureLoc Mini-cell electrophoresis system. About 2.0 mg of pea vine waste biopolymer powder was dissolved in 40 μL of solution consisting of 16 μLof NuPAGE LDS sample buffer, 4 μL ofNuPAGE reducing agent, and 20 μL of deionized water. The mixture was heated at 70 °C for 10 min to denature

the proteins, where after the samples were loaded on a graduated NuPAGE Bis-Tris Mini Gel alongside the standard marker and blank samples. The gel was then put into a buffer chamber and electrophoresed at a constant voltage of 200 V by a POWER PAC 1000 for 45 min. After that, the gel was washed with deionized water and immersed in protein stain for 1 h then rewashed with deionized water to form the separated protein bands.

As can be seen in the figure, there is no clear band observed from the protein gel.

Appendix IV

TEM figure of MFC from HL of mango peel (175)
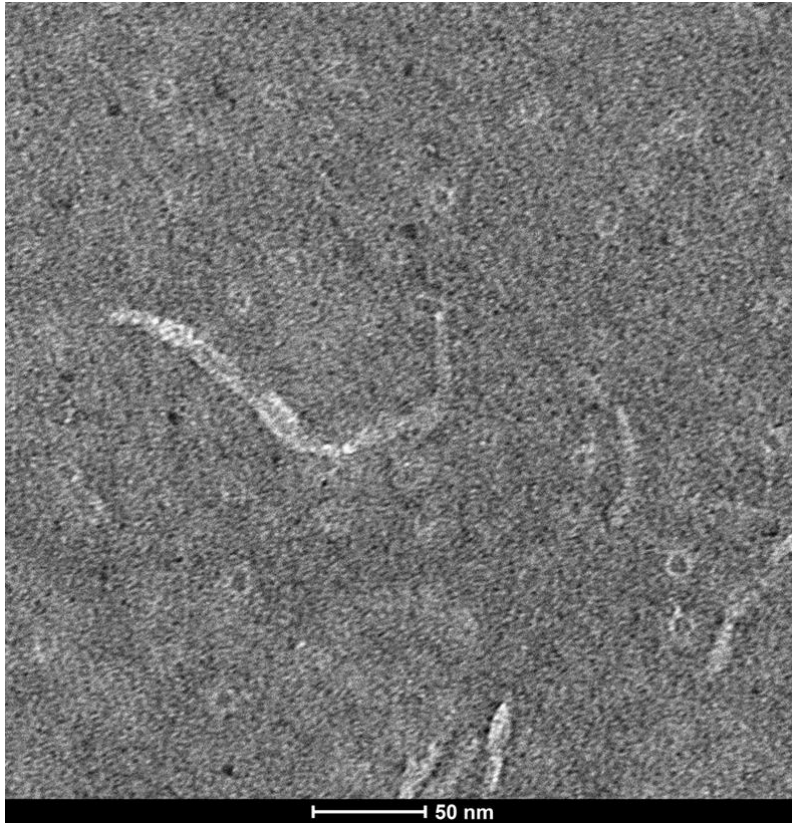
Appendix V

The peach peel after LPS (10 min)

The peach turned into dark color as soon as it was put into the hot lye solution. It can

be seen that the flesh was severely influenced after 10 min's heating.

Abbreviations

SDG - Sustainable Development Goals

FSCW – Food Supply Chain Waste

GalA - D-galacturonic Acid

HG – Homogalacturonan

DE - Degree of Esterification

HM – High Methoxyl

LM - Low Methoxyl

FT-IR - Fourier Transform – Infrared

UAE - Ultrasound-assisted Extraction

MWE - Microwave Extraction

SWE - Subcritical Water Extraction

MFC - Microfibrillated Cellulose

NFC - Nanofibrillar Cellulose

NCC - Nanocrystalline Cellulose

MCC - Microcrystalline Cellulose

CNF - Cellulose Nanofibril

CNC - Cellulose Nanocrystals

CMC - Cellulose Microcrystal

CMF - Cellulose Microfibril

BC - Bacterial Cellulose

CMNF - cellulose micro- and nanofibrils

PEF - Pulsed Electric Field

FAO - The Food and Agriculture Organization

MP – Mango Peels

PVW – Pea Vine Waste

PP- Peach Peel

PAO - Pheophorbide A Oxygenase

CAE - Conventional Acid Extraction

LPS – Lye Peeling Simulation

TGA - Thermogravimetric Analysis

NMR - Nuclear Magnetic Resonance

CP-MAS - Cross-polarization Magic Angle Spinning

GC-MS - Gas Chromatography–Mass Spectrometry

HPLC – High-performance Liquid Chromatography

CHN - Carbon, Hydrogen and Nitrogen Analysis

CV - Calorific Value

SEM - Scanning Electron Microscopy

TEM - Transmission Electron Microscopy

WHC - Water Holding Capacity

HL - Hydrothermal Liquefaction

CI – Crystallinity Index

SDS-PAGE - Sodium Dodecyl Sulfate Polyacrylamide Gel Electropho-resis